

IAEA TECDOC SERIES

IAEA-TECDOC-1796

Seismic Hazard Assessment in Site Evaluation for Nuclear Installations: Ground Motion Prediction Equations and Site Response



IAEA

International Atomic Energy Agency

IAEA SAFETY STANDARDS AND RELATED PUBLICATIONS

IAEA SAFETY STANDARDS

Under the terms of Article III of its Statute, the IAEA is authorized to establish or adopt standards of safety for protection of health and minimization of danger to life and property, and to provide for the application of these standards.

The publications by means of which the IAEA establishes standards are issued in the **IAEA Safety Standards Series**. This series covers nuclear safety, radiation safety, transport safety and waste safety. The publication categories in the series are **Safety Fundamentals**, **Safety Requirements** and **Safety Guides**.

Information on the IAEA's safety standards programme is available on the IAEA Internet site

<http://www-ns.iaea.org/standards/>

The site provides the texts in English of published and draft safety standards. The texts of safety standards issued in Arabic, Chinese, French, Russian and Spanish, the IAEA Safety Glossary and a status report for safety standards under development are also available. For further information, please contact the IAEA at: Vienna International Centre, PO Box 100, 1400 Vienna, Austria.

All users of IAEA safety standards are invited to inform the IAEA of experience in their use (e.g. as a basis for national regulations, for safety reviews and for training courses) for the purpose of ensuring that they continue to meet users' needs. Information may be provided via the IAEA Internet site or by post, as above, or by email to Official.Mail@iaea.org.

RELATED PUBLICATIONS

The IAEA provides for the application of the standards and, under the terms of Articles III and VIII.C of its Statute, makes available and fosters the exchange of information relating to peaceful nuclear activities and serves as an intermediary among its Member States for this purpose.

Reports on safety in nuclear activities are issued as **Safety Reports**, which provide practical examples and detailed methods that can be used in support of the safety standards.

Other safety related IAEA publications are issued as **Emergency Preparedness and Response** publications, **Radiological Assessment Reports**, the International Nuclear Safety Group's **INSAG Reports**, **Technical Reports** and **TECDOCs**. The IAEA also issues reports on radiological accidents, training manuals and practical manuals, and other special safety related publications.

Security related publications are issued in the **IAEA Nuclear Security Series**.

The **IAEA Nuclear Energy Series** comprises informational publications to encourage and assist research on, and the development and practical application of, nuclear energy for peaceful purposes. It includes reports and guides on the status of and advances in technology, and on experience, good practices and practical examples in the areas of nuclear power, the nuclear fuel cycle, radioactive waste management and decommissioning.

SEISMIC HAZARD ASSESSMENT
IN SITE EVALUATION
FOR NUCLEAR INSTALLATIONS:
GROUND MOTION PREDICTION
EQUATIONS AND SITE RESPONSE

The following States are Members of the International Atomic Energy Agency:

AFGHANISTAN	GEORGIA	OMAN
ALBANIA	GERMANY	PAKISTAN
ALGERIA	GHANA	PALAU
ANGOLA	GREECE	PANAMA
ANTIGUA AND BARBUDA	GUATEMALA	PAPUA NEW GUINEA
ARGENTINA	GUYANA	PARAGUAY
ARMENIA	HAITI	PERU
AUSTRALIA	HOLY SEE	PHILIPPINES
AUSTRIA	HONDURAS	POLAND
AZERBAIJAN	HUNGARY	PORTUGAL
BAHAMAS	ICELAND	QATAR
BAHRAIN	INDIA	REPUBLIC OF MOLDOVA
BANGLADESH	INDONESIA	ROMANIA
BARBADOS	IRAN, ISLAMIC REPUBLIC OF	RUSSIAN FEDERATION
BELARUS	IRAQ	RWANDA
BELGIUM	IRELAND	SAN MARINO
BELIZE	ISRAEL	SAUDI ARABIA
BENIN	ITALY	SENEGAL
BOLIVIA, PLURINATIONAL STATE OF	JAMAICA	SERBIA
BOSNIA AND HERZEGOVINA	JAPAN	SEYCHELLES
BOTSWANA	JORDAN	SIERRA LEONE
BRAZIL	KAZAKHSTAN	SINGAPORE
BRUNEI DARUSSALAM	KENYA	SLOVAKIA
BULGARIA	KOREA, REPUBLIC OF	SLOVENIA
BURKINA FASO	KUWAIT	SOUTH AFRICA
BURUNDI	KYRGYZSTAN	SPAIN
CAMBODIA	LAO PEOPLE'S DEMOCRATIC REPUBLIC	SRI LANKA
CAMEROON	LATVIA	SUDAN
CANADA	LEBANON	SWAZILAND
CENTRAL AFRICAN REPUBLIC	LESOTHO	SWEDEN
CHAD	LIBERIA	SWITZERLAND
CHILE	LIBYA	SYRIAN ARAB REPUBLIC
CHINA	LIECHTENSTEIN	TAJIKISTAN
COLOMBIA	LITHUANIA	THAILAND
CONGO	LUXEMBOURG	THE FORMER YUGOSLAV REPUBLIC OF MACEDONIA
COSTA RICA	MADAGASCAR	TOGO
CÔTE D'IVOIRE	MALAWI	TRINIDAD AND TOBAGO
CROATIA	MALAYSIA	TUNISIA
CUBA	MALI	TURKEY
CYPRUS	MALTA	TURKMENISTAN
CZECH REPUBLIC	MARSHALL ISLANDS	UGANDA
DEMOCRATIC REPUBLIC OF THE CONGO	MAURITANIA	UKRAINE
DENMARK	MAURITIUS	UNITED ARAB EMIRATES
DJIBOUTI	MEXICO	UNITED KINGDOM OF GREAT BRITAIN AND NORTHERN IRELAND
DOMINICA	MONACO	UNITED REPUBLIC OF TANZANIA
DOMINICAN REPUBLIC	MONGOLIA	UNITED STATES OF AMERICA
ECUADOR	MONTENEGRO	URUGUAY
EGYPT	MOROCCO	UZBEKISTAN
EL SALVADOR	MOZAMBIQUE	VANUATU
ERITREA	MYANMAR	VENEZUELA, BOLIVARIAN REPUBLIC OF
ESTONIA	NAMIBIA	VIET NAM
ETHIOPIA	NEPAL	YEMEN
FIJI	NETHERLANDS	ZAMBIA
FINLAND	NEW ZEALAND	ZIMBABWE
FRANCE	NICARAGUA	
GABON	NIGER	
	NIGERIA	
	NORWAY	

The Agency's Statute was approved on 23 October 1956 by the Conference on the Statute of the IAEA held at United Nations Headquarters, New York; it entered into force on 29 July 1957. The Headquarters of the Agency are situated in Vienna. Its principal objective is "to accelerate and enlarge the contribution of atomic energy to peace, health and prosperity throughout the world".

SEISMIC HAZARD ASSESSMENT
IN SITE EVALUATION
FOR NUCLEAR INSTALLATIONS:
GROUND MOTION PREDICTION
EQUATIONS AND SITE RESPONSE

COPYRIGHT NOTICE

All IAEA scientific and technical publications are protected by the terms of the Universal Copyright Convention as adopted in 1952 (Berne) and as revised in 1972 (Paris). The copyright has since been extended by the World Intellectual Property Organization (Geneva) to include electronic and virtual intellectual property. Permission to use whole or parts of texts contained in IAEA publications in printed or electronic form must be obtained and is usually subject to royalty agreements. Proposals for non-commercial reproductions and translations are welcomed and considered on a case-by-case basis. Enquiries should be addressed to the IAEA Publishing Section at:

Marketing and Sales Unit, Publishing Section
International Atomic Energy Agency
Vienna International Centre
PO Box 100
1400 Vienna, Austria
fax: +43 1 2600 29302
tel.: +43 1 2600 22417
email: sales.publications@iaea.org
<http://www.iaea.org/books>

For further information on this publication, please contact:

International Seismic Safety Centre
International Atomic Energy Agency
Vienna International Centre
PO Box 100
1400 Vienna, Austria
Email: Official.Mail@iaea.org

© IAEA, 2016
Printed by the IAEA in Austria
July 2016

IAEA Library Cataloguing in Publication Data

Names: International Atomic Energy Agency.
Title: Seismic hazard assessment in site evaluation for nuclear installations : ground motion prediction equations and site response / International Atomic Energy Agency.
Description: Vienna : International Atomic Energy Agency, 2016. | Series: IAEA TECDOC series, ISSN 1011-4289 ; no. 1796 | Includes bibliographical references.
Identifiers: IAEAL 16-01049 | ISBN 978-92-0-105516-3 (paperback : alk. paper)
Subjects: LCSH: Nuclear facilities — Location. | Earthquake hazard analysis. | Earthquake prediction.

FOREWORD

IAEA Safety Standards Series No. SSG-9, Seismic Hazards in Site Evaluation for Nuclear Installations, published in 2010, covers all aspects relating to seismic hazards. Detailed guidelines are, however, required to implement these recommendations.

One of the main objectives in seismic hazard assessment is the estimation of the ground motion that could occur during a future earthquake. Ground motion is usually estimated using a ground motion prediction equation (GMPE), which is an empirical function using earthquake magnitude, the distance from the seismic source to the site and other parameters such as local site conditions. The reliability of the equation strongly depends on the quality and the quantity of the utilized database because GMPEs are often based on regression analysis of observed ground motion data. For some areas, GMPEs based on simulated ground motions have been derived.

In the evaluation of the seismic hazard, it is essential to be able to predict strong ground motion from a dataset that includes near field recordings, as well as those from large magnitude earthquakes. However, data covering this range are still quite sparse. With the introduction of a large number of strong motion observation stations, such as K-NET in Japan, many records are now available in the range of interest. Using these data, new state of the art GMPEs have been developed and can be used to estimate ground motion. However, since local site conditions influence the prediction of ground motion at nuclear installation sites, GMPEs need to be modified by the local site response to be effective. This publication provides relevant information to Member States on how to consider GMPEs and site response in the context of seismic hazard assessments.

The contributions of all those who were involved in the drafting and review of this publication are greatly appreciated. K. Irikura (Japan) is acknowledged for coordinating the project, and C.J. Wu (Japan) is acknowledged for his role in developing this publication. The IAEA officer responsible for this publication was Y. Fukushima of the Division of Nuclear Installation Safety.

EDITORIAL NOTE

This publication has been prepared from the original material as submitted by the contributors and has not been edited by the editorial staff of the IAEA. The views expressed remain the responsibility of the contributors and do not necessarily represent the views of the IAEA or its Member States.

Neither the IAEA nor its Member States assume any responsibility for consequences which may arise from the use of this publication. This publication does not address questions of responsibility, legal or otherwise, for acts or omissions on the part of any person.

The use of particular designations of countries or territories does not imply any judgement by the publisher, the IAEA, as to the legal status of such countries or territories, of their authorities and institutions or of the delimitation of their boundaries.

The mention of names of specific companies or products (whether or not indicated as registered) does not imply any intention to infringe proprietary rights, nor should it be construed as an endorsement or recommendation on the part of the IAEA.

The IAEA has no responsibility for the persistence or accuracy of URLs for external or third party Internet web sites referred to in this publication and does not guarantee that any content on such web sites is, or will remain, accurate or appropriate.

CONTENTS

1.	INTRODUCTION.....	1
1.1.	BACKGROUND	1
1.2.	OBJECTIVE.....	2
1.3.	SCOPE	2
1.4.	STRUCTURE.....	2
2.	GROUND MOTION PREDICTION EQUATIONS	2
2.1.	BASICS OF GMPES FOR NUCLEAR INSTALLATIONS	4
2.1.1.	Important factors considered in GMPE	4
2.1.2.	Functional forms for GMPEs.....	27
2.1.3.	Uncertainty in GMPEs.....	32
2.1.4.	Database and limitation of GMPE	38
2.2.	GROUND MOTION SIMULATIONS	42
2.3.	SELECTION OF GMPES.....	44
2.3.1.	Introduction.....	44
2.3.2.	Priorities of criterion for the selection.....	45
2.3.3.	On the methods of ranking GMPEs based on observation data.....	46
2.4.	ADJUSTMENT OF GMPES	46
2.4.1.	Introduction.....	46
2.4.2.	Magnitude scale	47
2.4.3.	Extrapolation of GMPEs to small magnitudes.....	48
2.4.4.	Interpolation of supporting frequencies.....	48
2.4.5.	Style of faulting.....	48
2.4.6.	Source and path adjustment (V_S & κ)	48
2.4.7.	Single station sigma.....	49
2.4.8.	Near-source ground motion	50
3.	THE INTERFACE BETWEEN GMPES AND SITE RESPONSE.....	52
3.1.	INTRODUCTION	52
3.2.	APPROACHES TO DEALING WITH THE INTERFACE	52
3.2.1.	Preliminary examples	53
3.2.2.	The concept of reference soil configuration	53
4.	SITE RESPONSE	54
4.1.	BASICS OF SITE RESPONSE ASSESSMENT AND CRITICAL ASPECTS.....	54
4.1.1.	Physical interpretation of site response	56
4.1.2.	Site domain concept depending on wave length.....	58
4.1.3.	The role of nonlinearity	59
4.1.4.	The parameterization of site response	60
4.2.	THE THEORETICAL/COMPUTATIONAL APPROACH TO SITE RESPONSE EVALUATION.....	61
4.2.1.	The input ground motion	62
4.2.2.	Site characterization	64
4.2.3.	Numerical modelling.....	68
4.2.4.	Managing modelling uncertainty	72
4.3.	EMPIRICAL SITE RESPONSE EVALUATION	73

4.3.1.	Standard Spectral Ratio	73
4.3.2.	Receiver function	75
4.3.3.	Blind deconvolution	75
4.3.4.	Spectral modelling.....	76
5.	SUMMARIES	76
5.1.	GROUND MOTION PREDICTION EQUATION.....	77
5.2.	SITE RESPONSE.....	77
	APPENDIX: EXAMPLES OF AVAILABLE DATA	79
	REFERENCES.....	85
	DEFINITIONS	103
	ANNEX: DEVELOPMENT OF GMPE: JAPANESE EXAMPLE FOR VERY HARD ROCK CONDITION.....	107
	CONTRIBUTORS TO DRAFTING AND REVIEW	119

1. INTRODUCTION

1.1. BACKGROUND

This publication has been developed as a part of the work undertaken in the ISSC Extra Budgetary Project (ISSC-EBP). Work related to the seismic hazard is addressed in Working Area 1 (WA1) in the ISSC-EBP. The publication is developed under the Task 1.3 in WA1. The objective of WA1 is to develop guidelines to implement the recommendations of the Safety Guide, Seismic Hazards in Site Evaluation for Nuclear Installations, IAEA Safety Standards Series No SSG-9 (2010) [1].

Assessment of the ground motion hazard requires extensive data collection and the development of computational models including many elements (seismic source geometries, propagation pattern of seismic waves, etc.) requiring a careful integration. This publication deals with two topics that are commonly used in seismic hazard and site response analysis, and with an interface between these two types of analyses. The GMPE is a relationship used to estimate so called intensity measures and strong motion parameters at any site of interest. The GMPE provides a probability distribution of the seismic motion, conditional on magnitude, distance, and other parameters. Both, probabilistic and deterministic, estimates of the hazard for nuclear installations and other applications usually require the use of GMPEs.

Ground motion at any site can be seen as the combination of three contributions: characteristics of the source, long range seismic wave propagation (geometrical and anelastic attenuation, scattering and dispersion), and short scale wave field modification near the site of interest. Generally, GMPEs deal with all three elements through the use of simplified models. For the specific nuclear installation sites, the site effect requires more detailed evaluation than what is included in the output of a GMPE. Section 4 presents the controlling independent variables of the site response.

The seismic ground motion at any site shows an inherent variability due to the effects of source characteristics and wave propagation from the source to the site. The underlying process is complex and cannot be described in detail due to the lack of information and the nature of the simplifications inherent in a GMPE. To warrant their wide applicability, GMPEs have relatively simple mathematical forms depending on a relatively small number of independent variables and equation coefficients. Thus the predictions provided by GMPEs are presented with the use of probability distributions. The predicted ground motion is a probability distribution (usually in the form of a log normal distribution) whose characteristics (average and variance) are supplied with parametric relationships depending on independent variables (magnitude, hypocentral distance, etc.) and equation coefficients. Part of Section 2 focuses on the parametric form. Since several possible forms can be used and different sets of experimental data can be used to retrieve the relevant regression coefficients, multiple GMPEs often exist for the same area. The differences among acceptable GMPEs based on up to date collections of ground motion data is an expression of the epistemic uncertainty for predicted ground motion.

Some type of specification of site condition is used in the ground motion estimates given by the GMPEs. The site condition is also either implicit or precisely specified when generating ground motion for scenario earthquakes, depending on the method. However, as noted in SSG-9, a detailed site investigation is required for nuclear installations. Using the site data, the motions predicted using either GMPEs or scenario earthquakes need to be adjusted for the actual conditions. Section 3 discusses the interface between GMPEs or synthetic seismograms and detailed site response models. This interface between the GMPE and the site response

models is crucial, and needs to be handled with great care. For that reason it is discussed with more details in Section 4. As well as, the methods to adjust for the site condition are described in Section 4 of this publication.

1.2. OBJECTIVE

The objective of this publication is to provide the state-of-the-art practice and detailed technical elements related to ground motion evaluation by GMPEs and site response, so that the Member States could follow the recommendations of SSG-9 [1] on the estimation of strong ground motion for seismic hazard assessment or reassessment in site evaluation for nuclear installations.

1.3. SCOPE

The scope of this publication includes the basics of GMPE, ground motion simulation, selection and adjustment of GMPE, site characterization, and modelling of site response in order to improve seismic hazard assessment. The text aims at delineating the most important aspects of these topics (including up to date practices, criticalities and open problems) within a coherent frame. In particular, attention has been devoted to fill conceptual gaps among specific arguments (e.g. the use of empirical GMPEs vs. site response studies) that are generally examined separately. This publication cannot substitute for specific training in seismic response analysis or GMPEs parameterization. It is aimed at supplying a reference text for trained users not specifically aware of most recent developments in the above topics, who are responsible for planning preparatory seismic hazard analyses for siting of all nuclear installations¹ and/or providing constraints for anti-seismic design and retrofitting of existing structures.

1.4. STRUCTURE

Section 2 discusses GMPEs. Section 3 presents the interface between two topics of the GMPE and site response. Section 4 discusses the site response. Section 5 describes the summary for this publication. The Appendix introduces examples of available data and the Annex introduces GMPE for very hard rock.

2. GROUND MOTION PREDICTION EQUATIONS

A GMPE is an equation used to predict measures of seismic ground motion caused by an earthquake. The output of a GMPE is a probability distribution for the ground motion measure. The “classical” parameter is peak ground acceleration (PGA). However, in a modern form, GMPEs have been developed for several additional parameters. Most notable among these are the peak ground velocity (PGV) and response spectral ordinates. There are different types of response spectra. Most commonly, GMPEs predict the pseudo acceleration responses of a damped single degree of freedom oscillator at a range of periods. In the professional literature, GMPEs are sometimes given other names. One term that has been used is “regression model”, but that more properly describes the mathematical technique to calibrate

¹ ‘Nuclear installations’ includes: nuclear power plants; research reactors (including subcritical and critical assemblies) and any adjoining radioisotope production facilities; storage facilities for spent fuel; facilities for the enrichment of uranium; nuclear fuel fabrication facilities; conversion facilities; facilities for the reprocessing of spent fuel; facilities for the predisposal management of radioactive waste arising from nuclear fuel cycle facilities; and nuclear fuel cycle related research and development facilities.

unknown coefficients in the equation. Another term, used in SSG-9, is “attenuation relationships”, which technically refers to the amplitude decrease of the ground motion as the distance from a source increases, but does not include the effect of magnitude.

Let Y be the parameter that is to be predicted. Then a typical GMPE generally takes the generic form

$$\ln Y = f(X, \theta) + \delta \quad (1)$$

where $f(X, \theta)$ represents a function that may be simple or rather complicated, X is a vector representing the set of predictor variables, i.e. those parameters that are entered by the user into the equation to characterize the earthquake source (e.g. M , the event magnitude), the path (e.g. R , the distance from the source to the site), and often site conditions (e.g. V_{S30} , the time averaged shear velocity in the upper 30 m below the reference level). The symbol θ is intended to represent a vector of parameters that are generally chosen by some sort of optimization procedure based on data. The term δ represents the misfit of the data from the GMPE. For instance, a very simple equation (that illustrates the idea summarized by Eq. (1) in a concrete way) could be following.

$$\ln Y = c_1 + c_2 M + C_3 \ln R \quad (2)$$

The predictor variables (elements of X) would be earthquake magnitude M and earthquake source to site distance R . For an application, these would be provided by the user. The parameters that would be optimized (elements of θ) would be c_1 , c_2 , and c_3 . The values of these would be determined empirically in such a way to match as closely as possible some relevant observations of Y in past earthquakes.

The parameter Y requires some discussion. Ground motion parameter is a vector with two horizontal and one vertical component. Both horizontal and vertical motions are relevant for nuclear installations. The vertical component is sufficiently different from the horizontal components that it deserves a GMPE that is separate from the GMPE for horizontal motions. Since Y is a scalar but the horizontal ground motion is a vector, there are several approaches to converting the vector to a scalar, e.g. the geometric mean, a larger component, or vector summation. The method used to obtain the horizontal scalar amplitudes needs to be considered with the output of the GMPE, as alternative vectors to scalar conversions have differing statistical properties.

Figure 1 shows an example of a GMPE fit to a single earthquake. In this figure, it can be noticed that there is a considerable amount of variability of the actual data relative to the mean prediction. By creating a GMPE that incorporates more information about the source, path, and site conditions, some of this variability can be reduced. Because site and path properties vary with every datum, it is efficient to show plots of the term δ as a function of various predictor variables, in order to test whether that predictor is successfully modelled by Eq. (1).

The following sections expand on the above discussion. More detailed information of GMPE can be found in various review papers (e.g. [2–8]).

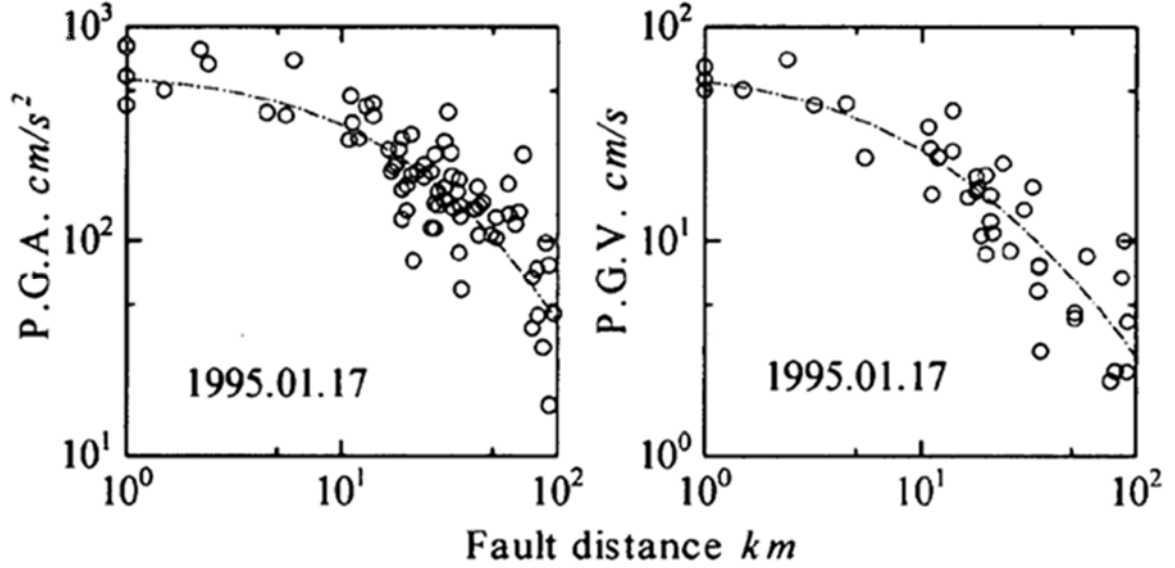


FIG. 1. An example of a regression model fit to a single earthquake, the 1995 M_w 6.9 Hyogo ken Nanbu (Kobe, Japan) earthquake. Reproduced with permission from Si and Midorikawa, 1999 [9].

2.1. BASICS OF GMPES FOR NUCLEAR INSTALLATIONS

2.1.1. Important factors considered in GMPE

Seismic source, path, site effects are the fundamental factors affecting the ground motion from an earthquake expected to be observed at nuclear installations. Generally the observation of ground motion at a station $O(\omega)$ can be represented as the multiplication of seismic source $S(\omega)$, wave propagation path $P(\omega)$, and site effect $G(\omega)$, as expressed in Eq. (3).

$$O(\omega) = S(\omega)P(\omega)G(\omega) \quad (3)$$

where, ω is the angular frequency, $S(\omega)$ represents the source characteristics, $P(\omega)$ represents the attenuation along the wave propagation path, and $G(\omega)$ shows the site amplification due to both the site response and the other effects. These factors are schematically shown in Fig. 2. Each of these, in turn, is affected by numerous physical factors and processes.

In GMPE, a set of simple but representative parameters is adopted to represent the effects of these factors. In the following subsections, many of these physical factors and processes will be introduced, and the parameters, that have been suggested for GMPEs, to represent them. Since ground motion prediction is an active research field, the state-of-the-art in ground motion prediction is continuously evolving, so that the recognition of additional processes and better ways of representing the processes discussed below, are expected.

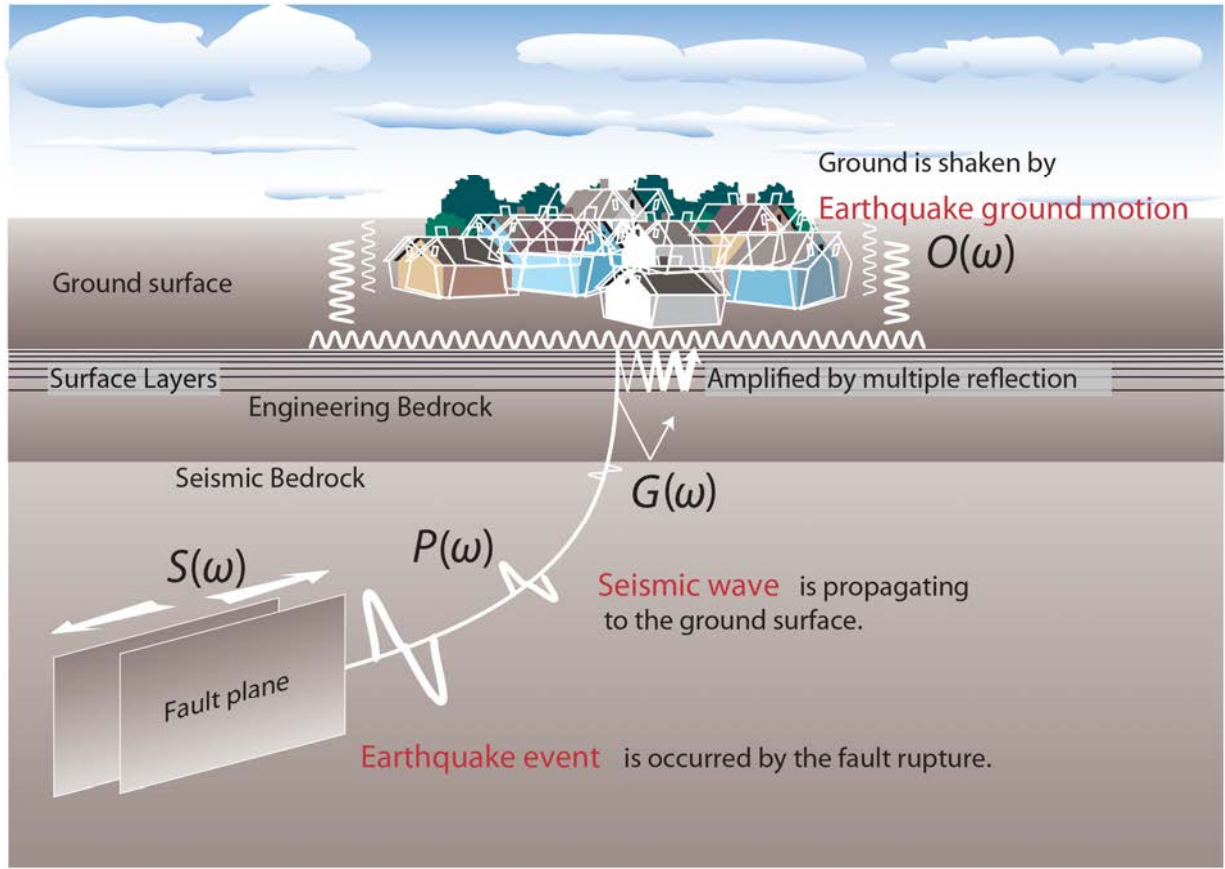


FIG. 2. Illustration of the important factors: seismic source (information about seismic fault, and the environment around the seismic fault, such as its size, location and orientation), path (characteristics about the path from seismic source to the reference interface between the path and the site, such as distance, “layer” velocities and attenuation), and site response (amplification factors from the reference interface to the surface. The reference interface may be engineering bedrock or seismic bedrock). The information on site classification for several countries or regions is shown in the Appendix.

2.1.1.1. Seismic source

The most fundamental parameter accounting for the seismic source in a GMPE is magnitude. Other parameters, including focal depth, tectonic regime, and style of faulting, are also used to represent the seismic source in some GMPEs. This section defines these parameters and gives some examples of their effects.

(1) Global earthquake parameters

Magnitude

The magnitude of an earthquake was originally defined by Richter in 1935 [10] as follows (Eq.4):

$$M_L = \log A - \log A_0(r_{epi}) \quad (4)$$

Where A is the amplitude recorded on a standard type of instrument, and $A_0(r_{epi})$ is a correction for the way that the amplitude of a reference earthquake decreases with epicentral distance. Thus the magnitude is a dimensionless number defined on a logarithmic scale in

which an increase of 1 magnitude unit corresponds to an increase in the amplitude of ground motions by a factor of 10.

The original scale defined by Richter is only valid for distances about greater than 600 km from the source. The scale was almost immediately adapted to records of events at farther distances, recorded on different types of instruments. Subsequently, seismic instrumentation and seismological theory have evolved dramatically. These factors have contributed to a proliferation of magnitude scales. All of these scales are calibrated, to the extent possible, to give the same magnitude for an earthquake as per Richter's original definition. However there are theoretical reasons why perfect correlation is impossible (e.g. [11]).

Several different magnitude definitions have been used in the GMPEs, including surface wave magnitude (M_S) Gutenberg in 1945 [12], local magnitude (M_L) Richter in 1935 [10], Japan Meteorological Agency magnitude (M_{JMA}) Tsuboi in 1954 [13] and moment magnitude (M_W) Hanks and Kanamori in 1979 [14]. However, as shown in Fig. 3, except for M_W , most of the magnitudes saturate for large earthquakes, that is, the increase of magnitudes become obviously smaller than the increase of seismic moment. Because M_W is routinely reported recently, and is directly related to seismic moment, most GMPEs now use M_W as the magnitude. In cases where M_W is unknown, M_W can be estimated based on its correlation with other magnitude scales, as shown in Fig. 3. However, it needs to be recognized that such conversions are always accompanied by uncertainties in the relationships between the magnitudes.

The amplitudes of ground motion generally increase with the increase of magnitude. However, just as some magnitude scales that are based on shorter periods of ground motion (e.g. body wave magnitude m_b , M_L) tend to saturate as the earthquake size increases (Fig. 3), therefore also peak acceleration and other ground motion parameters that measure the high frequencies in the seismic spectrum will tend to increase slowly or even saturate as magnitude increases.

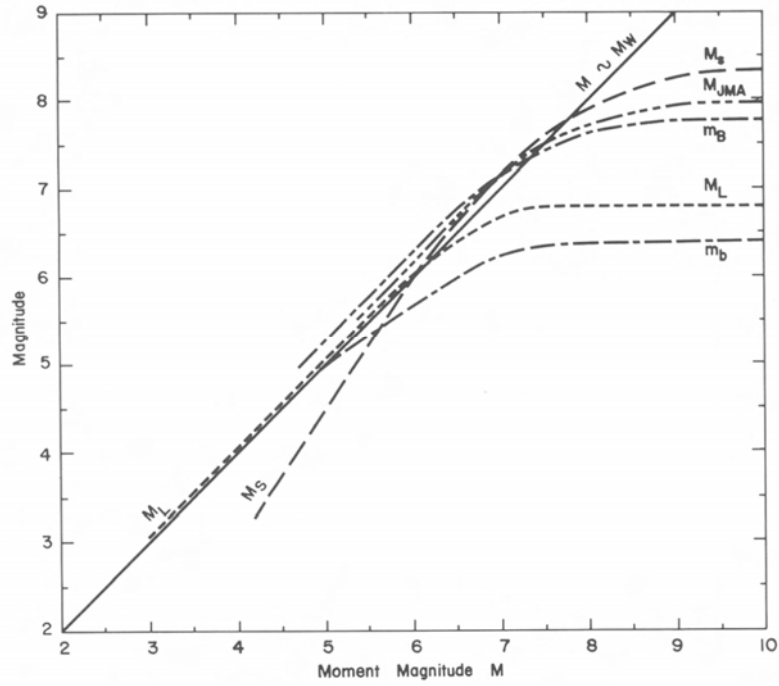


FIG. 3. Example of the correlation between different magnitudes. Reproduced with permission from Heaton et al. in 1986 [10].

Focal depth

Focal depth is the depth from surface to the hypocentre of an earthquake, which is the point where the rupture initiates. While the hypocentral depth is generally well resolved, data from well recorded earthquakes shows that energy radiates from a range of depths, and that the hypocentre may be anywhere within this range. Some GMPEs, recognizing this, use the depth to the centre of fault plane instead of hypocentral depth as a parameter (e.g. [9]). This parameter has been adopted in many GMPEs (e.g. [9, 15–19]). Some models also use the depth to the top of rupture (e.g. [20–22]).

Figure 4 shows the distribution of focal depths of the earthquakes used in the development of GMPE proposed by Si and Midorikawa in 1999 [9]. In their GMPEs, for the same fault distance, the strong ground motion from a deeper earthquake is stronger on average, i.e. strong ground motion scales positively with the focal depth, Si and Midorikawa in 1999 [9] suggest two reasons:

- (1) The average stress drop scales positively with focal depth;
- (2) The attenuation rate along the path is expected to be smaller in deeper layers than in shallower layers of the earth crust. Models cited above that use the depth to the top of rupture also find increased amplitudes as that depth measure increases.

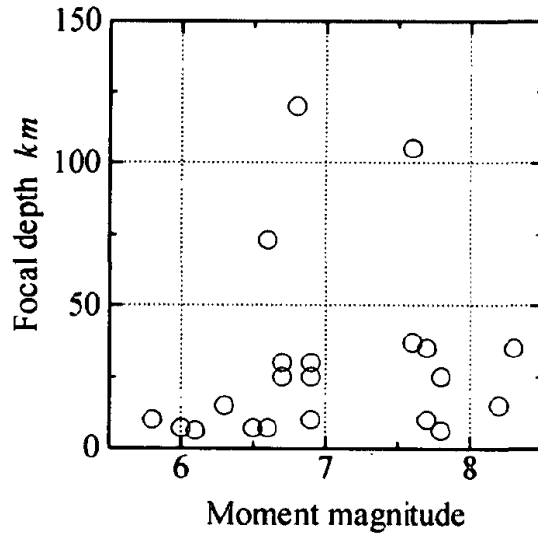


FIG. 4. The distribution of focal depth for earthquakes used in the development of GMPE. Reproduced with permission from Si and Midorikawa in 1999 [9].

Tectonic environment

Ground motions have been found to differ in different tectonic regimes or environments. Three categories of GMPEs are typically used in seismic hazard assessments (e.g. [4, 23]). These are stable continental regions (SCR), shallow earthquakes in active tectonic regions (ACR), and subduction zones (SZ). North American examples of these three types of tectonic environments are: SCR: eastern and central North America (east of the Rocky Mountains); ACR: active western states of the United States of America (USA) (e.g. from California to New Mexico, and north to Washington and Montana); and SZ: Cascadia subduction zone off the coast of northern California, Oregon, Washington, and southern British Columbia.

Additional subdivisions are possible. For instance Allman and Shearer in 2009 [24] divided active continental earthquakes into three regimes or environments: continental extension, continental transform, and continental collision, and found that the average stress drops for each tectonic regime are slightly different, although the ranges overlap considerably. On the other hand, crustal earthquakes outside of SZ cannot always be easily separated into either the stable or active categories as global tectonics demonstrate a continuum of deformation rates between stable regions and the most active regions. Furthermore, even the SCR category is composed of a variety of wave propagation properties. For instance, geometrical spreading, attenuation (Q) is lower in France than in Scandinavia [25] and zones of different Q are also found in eastern North America (e.g. [26]). A global survey finds regions that now may seem stable but have had tectonic activity at a range of different geological ages. Thus the categories of SCR and ACR are perhaps best regarded as idealized end members of a continuous distribution.

Eastern and central North America are characterized as SCR due to low rates of earthquakes, little to no mountain building in the past 100 million years or more, relatively low heat flow, and geodetic deformation rates that are quite low over the past 20 years of GPS monitoring. An ACR is characterized by measurable strain rates (i.e. mostly $>10^{-9}$ per year), conspicuous mountain building, and high heat flow. The ACR of the western US differs from the SCR (central and eastern US) in focal depths and stress drops, and in Q and site response of ground motion. The regions thus need to be modelled by different GMPEs (e.g. [20, 27]).

The earthquakes in subduction zones may occur as SZ interface (interplate) earthquakes, ACR crustal earthquakes above the subduction interface, and intraslab (intraplate) earthquake in the downgoing slab. Additional earthquakes occur in the outer rise seaward of the trench (OR). OR events are generally sufficiently distant from land that they are of less concern for strong motion hazards, but they may cause dangerous tsunamis.

In large and well delineated tectonic environments, it is possible to develop GMPEs for each specific tectonic environment as in the models identified above. In a region like Japan, the approach that has been used is to develop a unified GMPE for all of the regional earthquakes (e.g. [9, 18, 19, 28]). This is possible because all of the earthquakes in that region are affected by the same regional crustal structure and attenuation. In these models, intraplate earthquakes produces stronger ground motion than interplate or crustal earthquakes. However, in general the selection of GMPEs is more likely to require dealing with a trade-off between the use of limited data from a small and more homogeneous region, and sufficient data to adequately constrain the GMPE from a very large region or collection of less homogeneous regions.

Style of faulting

Style of faulting is categorized into three different “end member” types that are: strike slip, normal, and reverse (or thrust) slip faulting as shown in Fig. 5 (see also [29]). Oblique slip earthquakes are also common. An oblique normal earthquake would have components of both normal and strike slip displacement. An oblique reverse earthquake would have components of both reverse and strike slip displacement. The rake angle is used to define the direction of slip on the fault rupture plane. By convention the rake is measured from the horizontal, so a rake of 0 or 180 degrees represents a strike slip earthquake. A rake of 90 degrees represents reverse faulting, and a rake of 270 (or -90) degrees represents normal faulting. The rake is not necessarily constant over the entire rupture of a large fault.

Some models (e.g. [20–22], [30]) predict different ground motions for reverse, strike slip and normal faulting earthquakes. The style may be added as a simple categorical term depending on the rake. According to these models, an earthquake of reverse faulting could generate the strongest ground motion, while lowest for normal faulting and middle level for strike slip faulting. This might seem reasonable, considering that intuitively large horizontal forces are needed in reverse faulting to push up a mountain range against gravity in addition to overcoming friction, while strike slip faulting only moves rock horizontally. However, at the depths where large earthquakes release most of their energy, the frictional forces may dominate, so in the models cited above this term is not necessarily a major effect, and some models do not include it at all.

Schematic diagram of a focal mechanism

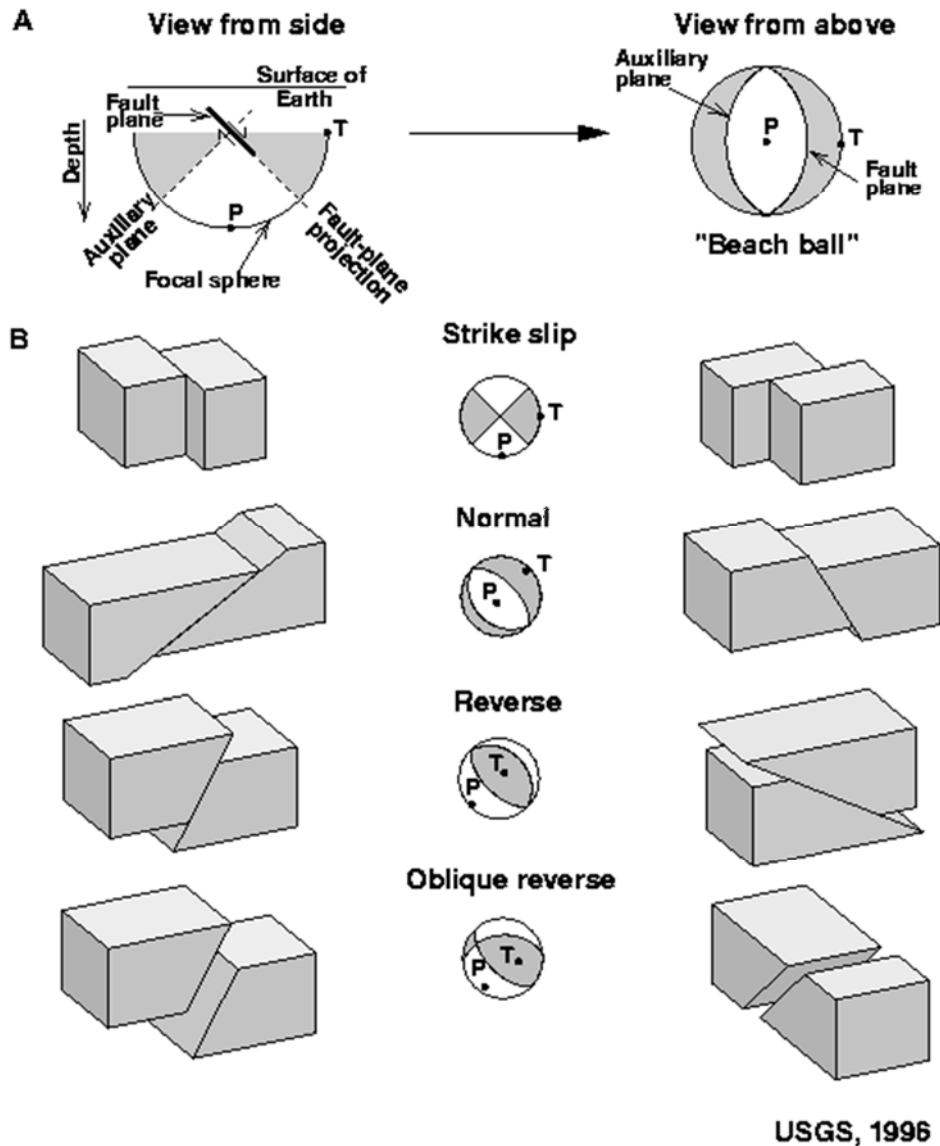


FIG. 5. Definition of earthquakes with different style of faulting. Reproduced with permission from <http://earthquake.usgs.gov/learn/topics/images/beachball.gif>

Stress drop

Stress drop of earthquakes is measured in two different ways, as shown in Fig. 6. The first one is often referred to as the static stress drop, and measures the average differences in the shear stress across a fault before and after an earthquake. For crustal earthquakes, the static stress drop is often about 3 MPa (e.g. [24, 31]), but there is an order of magnitude variation among earthquakes in a region or even aftershock sequence. Theoretically, the static stress drop is proportional to the ratio of the slip on the fault to the fault dimension; for a rectangular fault the denominator uses the smaller dimension (the width) rather than the longer dimension (the length).

The second stress drop is often referred to as the dynamic stress or the apparent stress. This measures the stress that drives the slip on the fault after static friction has been overcome. It may theoretically be much greater than the static stress drop since the fault may have low to zero friction during sliding, but at the end of the earthquake the slip on the fault might be arrested before the fault slips to a condition of zero stress. The energy radiated by the fault is proportional to the dynamic stress drop.

In the simulation of strong ground motion based on theoretical or empirical Green's function methods or stochastic methods, the stress drop parameter, together with the seismic moment, controls the corner frequency and thus the flat level of Fourier spectrum of ground motion above the corner frequency (e.g. [32, 33]). With this in mind, Hanks (1982) [34] suggested using the flat level of the Fourier amplitude spectra to find an estimate of the stress drop, which he calls "RMS stress drop". Unfortunately, since the measurement of stress drop has large uncertainties, only a few GMPEs (e.g. [35]) directly adopt stress drop as an explanatory parameter.

Another approach to incorporating the stress drop may be through the structural maturity of the fault. Radiguet et al. (2009) [36] recognized that ground motions from mature faults are systematically smaller than from immature faults. Mature faults have well developed surface expression, higher slip rate and total slip, greater total fault length, and have been active for longer times. As pointed out by Radiguet et al. (2009) [36], all of these factors can be plausibly identified as contributors to lower stress drop, and thus lower ground motions.

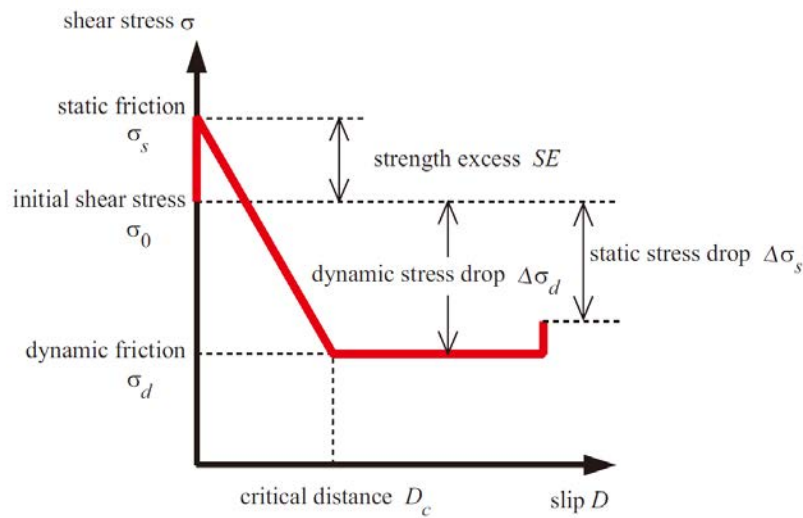


FIG. 6. Illustration for the definition of stress drop. Reproduced with permission from Dan et al., 2007 [37].

(2) Parameters for near field ground motion

Hanging wall

The observation stations located near a seismic source fault can be divided into hanging wall stations and footwall stations, as shown in Fig. 7. Abrahamson and Somerville (1996) [38], analysed the recordings derived at hanging wall and footwall stations during the 1994 Northridge earthquake and the other several crustal earthquakes in the USA and found that the peak horizontal accelerations on the hanging wall over the distance range of 10 to 20 km are up to a 50% larger than the median amplitude for the earthquakes. In contrast, the peak accelerations on the footwall are not significantly different from the median amplitude over this distance range. This is called the hanging wall effect on ground motion. Based on the data available at that time, in 2008 Abrahamson and Silva [20] developed a modification function for the hanging wall effect (Fig. 8). By using this modification function (F_{HW}), the prediction by a GMPE (A_{GMPE}) can be modified to include the hanging wall effect as expressed in Eq. (5).

$$A_{GMPE_HW} = A_{GMPE} \times F_{HW} \quad (5)$$

Several different models for the hanging wall effect and where it applies have been proposed in recent GMPEs (e.g. [20–22]). Due to the fact that the hanging wall data is sparse, approaches to parameterize this effect remain an active area for research.

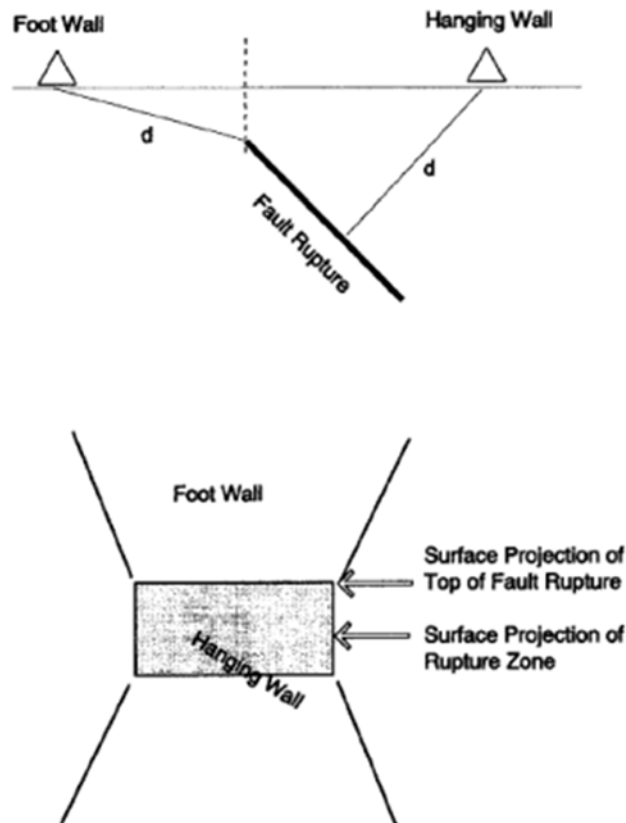


FIG. 7. Definition of footwall and hanging wall sites used in this analysis. The separation point is the vertical projection of the top of the rupture (upper). Stations off the ends of the fault are excluded (lower) [38].

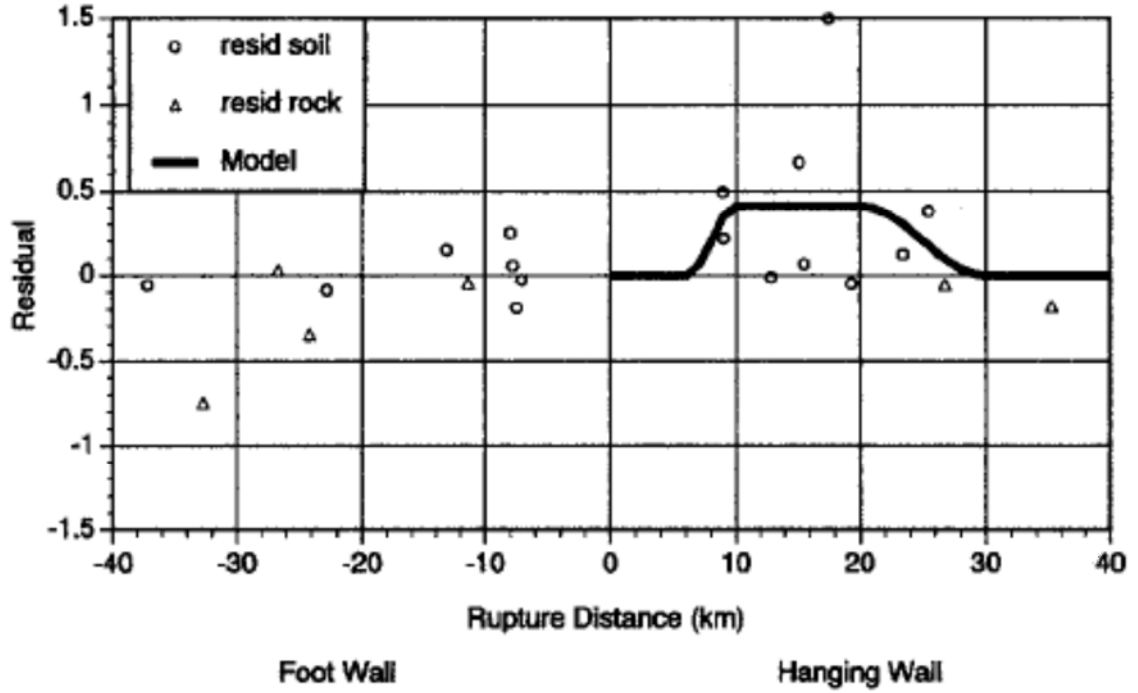


FIG. 8. An example of a modification function for the hanging wall effect [38].

Directivity

A modification of GMPE to include directivity effects were first proposed by Somerville et al. (1997) [31]. In their analysis, the observed ground motion at stations located in the forward direction of rupture propagation is larger than the one from the observations in the backward direction. An example of the forward direction observation station is shown in Fig. 9. One approach to define the modelling parameters is shown in Fig. 10.

Based on the analysis of observations from 20 earthquakes, Somerville et al. (1997) [31] found that, the propagation of rupture towards a site causes larger ground motion amplitudes at predominant periods longer than 0.6 second and shorter strong motion durations than for average directivity conditions. That is, the rupture directivity causes spatial variations in the amplitude and duration of ground motions around faults. Based on the data available at that time, they suggested a modification function to account for the forward directivity effect, as shown in Fig. 11. By using this modification function (F_{DIR}), the prediction by a GMPE (A_{GMPE}) can be modified to include the rupture directivity effect (A_{GMPE_DIR}) as explained in Eq. (6).

$$A_{GMPE_DIR} = A_{GMPE} \times F_{DIR} \quad (6)$$

Besides the method proposed by Somerville et al. (1997) [31] other methods have been also suggested (e.g. [39]). Recently, in the Next Generation Attenuation relationships (NGA) West2 project, four alternative models for directivity effects have been proposed [40]. However, though they make progress towards improvement to the directivity model, they concluded that the current version of directivity models is still not satisfactory and indeed more investigation is needed [40].

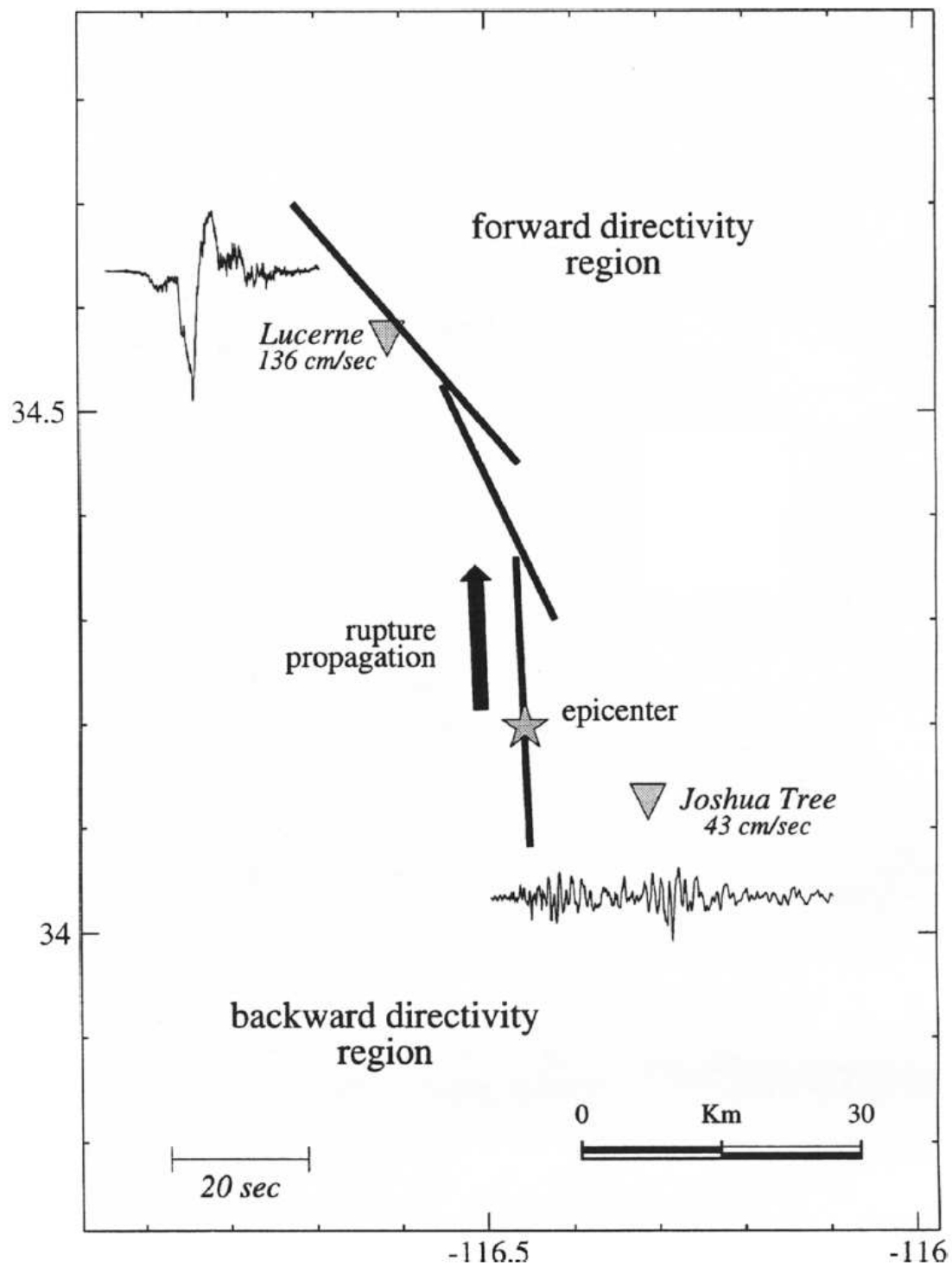


FIG. 9. Map of the Landers region showing the location of the fault plane of the 1992 Landers earthquake and recordings at Lucerne and Joshua. The strike normal velocity waveforms at the two stations show rupture directivity effects in forward and backward direction respectively (Somerville et al., 1997 [31]).

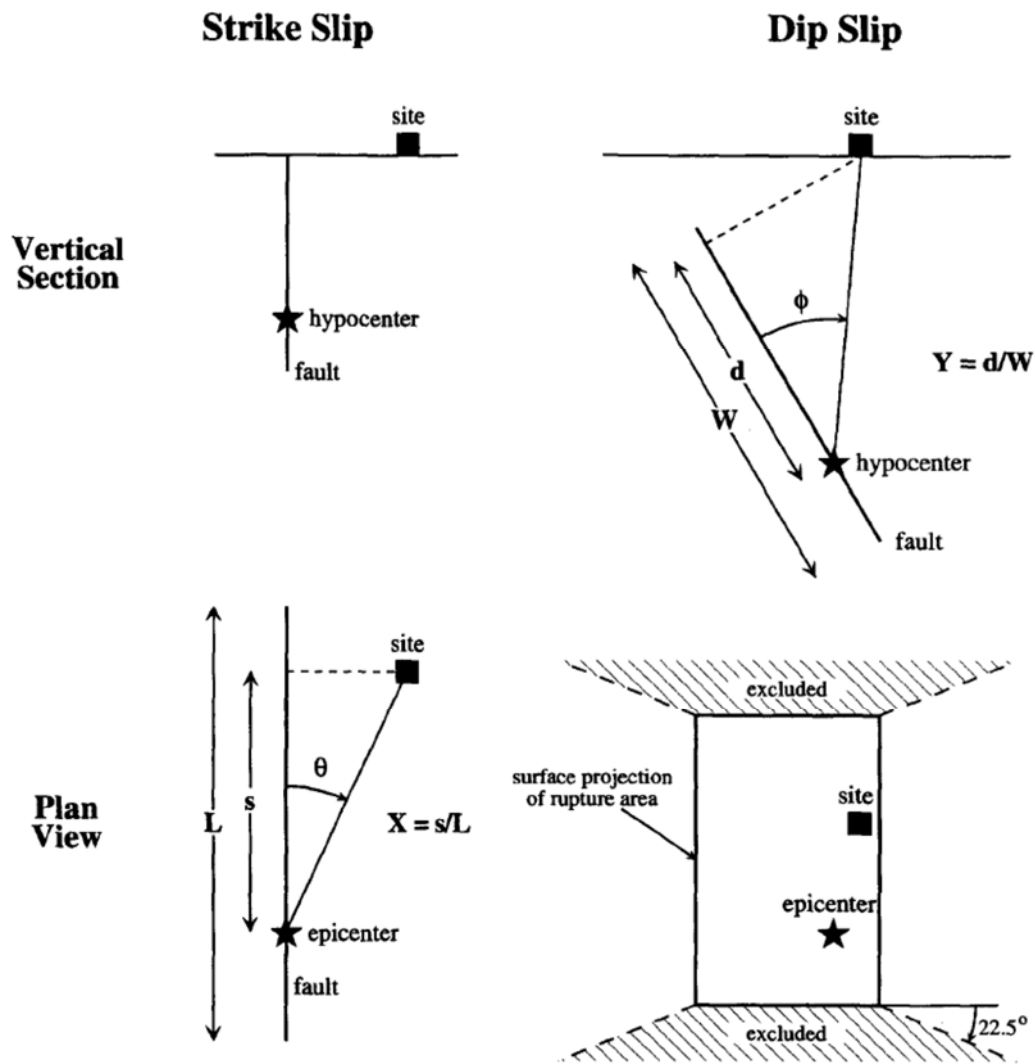


FIG. 10. Illustration of parameters used in the modelling of directivity effects [31].

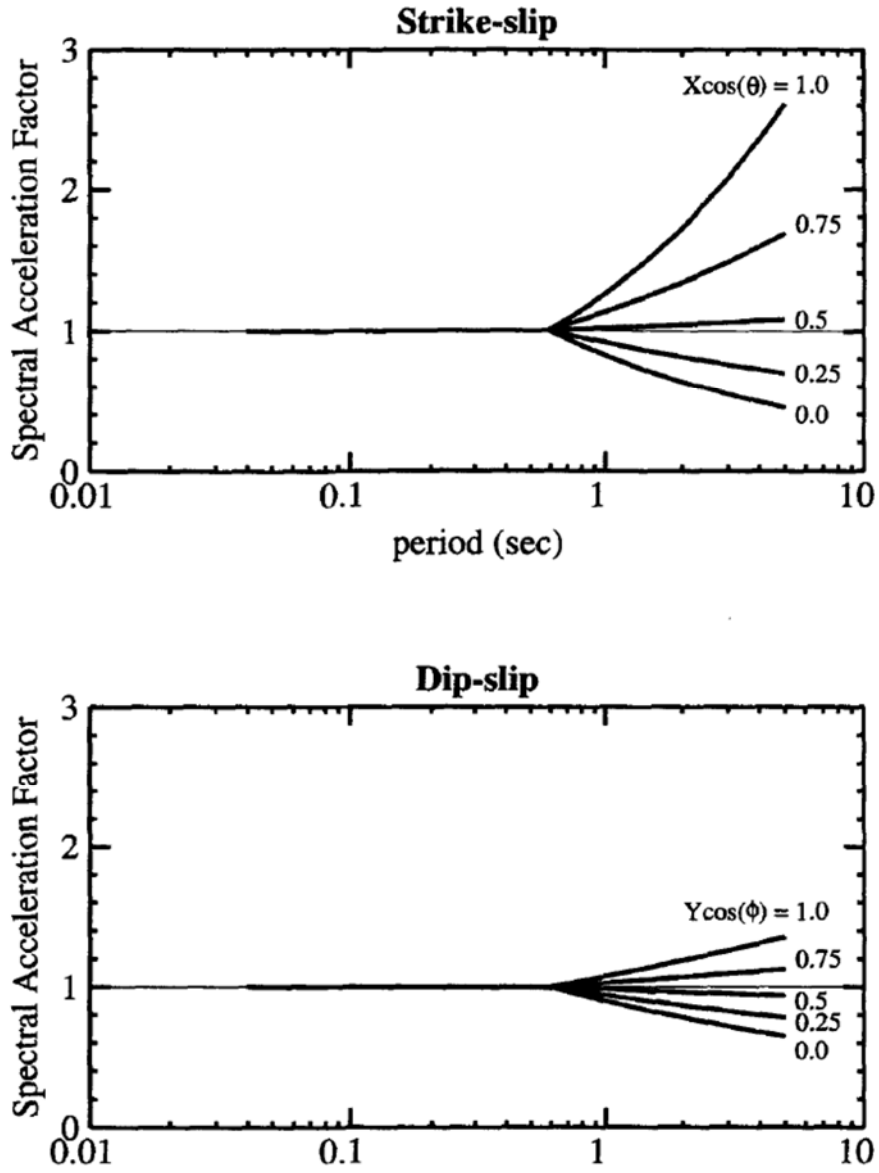


FIG. 11. Empirical model of directivity effect for modifying GMPE [31].

Buried rupture

Somerville (2003) [41] suggested that the ground motion from earthquakes that produce large surface rupture seems to be systematically weaker than ground motion from earthquakes with a subsurface rupture as shown in Fig. 12. Especially for the 1999 Chi-Chi earthquake and Izmit earthquake, the ground motions at short and intermediate periods (0.1-3.0 s) are about 40% weaker than current GMPE predictions.

Kagawa and Irikura (2004) [42] found that this results may be caused by shallower depths of the strong motion generation area (SMGA) for surface rupturing events compared to buried rupture events as shown in Fig. 13. They found that the total rupture area of buried rupture earthquakes is 1.5 times smaller than that of surface rupture earthquakes having the same seismic moment, and that deep SMGAs have about three times larger effective stress drops and two times higher slip velocities than shallow SMGAs.

However, currently there is no effective modification function for GMPEs to include the effect by larger strong motion caused by the buried rupture earthquake, though as mentioned above, some GMPEs (e.g. [20]) and NGA West models use the parameter of the depth to the top of the fault plane to account for the effects of buried rupture.

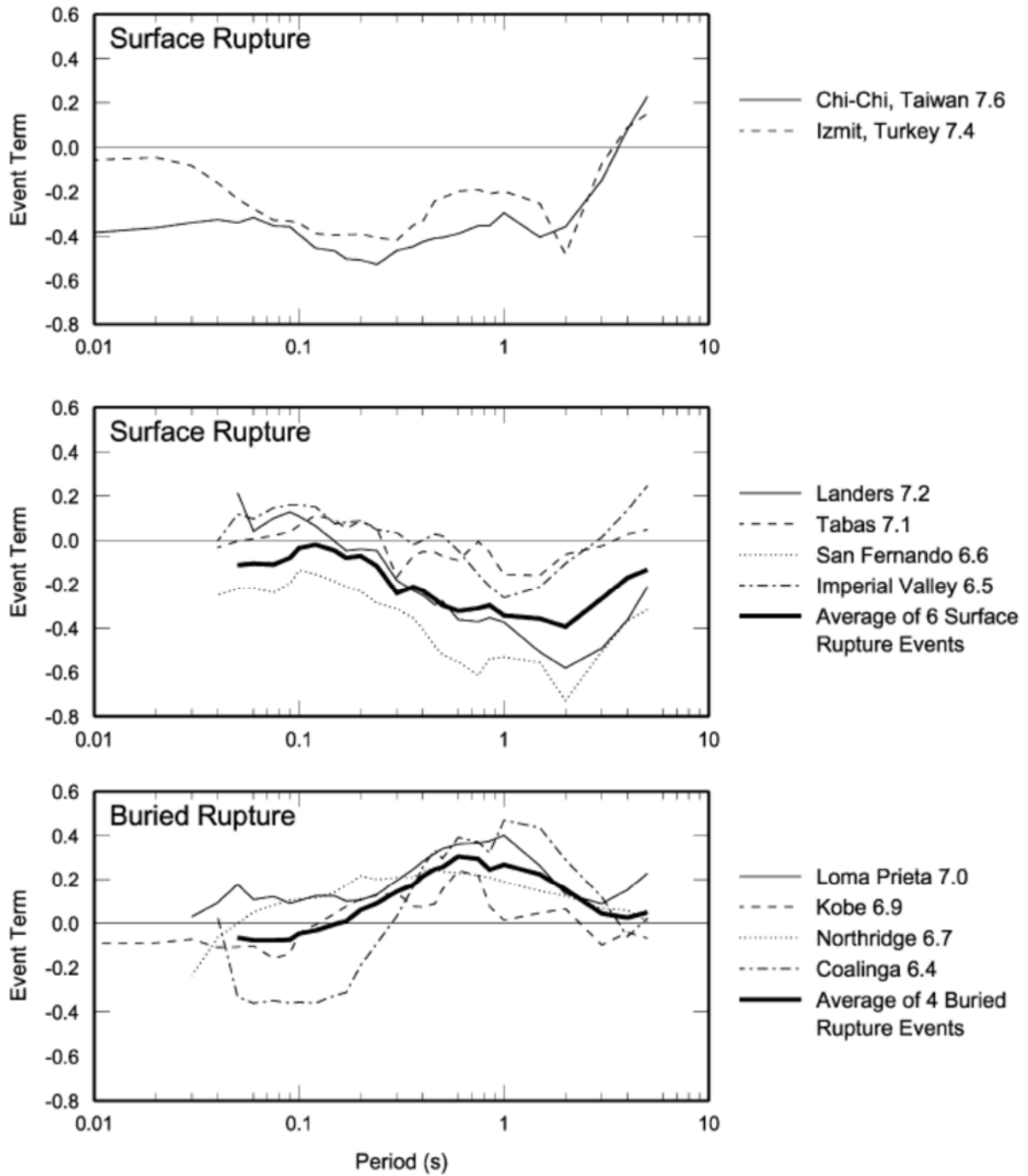


FIG. 12. Comparison of the response spectral amplitude of individual earthquakes, averaged over recording sites, with the amplitude of the average earthquake as represented by the model of Abrahamson and Silva (1997) [43] shown as the zero line, which accounts for the magnitude, closest distance and site category. The event terms (residuals) are shown as the natural logarithm of the event/model ratio: $+0.2$ indicates event exceeding the model by a factor of 1.22, and -0.2 indicates event at 0.82 of model value. Reproduced with the permission from Somerville, 2003 [41].

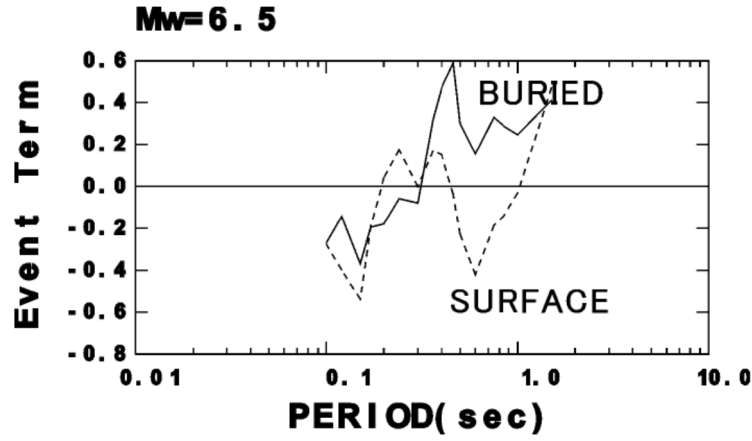


FIG. 13. Comparison of the simulated response spectra with the GMPE of Abrahamson and Silva (1997) [43]. Reproduced with the permission from Kagawa and Irikura, 2004 [42].

2.1.1.2. Path effects

In a GMPE, the path is primarily represented by the distance from seismic source to a site. Figure 14 shows some definitions of distance practically used in GMPEs [4]. Among them, the distances measured from fault plane to observation station (r_{rup}) is perhaps the most commonly used in modern GMPEs.

In addition to the above distance measurements, an equivalent hypocentral distance (EHD) has also been proposed. EHD represents the distance from a virtual point source that provides the same energy to the site as does a finite size fault [44]. Currently, still only few authors use this distance measurement to develop their GMPEs (e.g. [9, 45, 46]).

For small earthquakes (e.g. $M < 5$) the fault dimension is generally not larger than the uncertainty in the location, so a common approximation is $r_{hypo} \approx r_{rup}$. Generally, the path effects can be modelled as a contribution from geometric spreading and a contribution from inelastic (intrinsic and scattering) attenuation term.

The geometric attenuation depends on the distance, velocity structure, and period of the seismic waves. The geometric attenuation is different for body waves, and surface waves. In an unbounded elastic medium, the amplitude of a body wave decreases with distance r at a rate of r^{-1} , where r generically represents the source to station distance. Thus near the earthquake source, a distance dependence of r^{-1} is generally expected to be a good approximation. Surface waves only exist due to the waveguide caused by low seismic velocities of the crust. Being trapped in this waveguide, the amplitude of surface waves decrease at a nominal rate of $r^{-0.5}$. In the near field area, the seismic ground motion is controlled by body waves, while surface waves become more important as the distance increases. GMPEs often set the geometrical spreading factor as a variable, i.e. r^{-c} where the factor c may depend on the distance range. In a GMPE, which predicts the logarithm of the ground motion, the geometrical spreading generally takes the form $c \cdot \ln(r)$.

The anelastic attenuation arises from energy absorption and scattering along the path, and is quantified with a quality parameter Q . The Q is spatially variable, which contributes to the regional dependence of ground motion attenuation characteristics.

In a uniform material, in addition to the effect of geometrical spreading, the amplitude decreases by the additional factor of $\exp\left(\frac{-\pi r f}{Qv}\right)$, where v is the velocity of the seismic wave and f is frequency. Thus in a GMPE, which predicts the logarithm of the ground motion, the attenuation term enters as $-c_i r$ where c_i is determined from the data and generally depends on the frequency of the waves. As an example of regional variations in Q , Fig. 15 shows the regional variation of Q in the USA, and Fig. 16 shows the impact of regional variation in Q in Japan on attenuation of ground motions from two earthquakes. Other similar phenomena were mentioned in Morikawa et al. 2003 [48].

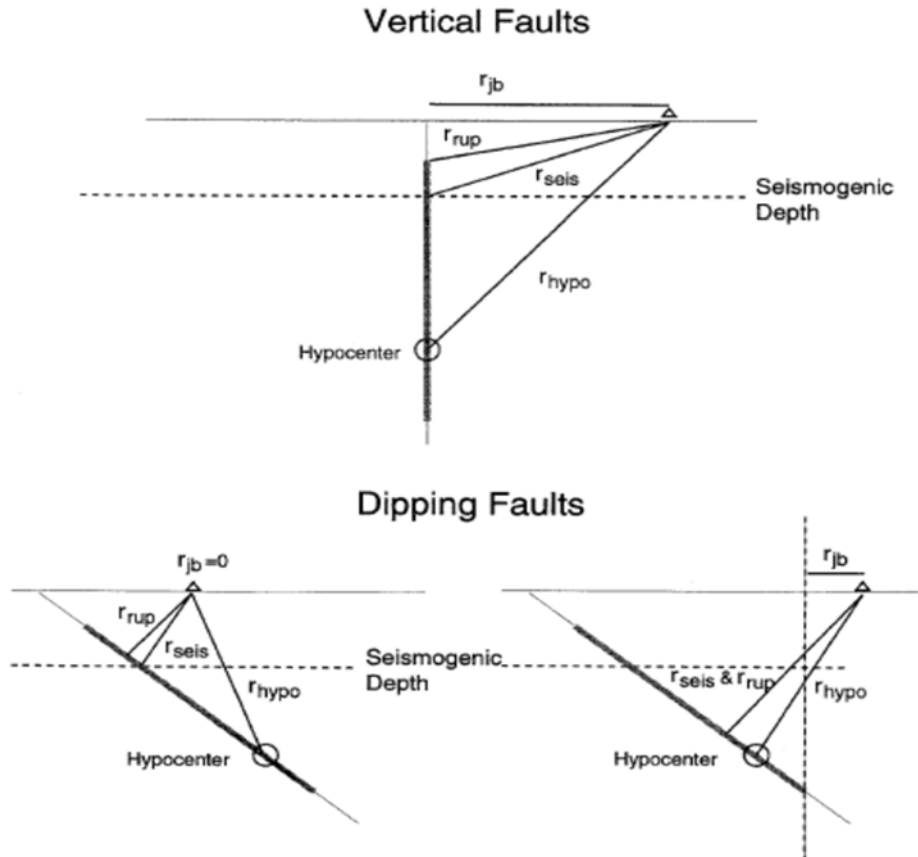


FIG. 14. Illustration of different definitions of distance. The four distances represented here are, the hypocentral distance, r_{hypo} ; closest distance to rupture zone, r_{rup} ; closest distance to surface projection of rupture zone, r_{jb} ; and closest distance to seismogenic rupture, r_{seis} [4].

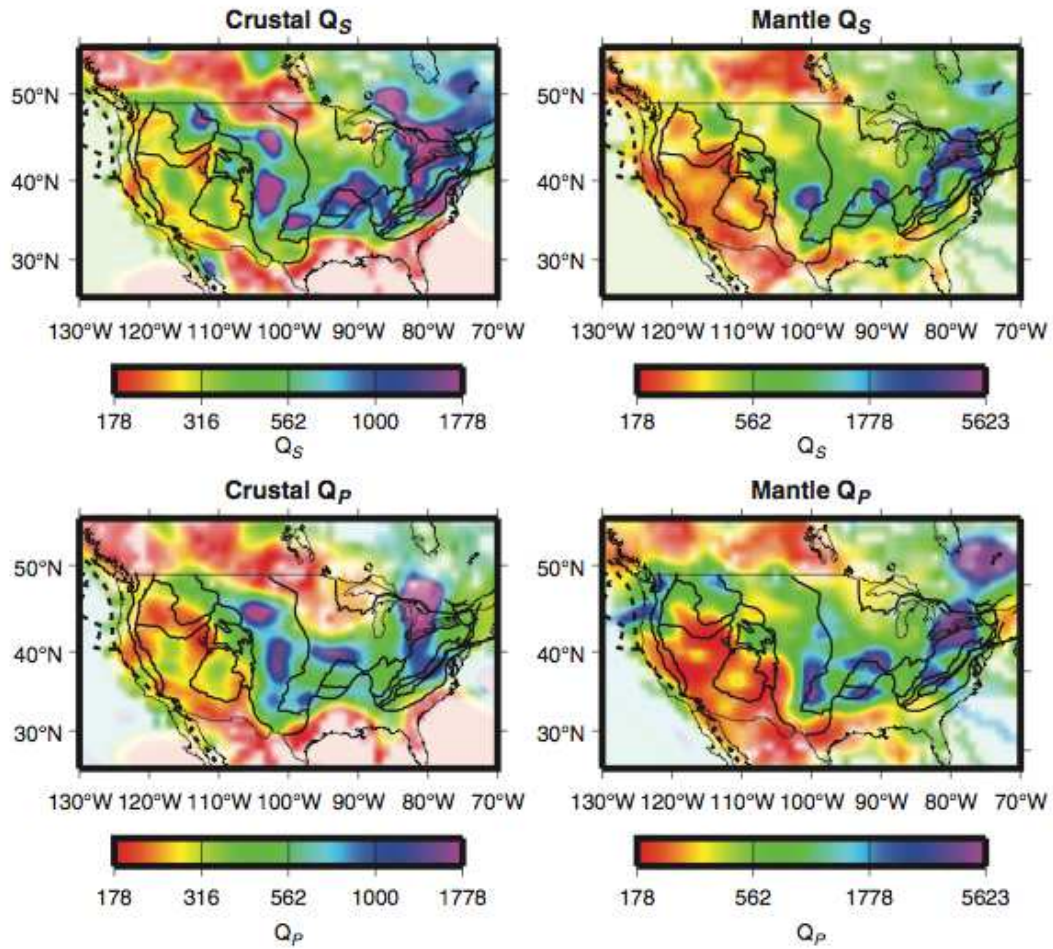


FIG. 15. Example for regional variability of Q in the United States of America [26].

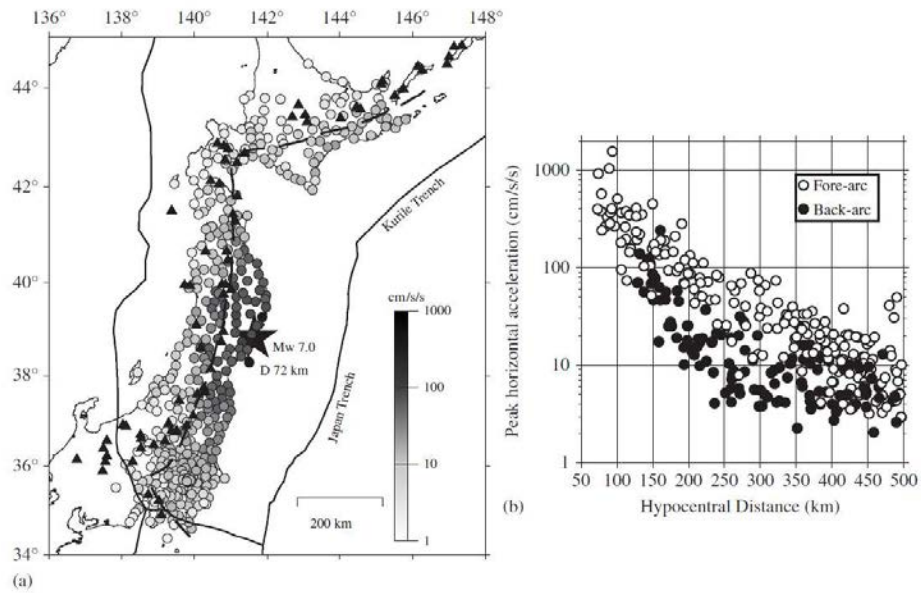


FIG. 16. Examples for different attenuation rate for short period ground motion due to the low Q_s region underneath the volcanic front. Reproduced with the permission from Dhakal et al., 2010 [47].

Focal depth dependency

For several reasons, the geometric attenuation for deeper earthquakes differs from that of shallow earthquakes (Fig. 17. e.g. [49–51]). There are several physical effects that contribute to this difference, and details are explained below. Deeper earthquakes are less efficient in exciting surface waves, so body wave spreading is a more dominant effect. Up-going waves originating from earthquakes below the Moho encounter, a relatively strong reflection coefficient at the Moho, decreasing the amplitudes in the crust, and that reflection coefficient depends on the angle of incidence and thus the epicentral distance. Deeper events tend to have higher stress drops, but the seismic waves often encounter lower Q paths through the upper mantle and the crust.

As one example of the difference in geometrical spreading, Midorikwa and Ohtake (2002) [49] proposed using the Eq. (7) to model the differences in attenuation rate for earthquakes with different focal depth, D (Fig. 18).

$$\begin{aligned} \log A &= b - \log(X + C) - kX & (D \leq 30 \text{ km}) \\ b + 0.6 \log(1.7D + C) - 1.6 \log(X + C) - kX & & (D > 30 \text{ km}) \end{aligned} \quad (7)$$

Where X is the distance from the fault or hypocenter to site in km, C and k are the constant coefficients.

Thus they find a faster geometrical spreading for deep events ($c=1.6$) than for shallow events ($c=1.0$).

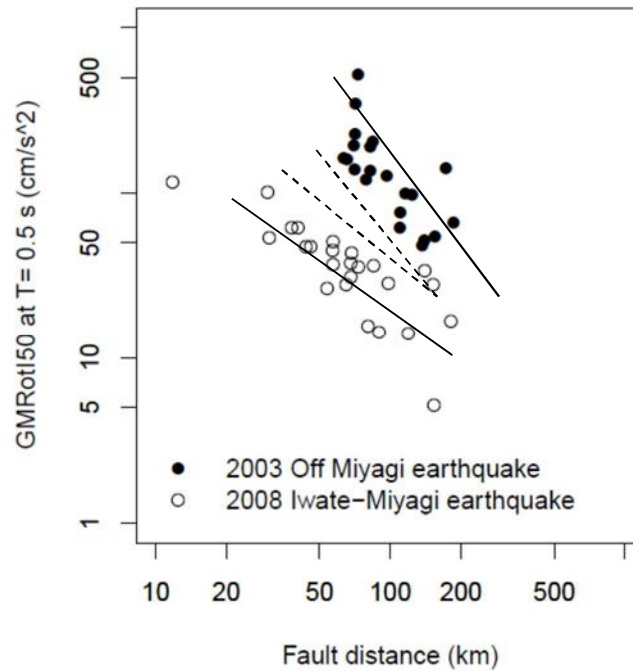


FIG. 17. Examples for different attenuation rate for short period ground motion due to different focal depths (open circles): M7.0 Off Miyagi earthquake on 2003/05/26, focal depth 71 km; solid circles: M6.9 Iwate Miyagi earthquake on 2008/06/14, focal depth 9km; solid lines show regression curves for data from the two earthquakes, and broken lines illustrate the different attenuation rates for the two black lines. All data are adopted from the database of Si et al., 2013 [28]. Reproduced with the permission from H. Si.

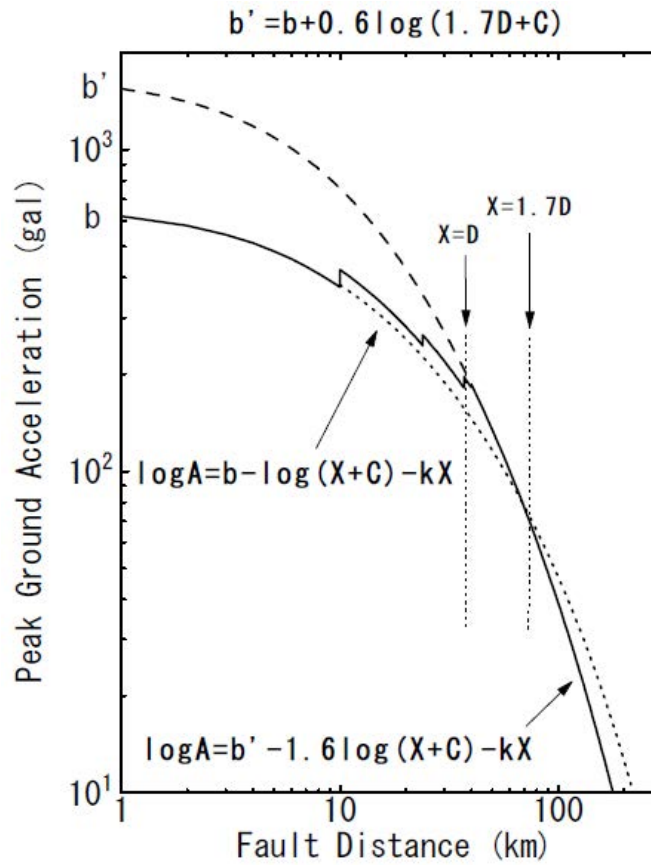


FIG.18. Modelling the effects of focal depth on attenuation rate for PGA. Dotted and solid lines show attenuation model without or with effects of focal depth, respectively, inferred from a layered crustal model and a focal depth of 40 km. Reproduced with the permission from [49].

Magnitude dependency for attenuation rate

Several researchers found that the attenuation rate for smaller earthquakes is steeper than that for larger earthquakes (e.g. [52–55]).

Figure 19 shows some examples of the comparison of the observations for small earthquakes and the prediction by GMPEs represent the attenuation rate for moderate or large earthquake. From this figure, the observations of small earthquakes show steeper decay than GMPEs that are for moderate or large earthquakes. This implies that the attenuation rate for small earthquakes maybe different from moderate or large earthquakes.

Anderson (2000) [56] uses three techniques to simulate ground motions with different magnitude, and found that ground motion decays less rapidly with distance for larger magnitude earthquakes, so that there is a distance dependent magnitude saturation. He explained this phenomenon as follows: at longer distances the Green's functions are more complex due to various arrivals spread out over a longer duration of time. A larger earthquake, with more subevents spread over a greater time period, will have constructive interference among the various arrivals from each subevent, and the longer durations of the subevent signals at larger distances will cause a proportionately greater increase in the amplitude than what typically occurs at shorter distances (Fig. 20).

Si et al. (2012) [55] simulated the wave propagation from small and moderate earthquakes based on the Finite Difference Method (FDM), and found that:

- (1) The attenuation rate for small earthquakes, $X^{-1.6}$, being higher than that for body waves may be caused by the reflection loss on the discontinuities in Earth structure;
- (2) For moderate earthquakes, the reflection loss is almost cancelled by the predominant surface waves (attenuation rate is $X^{-0.5}$). Consequently, the attenuation rate is the same as for body waves ($X^{-1.0}$) (Fig. 21). This result implies that the difference in attenuation rates between small and moderate earthquake may be significant, but between moderate and large earthquakes, the difference may not be significant.

The above results show a further investigation is needed for this issue.

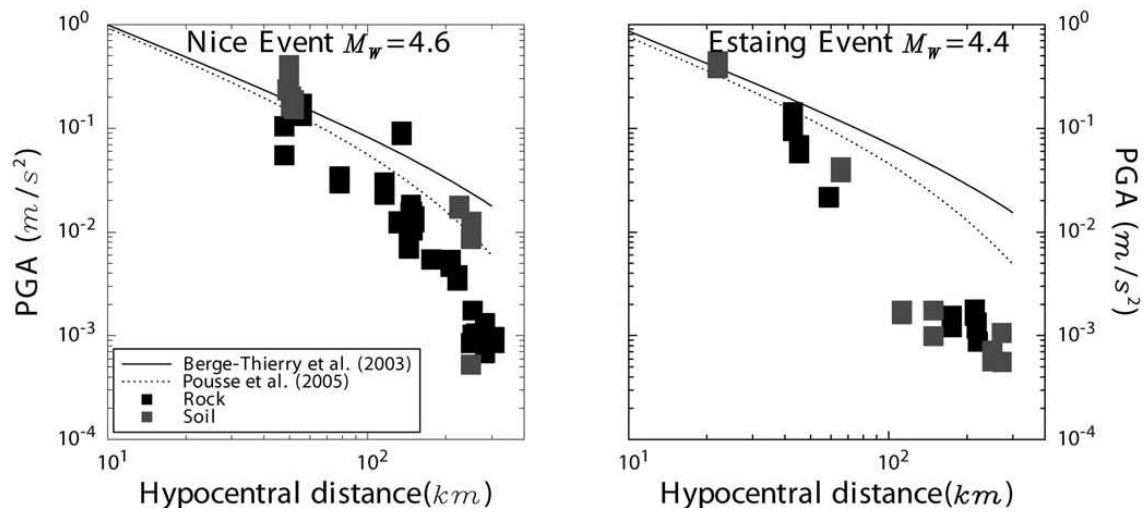


FIG. 19. Examples of different attenuation characteristics for small and moderate events from large earthquake (Cotton et al., 2008 [52]). The GMPEs shown in the figures represent the attenuation rate for moderate or large earthquakes for this size of events.

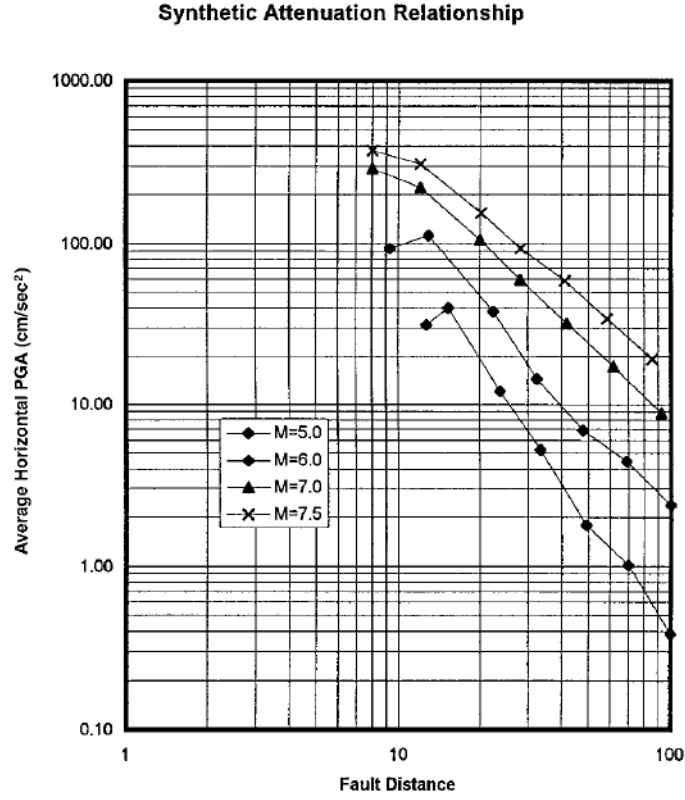


FIG. 20. PGAs as a function of the fault distance. Each ordinate is the average PGAs obtained from 50 realizations of the random parameters in the composite source model. Curves are for magnitudes 5.0, 6.0, 7.0, and 7.5 [56].

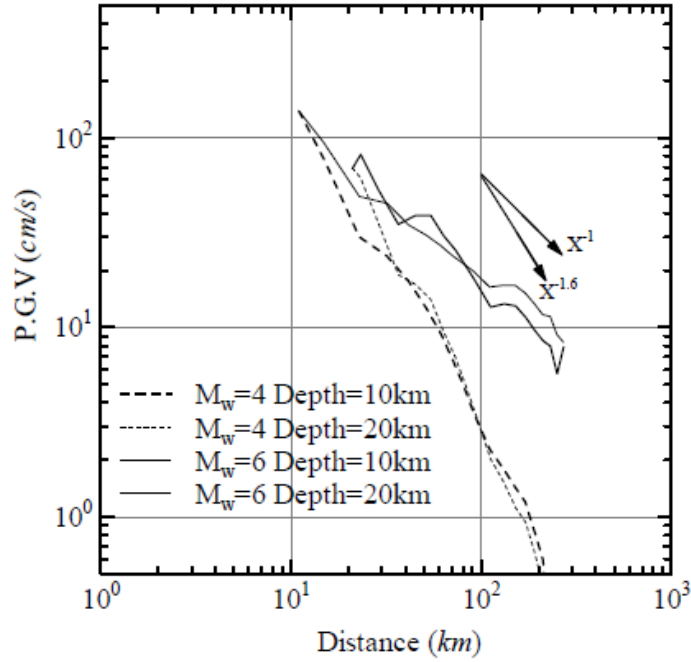


FIG. 21. Simulation results for different attenuation rates for small and moderate earthquakes. Curves are for magnitudes 4.0 and 6.0 with different focal depth [55].

2.1.1.3. Recording site conditions

In recent GMPEs the influence of local conditions are often included in a shear wave velocity term. Being aware that site response requires specific analyses (see Section 4), accounting for the average effect of local soil conditions is required for development of GMPEs. In fact, except perhaps for borehole data (e.g. [28]).

In general, site conditions are ground motion observations significantly affected by site response. In this situation, roughly accounting for site response by simultaneously inverting for propagation source and site effects is essential for reliable parameterization of propagation and source effects in GMPEs evaluated in terms of site categories that are determined by considering simple proxies. Some of these proxies are introduced below.

V_{S30} : V_{S30} is the travel time weighted average shear wave velocity in the top 30 m below the surface or any depth of interest (e.g. engineering bedrock), defined as Eq. (8).

$$V_{S30} = \frac{30}{\sum_{i=1}^N \frac{H_i}{V_i}} \quad (8)$$

Where, H_i and V_i are the thickness (m) and the shear wave velocity (m/s) of the i -th layer in the topmost 30 m of sediments.

For empirical evaluation of spectral amplification (AF), V_{S30} is widely used as an explanatory parameter (e.g. [57, 58]). As an example of the way it is used in a GMPE, Boore and Joyner (1997) [59] used the ratio of V_{S30} over V_{REF} .

$$\ln AF = b \ln (V_{S30}/V_{REF}) \quad (9)$$

In Eq. (9), V_{REF} is a parameter of the GMPE, not an explanatory variable.

V_{REF} is taken as 1100m/s for some NGA models [20] and 700 m/s in Japan [58].

Depth to bedrock: For longer predominant period components, e.g. for $T > 0.6$ s or 0.75 s, several studies use the depth to bedrock to represent the basin effect (e.g. [28, 60–63]). In the NGA models, the database provides two parameters to the modellers: $Z_{1.0}$, and $Z_{2.5}$. These represent the depths to rock with shear velocities of 1.0 and 2.5 km/s respectively.

Recently Si et al. (2013) [28] suggested a new parameter defined by the ratio of V_{S30} and the shear wave velocity of the reference basement V_{BASE} , which is corresponding to seismic bedrock. That is, $V_{S30}RT = V_{S30} / V_{BASE}$, for which, amplification factors are represented as a combination of function of $V_{S30}RT$, and H , the depth of sediments affecting relative long period ground motion.

Kappa: The spectral decay parameter kappa (κ) has been found to be useful in engineering studies to characterize the Fourier spectrum of ground motion, Ktenidou et al., 2014 [64] and Anderson and Hough (1984) [65] found that the high-frequency Fourier spectrum of acceleration at the surface for frequencies above 2 Hz during earthquakes with $M > 5$ behaves as

$$a(f) = A_0 e^{-\pi \kappa f} \quad (10)$$

shown in Fig. 22. In Eq. (10), A_0 gives the intercept of the line, but is only relevant to the spectral level for frequencies above the corner frequency. In addition, they found that κ depends on both the station and the distance from the source to the station. They suggested that the parameter κ for a site can be modelled as expressed in the Eq. 11.

$$\kappa = \kappa_0 + \tilde{\kappa}(r_{epi}) \quad (11)$$

where κ_0 is a station parameter, r_{epi} is the epicentral distance, and $\tilde{\kappa}(r_{epi})$ gives a distance dependence related to the entire path. To uniquely partition the observations, it is assumed that $\tilde{\kappa}(0) = 0$

The distance dependence $\tilde{\kappa}(r_{epi})$ has been treated as a linear function of r_{epi} , but in 1986 [66] and in 1991 [67] Anderson considered that it will generally be nonlinear. The distance dependence of κ indicates that κ is related to the attenuation of seismic waves in earth. More recent research has demonstrated that there is also a source contribution, κ_s , with zero mean (e.g. [68–70]) as described in the Eq. 12:

$$\kappa_r = \kappa_0 + \kappa_s + \tilde{\kappa}(r_{epi}) \quad (12)$$

The parameter κ has an important effect on strong earthquake ground motions, as it filters the high-frequency part of the spectrum and thus influences PGA. The units of κ are seconds. Typical values of κ at distances close to the source are in the range of ~ 0.01 s or less in regions of very hard rock to ~ 0.10 s in regions with very deep, soft sediments (e.g. [71]). In spite of its strong influence, it has not yet been incorporated into GMPEs, but when GMPEs are adjusted to a new region, correcting for regional differences in κ becomes an important consideration. Laurendeau et al. (2013) [72] have suggested an approach to incorporating κ into GMPEs.

Nonlinearity: Several GMPEs include an adjustment for nonlinear site amplification. The adjustments are often somewhat complicated functions depending of both soil profile and the predicted PGA at the site (e.g. [62, 73–77]). Because nonlinear effects are recommended to be treated outside of the GMPEs for nuclear facilities they are discussed extensively in Section 4.

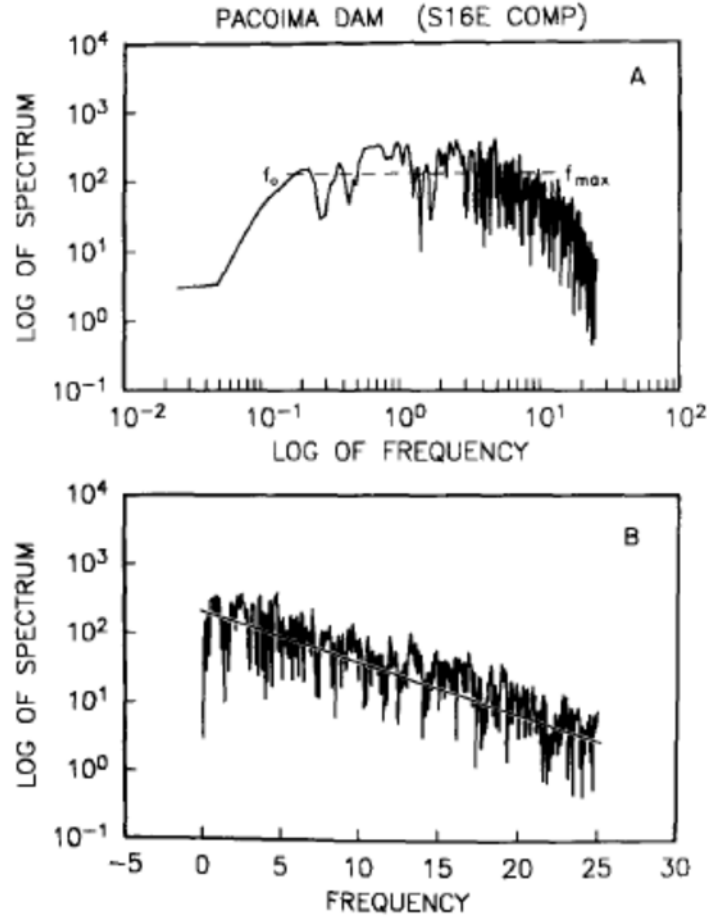


FIG. 22. Fourier amplitude spectrum of acceleration for the N16°E component of the Pacoima Dam accelerogram, San Fernando, California, earthquake of 9 February 1971. (A) Log-log axes. (B) Linear-log axes (Anderson and Hough, 1984 [65]). The linear approximation to the spectrum in part B has the form $e^{-\pi k f}$.

2.1.2. Functional forms for GMPEs

There is a wide variety of functional forms, resulting from the idea that the GMPE is a model for the ground motions. The philosophy of model building has varied considerably from one model developer to another. Therefore, while one can identify some common forms, a user needs to recognize that there are many other GMPEs that use variations or include additional terms which are not mentioned here.

Usually, the model for a GMPE, making the form in Eq. (2) more explicit, has been written in Eq. (13).

$$\log A = f(M, \text{etc.}) + g(X, \text{etc.}) + c + \delta \quad (13)$$

In this equation $f(M, \text{etc.})$ includes terms accounting for the seismic source, including the terms for magnitude (M), faulting style, focal depth (D), and tectonic regime, and $g(X, \text{etc.})$ represents the path term (including depth dependency and magnitude dependency).

(1) Source term $f(M, \text{etc.})$

For $f(M, \text{etc.})$, one often used functional form for the magnitude dependence is $aM+c$ a linear function for M . Terms of bM^2 or $b(M-M_c)^2$ have been introduced to allow for the magnitude saturation of ground motion (e.g. [20, 30, 43, 78–80]).

Figures 23 and 24 show the magnitude dependency from typical regression analysis results. Boore and Atkinson's (2008) [30] results show a saturation to magnitude at a relatively low hinge magnitude of about 7 for some periods. For lower magnitudes, their model shows a multiple linear or nonlinear scaling with magnitude. Si et al. (2013) [28] shows a hinge magnitude of about 7.5 for long period components and as shown in Fig. 25 about 8.3 for short period components. Si et al. (2013) [28] suggested a bilinear model for the scaling of magnitude for their data, while Boore and Atkinson (2008) [30] and others used a more complicated curve for the scaling of magnitude. On the other hand, Douglas and Jousset (2011) [81] present analysis showing that the magnitude scaling of GMPEs is nonlinear below $M<5$.

A comparison between the $M_w8.3$ Tokachi-oki and $M_w9.1$ Tohoku earthquakes in Japan was indicated in Fig. 25. Both occurred in the same tectonic region and no remarkable difference among the observations can be seen, although the difference of the earthquake size is remarkable. In these figures, GMPEs for corresponding M_w are also indicated and an overestimation for the $M_w9.1$ Tohoku earthquake can be seen. The saturation of amplitudes with increasing earthquake magnitude can be also recognized with this comparison.

The physical background for such scaling model can be partly explained based on the seismic source spectra (e.g. [80, 82]). Figure 26 shows the scaling with magnitude and the amplitude of the ground motion directly calculated from the Fourier amplitude source spectra, and shows that, at short or intermediate periods, the scaling tends to be a linear model; however, at long periods, it tends to be multilinear model, or bilinear model for earthquakes larger than about M_w6 . This result is roughly consistent with the results based on the analysis of observational data, as shown in Fig. 24. Differences from observations arise because Fig. 26 represents the spectral shape in the far field from a point source equivalent of the earthquake. Near the fault, the spectrum mainly represents the effects of slip on the nearest part of the fault, instead. Thus, the saturation of spectral amplitudes at large magnitudes tends to be more complex than the prediction of the model in Fig. 26.

To represent the source characteristics, the other parameters described in Section 2.1.1 are also used. Focal depth as a parameter in GMPEs appears generally as a linear function of H a log scale, e.g. dH , where H is the focal depth, and d is a parameter found by regression, generally showing positive values. In one study in Japan, for example, the d values are estimated to be slightly larger for PGA and for short period response spectral accelerations than for PGV or longer periods [9]. Tectonic environment appears as a categorical variable in GMPEs (e.g. [9]), where often researchers develop distinct models for different tectonic regimes (e.g. [27]). The modelling of the faulting style is often performed treating strike slip, reverse and normal faulting earthquakes as distinct categories. Some recent results find the ground motion from normal faulting earthquakes seems to be weaker than from reverse slip or strike slip events (e.g. NGA and NGA West 2 models). However, recent observations indicate uncertainties for the effects of the faulting style (e.g. [83]). This issue may need further investigation.

(2) Path Term

As described in Section 2.1.1.2, path effects depend on wave types, velocity and Q profile, focal depth and probably magnitude. In some models, the path term can be simply considered in the form shown in Eq. (14).

$$g(X) = b \log(X + C) - kX \quad (14)$$

In the equation, b is a regression coefficient showing attenuation by geometric spreading. In some models, b is forced to the values of -1 for body waves (e.g. [9]), and -0.5 for surface wave (e.g. [84]). Some GMPEs relate the regression coefficient b with magnitude (e.g., NGA models). As suggested by Midorikawa and Ohtake (2002) [49], this term shows the dependency on focal depth (see Section 2.1.1.2).

Numerically, the parameters b representing geometrical spreading and k representing attenuation will tend to be inversely correlated: a more rapid geometrical spreading can be compensated with a smaller loss due to Q .

C shows the saturation of near field ground motions, depending on magnitude. Campbell, 1981 [85] explains that, the parameter C modulates PGA attenuation at distances close to the fault where little geometrical attenuation is expected. The distance at which the transition from far field to near field attenuation occurs is probably proportional to the size of the fault rupture zone, especially the fault length for the larger shallow focus events. Since fault rupture dimensions scale exponentially with magnitude, it would be expected that C also scales exponentially with magnitude. Therefore, the following relationship is often used to model C as following Campbell, 1981 [85].

$$C = c_1 \exp(c_2 M) \quad (15)$$

Where, c_1 and c_2 are regression coefficients.

For this term, an alternative function form is a constant for crustal earthquake, without dependence on magnitude (e.g. [20, 86]).

Note that functional forms for the models may be dependent on the distance definition (e.g. [9]).

(3) Terms accounting for the recording site condition

In applications of GMPEs, the site effects are generally evaluated by the relationship between the soil parameters and amplification factor. These relationships are in general described in Section 2.1.1.3. Note that if the GMPE is defined on hard rock, the site condition term can be approximated as zero on average for reference rock conditions. In this case, the site effect can be evaluated based on either the site response analysis described in Section 4 of this publication, or be evaluated by the soil parameters and amplification factors.

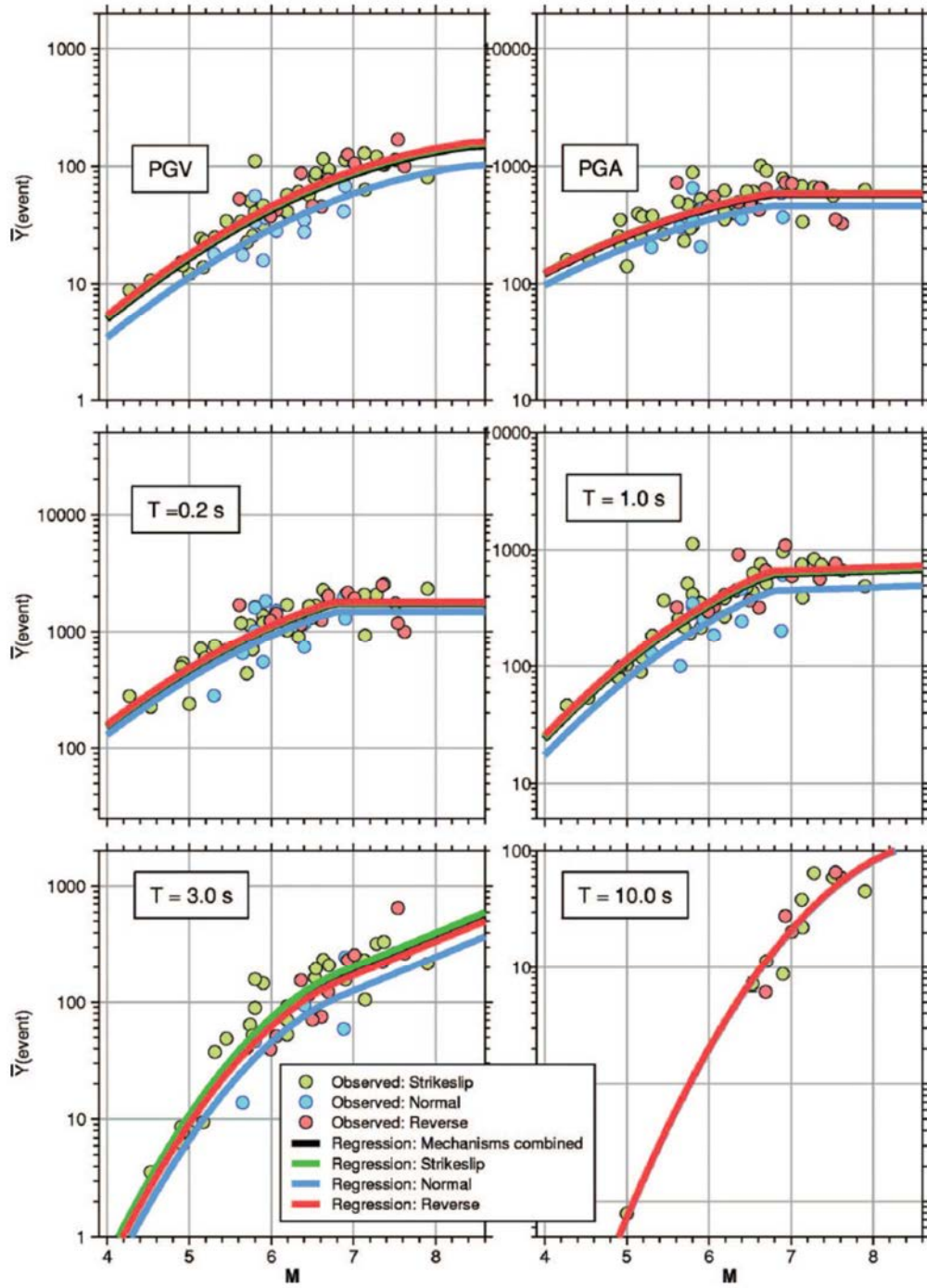


FIG. 23. Examples for magnitude saturation in GMPEs. Reproduced with the permission from Boore and Atkinson, 2008 [30].

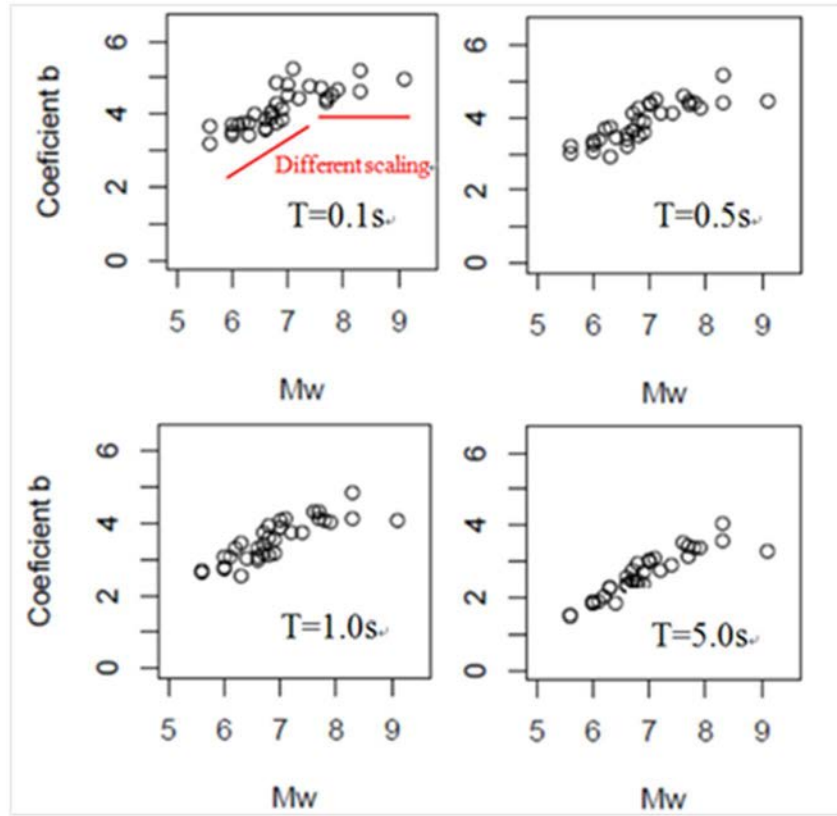


FIG. 24. Examples for bilinear magnitude saturation in GMPEs. Reproduced with permission from Si et al., 2013 [28].

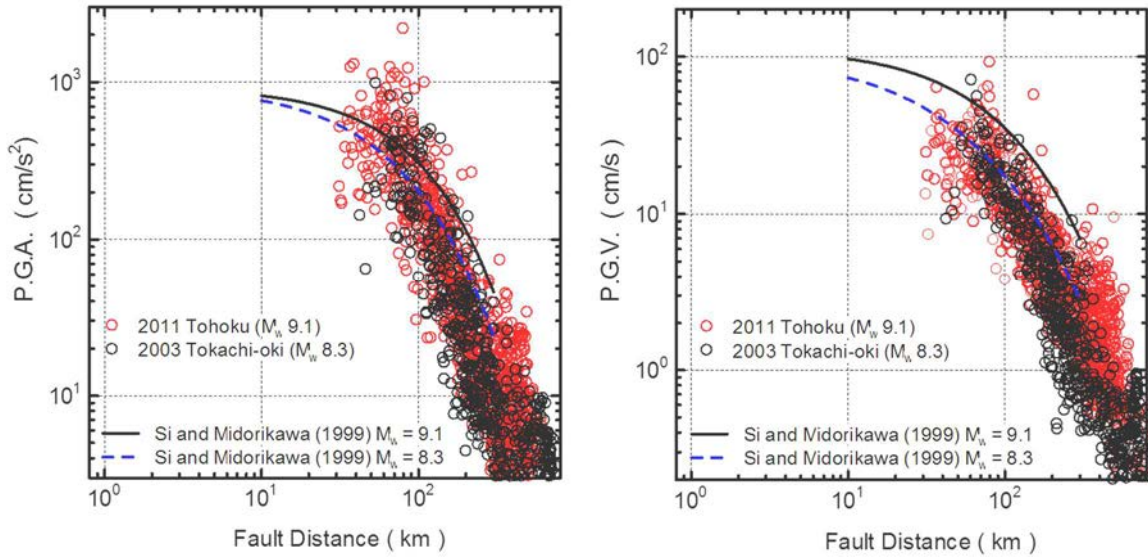


FIG. 25. Comparison of observed ground motion in the $M_w 8.3$ Tokachi-oki and $M_w 9.1$ Tohoku earthquakes. Reproduced with the permission from Si et al., 2011 [87].

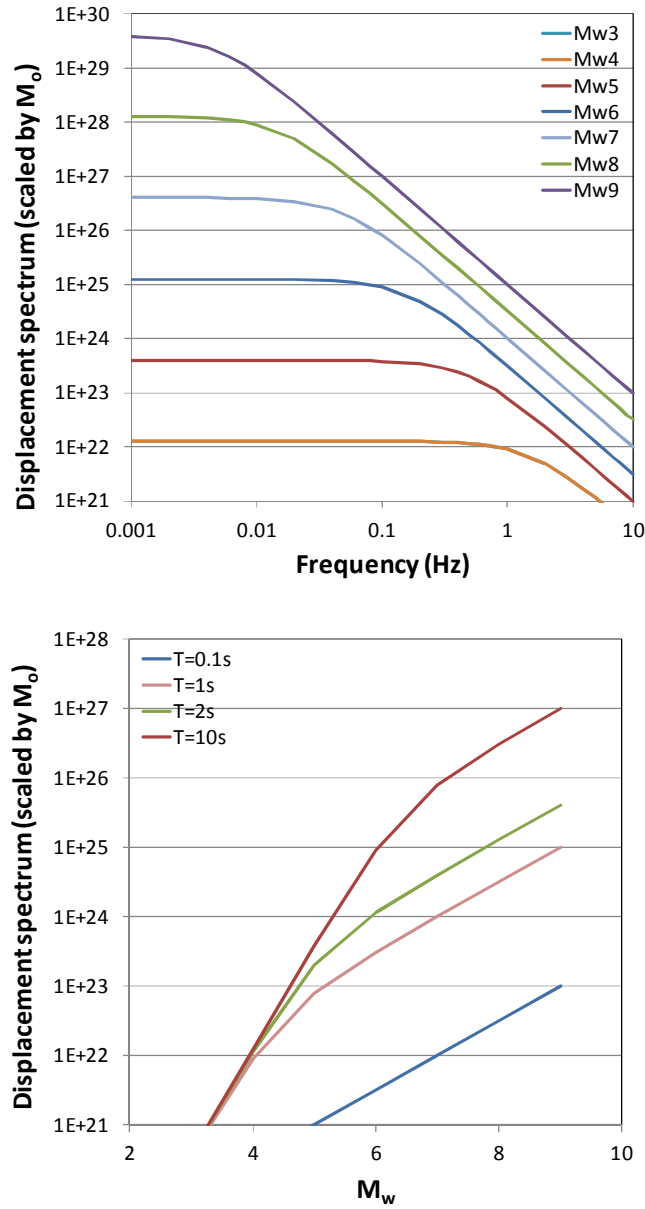


FIG. 26. Illustration of scaling law for source spectra. (upper: shape of the far field displacement spectra; lower: amplitude of the displacement spectra at different periods versus M_w). Reproduced with the permission from Si et al., 2013 [28].

2.1.3. Uncertainty in GMPEs

The introduction noted that a GMPE describes a probability distribution for the measure of the ground motion that it aims to predict. This property of GMPEs is essential to their value in estimating ground motions. While the previous section focused on the information that is needed to predict the mean value of the ground motion, this section focuses on the probability distribution.

Several studies have considered the shape of the probability distribution. The empirical evidence seems to be uniformly supportive of the hypothesis that the distribution is lognormal or stated in an equivalent way that the distribution of $\ln Y_i$ follows a normal or Gaussian, distribution (e.g. [88]). The standard deviation of this Gaussian distribution of $\ln Y_i$ is given the generic designation σ (sigma).

Equation 16 noted that for any particular measurement of ground motion from Eq. (1), Y_i , one can write

$$\ln Y_i = f(X_i, \theta) + \delta_i \quad (16)$$

Where $f(X_i, \theta)$ is the GMPE and δ_i is the difference between the prediction and the observation. The variability can be defined by the total uncertainty, σ_T as given in the Eq. 17.

$$\sigma_T = \sqrt{\frac{1}{N} \sum \delta_i^2} \quad (17)$$

where the total number of observations is N . In this equation, δ_i is the difference between the logarithms of the observation and the prediction given by the model, as defined by Eq. (16).

The total uncertainty, σ_T , can be divided into aleatory and epistemic contributions. Aleatory variability is conceptually associated with true randomness in a process, while epistemic uncertainty is uncertainty due to a lack of knowledge. To help explain these concepts, Table 1 identifies four parameters that are relevant for a GMPE. For any set of predictive parameters X_i relevant to the observation Y_i , the value of $f(X_i, \theta)$ is designated as μ in Table 1. Assuming the probability distribution to be lognormal, the standard deviation is designated as σ in the table.

In reality, the values of μ and σ are not known exactly. Typically, the users of these models will make the assumption that the true values will be close to the best estimate, and the range of possibilities is described by separate normal distributions of μ and σ . The widths of these probability distributions are designated in Table 1 as σ_μ and σ_σ respectively. It is not necessary for the distributions of possible ranges of μ and σ to be symmetrical. Given the long tails of lognormal distributions, positive tails on the distribution for μ can have a strong impact in increasing the hazard, so it is important to consider carefully what the data and models imply in developing the distributions for possible values of μ and σ . From this discussion, the epistemic uncertainty of μ and σ can potentially be reduced through gathering additional data, while the aleatory variability is a property not similarly reducible.

TABLE 1. PARAMETERS THAT DESCRIBE EPISTEMIC UNCERTAINTY AND RANDOM VARIABILITY IN SEISMIC HAZARD ASSESSMENT

	Central value	Random (aleatory) variability of central value
Best estimate	median (μ)	sigma (σ)
Epistemic uncertainty in true value of best estimate (standard error of best estimate)	σ_μ	σ_σ

Figure 27 contains an example to further elaborate on the concepts of aleatory and epistemic uncertainty. Fig. 27 (a) shows an example of four GMPE models compared to the peak accelerations observed in a single earthquake. On this figure, one can see two major features. The first is that the observations are generally quite high compared to the models. The second is that there is a considerable variability in the actual data.

In Fig. 27 (b), each observation has been adjusted in two ways. First, a site specific term, customized for that site, and intended to convert that observation to the PGA that would be observed on a site with $V_{S30}=760$ m/s, has been applied to each point. The consequence is that all the points in Fig. 27 (b) are clustered closer to a horizontal trend. This tighter clustering is evidence that as a result of this adjustment σ has been reduced. In this case, for distances less than 100 km, where the predictions are most critical, σ has apparently decreased from about 0.59 to 0.42. Second, not visible in this figure, a small additional event term adjustment has also been applied.

An equation to explain what happened between Figs 27 (a) and (b) expands the misfit term of Eq. (16) to include the site specific and event terms. δ_i in the equation can be deployed as following.

$$\ln Y_i = f(X_i, \theta) + S_i + E + \delta_i^{II} \quad (18)$$

Where S_i is the station term associated with each record, and E is the event term, and δ_i^{II} is the path term for this station. In a network of stations that have recorded multiple earthquakes, the unique value of the station terms S_i can be found for each station as it was in the case given by Kawase and Matsuo (2004) [89]. They found the station terms S_i by averaging δ_i over all of the records obtained from a single station. On the other hand, E is determined specifically for this earthquake.

The first difference between Figs 27 (a) and (b), then is that the station terms, which are conceptually measurable, have improved the GMPE given in Eq. (18) compared to the model given in Eq. (16). Since the station terms S_i are measurable (and had been measured before this earthquake occurred) they are epistemic uncertainties. The event term E was not knowable in advance, and may differ for future earthquakes in the region, so E is an aleatory variable. Its distribution could be determined by determining E for several earthquakes in the region, but knowing the values from several past earthquakes would probably not necessarily help to anticipate its value in future events.

The standard deviation associated with δ_i'' may be designated as, say, σ'' and is found by Eq. 17. The relationship between σ'' and σ_T is approximated in Eq. 19.

$$\sigma_T^2 = \sigma_s^2 + \tau^2 + (\sigma'')^2 \quad (19)$$

Where σ_s measures the uncertainty due to station to station variations of the site terms and τ represents the variance associated with the event terms. The uncertainty measured by σ_s is an epistemic uncertainty. The single station sigma σ_{ss} is given in Eq. 20.

$$\sigma_{ss}^2 = \tau^2 + (\sigma'')^2 \quad (20)$$

The single station sigma is presumed to represent more specifically the aleatory variability for predicting the ground motion at the site. High values of the variability tend to increase the hazard estimate at a site. Thus making measurements at a site of a nuclear installation to determine the site term is beneficial for a more accurate estimate of the ground motion hazard.

In summary, by understanding the various contributions to the total uncertainty, it becomes possible to obtain a more accurate estimate of the ground motion hazard. This discussion only describes some of the multiple contributions to the total uncertainty. Morikawa et al. (2008) [90] studied contributions to ground motion uncertainty determined from observed records. Al Atik et al (2010) [91] presented a model for more contributions to sigma. Studies to understand and reduce uncertainties are an important frontier in ground motion prediction.

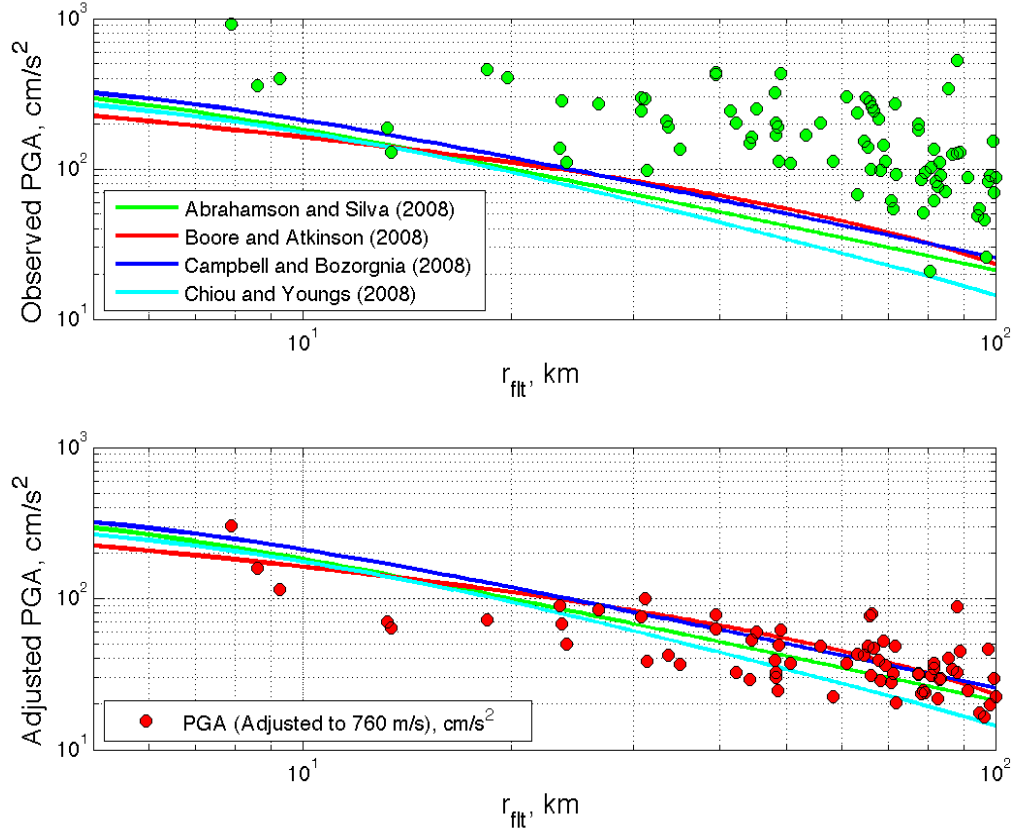


FIG. 27. Observed peak acceleration as a function of fault distance (r_{fit}) during the Fukushima Hamadori, Japan, earthquake of April 11, 2011 (M_w 6.7). Upper: raw peak observations, compared with four NGA-1 GMPEs. The parameters of the GMPE include a site term of $V_{S30}=400$ m/s, which is roughly the network average for K-NET and KiK-net. Lower: Peak acceleration after site specific adjustments derived from small earthquakes by Kawase and Matsuo (2004)[89] have been applied to correct each peak value to $V_{S30}=760$ m/s. The GMPEs also use a site term of $V_{S30}=760$ m/s. (Anderson et al., 2013 [83]).

2.1.3.1. Aleatory variability

Considering the example discussed in conjunction with Fig. 27, some contributions to aleatory variability, i.e. uncertainty that is due to true randomness in earthquake processes, can be identified. This discussion is not intended to be complete, but rather to identify some obvious uncertainties of this type. The greatest one is associated with the source. Consider only the set of sources with the same moment magnitude M_w . The individual sources have a certain finite size, but the same moment can be achieved with a smaller fault area and higher slip or a larger fault area with smaller slip (these differences are characterized with a parameter called the static stress drop, see earlier section). The roughness of one fault may vary from the roughness of another. The slip can be distributed in different ways over the fault surface, and the location of the epicentre on that fault can also vary, resulting in uncertain amounts of directivity in repeated earthquakes on the same fault. The speed at which the rupture crosses the fault, called the rupture velocity, can be variable. Finally the time required for the fault to slip at each point can vary. At present, seismologists do not believe that they can predict any of these variables for a specific fault, so they are regarded as true randomness that cannot be reduced by taking additional measurements.

Aleatory variability also appears in the earthquake source process. A prominent case is the locations of earthquakes in a zone of diffuse seismicity. Similarly, consider a fault segment that has a Gutenberg-Richter distribution of events with small magnitudes, and large earthquakes that rupture the entire fault segment. With this distribution, small earthquakes are modelled as having random locations on the fault surface as another form of aleatory variability.

In a region with extremely dense observations (as well as high seismicity) as in Japan,, several records can be observed from one specific source at several specific observation stations, such as in the case of records from a main shock and from some foreshocks and aftershocks. In this case, the variability of the observed records due to the site effect can be eliminated, since the site effect is unique at the particular observation station. In addition, the path effect can also be avoided, since the seismic wave rays propagate by a unique path from the source to the observation station. The variability among the source mechanisms can also be neglected, since the mechanism of the events is unique between the foreshocks, main shocks and aftershocks. The biggest influence is the difference in size between the foreshocks, main shock and aftershocks. However, the individual sizes can be interpolated to a certain size of earthquake by using a GMPE in the region, the variability of this difference in size can also be normalized. With regard to this condition, Morikawa et al. (2008) [90] demonstrated that

“The minimum uncertainty determined is about 0.15, which corresponds to $10^{0.15} \approx 1.41 \approx \sqrt{2}$ on the linear scale. This value corresponds to the random summation of incoherent high-frequency phases, which is the root mean square between two conjugate eigenvectors.”

Thus, the mathematical lower bound of the aleatory variability might be about 0.15 in the base ten logarithm.

2.1.3.2. *Epistemic uncertainty*

The contributions of the epistemic uncertainties can be also identified. This discussion is not intended to be complete. Variations exist in the regional velocity model and attenuation model over the entire region between the sources of each station. The station term may be approximated as a single constant as used in Eq. (18), but in reality probably depends on the direction from the station to the earthquake, the depth of the earthquake, the frequency content radiated by the source, and the amplitude of the incoming motion, since the site may respond in a nonlinear manner to large amplitude motions. All of these factors can conceptually be measured, but they are rarely known, so they would be examples of uncertainties due to lack of knowledge, the definition of epistemic uncertainty.

Equation 20 is often used in the discussion of uncertainty, but it is flawed in that it mixes aleatory and epistemic uncertainty together. The assumption behind Eq. (19) is that the aleatory and epistemic distributions are both lognormal, with standard deviations given by σ'' and σ_s , respectively. However a lognormal distribution has extremely long tails and the site response cannot really follow such a distribution in which the site amplifications are essentially unbounded. The physics of wave propagation puts bounds on the site terms S_i . Similarly the physics of the strength of the rock materials puts bounds on the residuals related to the earthquake source, associated with δ_i'' . The bulk of distribution can be represented approximately with a lognormal distribution with the variance of Eq. (19), but long tails are probably unrealistic.

The value of the aleatory variability, after as many epistemic uncertainties as possible have been removed, is one measure by which the quality of a GMPE can be evaluated. A good estimate of the aleatory variability is essential input for a good estimate of the seismic hazard when a GMPE is applied to the site of a nuclear installation. However, as discussed in Section 2.3, there are many other criteria for screening of GMPEs, and many reasons why GMPEs with high values of aleatory variability may be unacceptable for use in nuclear installations.

2.1.4. Database and limitation of GMPE

In the best case, in order to develop a GMPE, one compiles a database of strong motion records that includes source, path, and site information. For example, the PEER NGA West 2 Flatfile (<http://peer.berkeley.edu/nga/>) described by Ancheta et al. (2013) [92] compiles the necessary information for strong motion records obtained from earthquakes worldwide in active continental crustal regions. The publication by Ancheta et al. (2013) [92] is a resource for a detailed description of the steps required to compile a complete database for GMPE development. This section briefly summarizes the desired information.

When this desired database is not available, then there are other strategies that can be pursued (see Section 2.2).

2.1.4.1. Source information

The seismic source information used in the development of GMPE includes information on magnitude, source model and related parameters, location and environment of the seismic source.

For magnitude, generally the local magnitude M_L , surface wave magnitude M_S , Japan Meteorological Agency magnitude M_{JMA} , etc. are estimated from the amplitude of the observed seismograms, hence they have no direct physical meaning. On the other hand, the moment magnitude M_W is defined from the seismic moment of a physical parameter, but used to be available only from very large earthquakes, since fault dimensions, rigidity and slip dislocation are required to estimate the seismic moment. Now these are systematically determined by seismic source inversion through fitting simulated and observed wave forms.

Some often used sources of earthquake information including earthquake magnitude are listed in the Appendix. For these data sources, the information includes not only the seismic moment but also the strike, dip, rake angles, and location of the earthquakes. The mechanisms are useful to segregate strike slip, reverse and normal source mechanisms. The source mechanism is also useful to define the types of crustal, slab and interplate events. In general, crustal events have strike or reverse oblique features in compressional regions, whereas normal events in the tensional regions and slab events seem to be normal, too, due to down dip extension of the slab, and interplate events have reverse mechanism at the dipping plate boundary.

In the development of GMPEs, information on finite source models is also needed for earthquakes which cannot be approximated as a point source. The source models are generally derived from source inversion based on the seismic wave, tsunami, geodesy, and intensity data. These data can be taken from specific research studies. Some of the source models are compiled on the websites and shown in the Appendix

2.1.4.2. *Site information*

Since ground motion recording stations supply basic information for the parameterization of GMPEs, complete seismic characterization of these sites is of major concern. In particular, separating long range propagation and source effects from the effects of local geomorphological conditions (see Section 4) requires a clear identification of these latter ones before the relevant accelerometric data are used in statistical analyses to derive GMPEs. In many cases this aspect is overlooked and can significantly contribute to the large dispersion associated with the resulting GMPEs. Another aspect contributing to the aleatory variability of GMPEs is the eventual location of ground motion recording stations inside buildings or large human made structures (e.g. dams): except in the case that dynamic influence of the building is expected to be small (e.g. ground floor or basement) or accounted for by using suitable deconvolution procedures to eliminate the contribution of building response, these sites need to be avoided due to the possible distortions induced by the building dynamics and a free field configuration is preferred. In any case, these sites need to be clearly indicated in the database and their impact considered when GMPEs are parameterized.

A complete characterization of site conditions requires a number of elements:

- (1) Geological characterization at the local scale (1:2000–1:5000) including lithological characterization of the main geological bodies and relevant discontinuities (faults, geological unconformities, etc.) around the station;
- (2) Geomorphological characterization including local morphology, eventual ground instabilities (landslides active or silent);
- (3) Geophysical (local V_s profile to any depth, major impedance contrasts in the surroundings of the site and resonance frequency) and geotechnical (in situ tests, laboratory) characterization.

In principle, all these features need to be documented but rarely is this the case, except for Japanese observation networks in the extremely high seismicity area. As an example, just a relatively small subset (of the order of tens) out of more than 400 ground motion recording stations included in the Italian accelerometric network [93] have been characterized in such a complete way.

More commonly, a rough characterization is provided in terms of soil and topographic classes (e.g. Lithostratigraphic classification estimated and based on in situ measurements, topography classification). Examples of this classification are provided in CEN (2004) [94] and NEHRP [95], which are given in the Appendix. To be applied, these classifications require specific surveys and field measurements (see e.g. procedures adopted to characterize sites included in the Turkish accelerometric network [96]). However, in many cases, the above classification is provided very roughly on the basis of large scale geological maps (1:100000 or more). The lack of an effective geological/geophysical/geotechnical characterization of ground motion observation stations is one of the most important sources of both epistemic uncertainty and aleatory variability affecting GMPEs.

2.1.4.3. *Time histories*

The starting point for the development of GMPEs is strong motion accelerograms. In the Appendix web sites are listed that are sources for records from some of the currently active

networks. This appendix is not complete, because the sources change often, so one always needs to carry out a new search and consult with experts on the region.

This section discusses some practical aspects of handling strong motion accelerograms. These accelerograms are also often called times series (or time histories) in the scientific literature. Such a typical accelerogram, recorded on a strong motion accelerograph, gives the acceleration of the ground as a function of time for three orthogonal components of ground motion: two horizontal components and the vertical component. Early instruments, mostly manufactured before 1980, recorded on film or some other analogue medium. Newer instruments record on digital media, ranging from digital cassette tapes to memory cards, or solid-state memories. Newer data are often sampled to indicate the acceleration at equally spaced points in time at a rate of 100 or 200 samples per second. In order to be useful, analog data needs to be digitized to obtain equally spaced time series. In many cases the digitization is not able to recover a time resolution finer than 50 samples per second. The digitization process introduces noise into the amplitudes of the ground motions. This is also true of newer digital recording instruments, but for these instruments the noise is generally smaller. The digital accelerograms at this point are referred to as raw accelerograms. They are called Volume I accelerograms, digitized in an extensive set of records in the late 1970s as “the Caltech Bluebooks”, e.g. [97]. The following are typical processing steps that are applied to the raw accelerograms:

- (1) Baseline correction. In brief, this is required because an accelerograph is sensitive to a static tilt of the ground. Because of this, the condition of zero acceleration is generally represented numerically by non-zero values on modern digital accelerometers. For older analogue instruments, the accelerogram is a trace on a film or paper, and the analyst needs to decide where zero acceleration goes through the trace. The analyst also needs to be aware that the zero level of acceleration may change during an earthquake. Very small errors in the baseline will cause unreasonable results when the accelerogram is integrated to find velocity or displacement of the ground, or convolved with an instrument response to find response spectral amplitudes at longer periods;
- (2) Instrument correction may be needed, depending on the characteristics of the sensors, to convert the recorded time series to acceleration;
- (3) Filtering may be needed to remove long period noise. This is sometimes not essential for digital records obtained on high-quality instrument, but is practically always needed for analog records;
- (4) Integration and calculation of response spectral amplitudes;
- (5) Deciding how to convert the vector that represents the two horizontal components of acceleration into a scalar.

Characteristics of the processing method and parameters need to be preserved in the ground motion database. The most essential record processing parameters to include in the database are the filter parameters and information about the frequency range over which the data may be considered to be reliable. This information provides limits on the frequency range over which the response spectra are reliable. Parameters that are not reliable, obviously, cannot be used for the determination of regression coefficients in GMPEs. Boore and Bommer in 2005 [98] provide a recent review of record processing procedures.

2.1.4.4. *Limitation of GMPEs*

This section addresses two types of limitations to GMPEs. The first is limitations due to the data that is available for their development. The second is limitations due to the assumptions about Earth models.

The first limitation is the constraint, or lack of constraint, available from the data. Once a database has been compiled, it is used to determine the values of the coefficients, θ in Eq. (1), that cause the functional form of the model to best match the data. The resulting model will generally achieve the best possible fit to the data in the range of magnitudes, distances, and other conditions where the data are abundant.

GMPEs not only are intended to fit the data where they are abundant, the GMPEs are also used to extrapolate to magnitudes and distances where data are sparse. To illustrate the significance of this point, Fig. 28 shows the distribution of data as a function of M and R from the NGA West 2 database. It is apparent that for $r < 5$ km, or for $M > 7.0$, the data are sparse compared with the data obtained at larger distances and smaller magnitudes. There are a few points in these ranges, but it is unreliable to base important conclusions on data from only one or two earthquakes. Within the ranges where data are sparse, the GMPEs are dependent on the selected functional form (Section 2.1.2) and thus the functional form can have a strong impact on ground motion estimates.

Plots similar to Fig. 28 need to be provided for all GMPEs, thus enabling the potential user to evaluate the completeness of the database for the range where it is to be applied.

Since a GMPE is generally constrained by the earthquake data used in the development, users need to pay attention to the span of the following parameters in the database:

- (1) Magnitude;
- (2) Distance;
- (3) Focal depth;
- (4) Recording site condition;
- (5) Tectonic environment; and
- (6) Regional dependency.

Application of the GMPE outside the span of the data represents extrapolation based on the parametric form of the equation, and requires great caution. The second limitation of GMPEs involves the effects of deviation of the Earth from a flat-layered configuration. This will be discussed in the next section, Section 2.2.

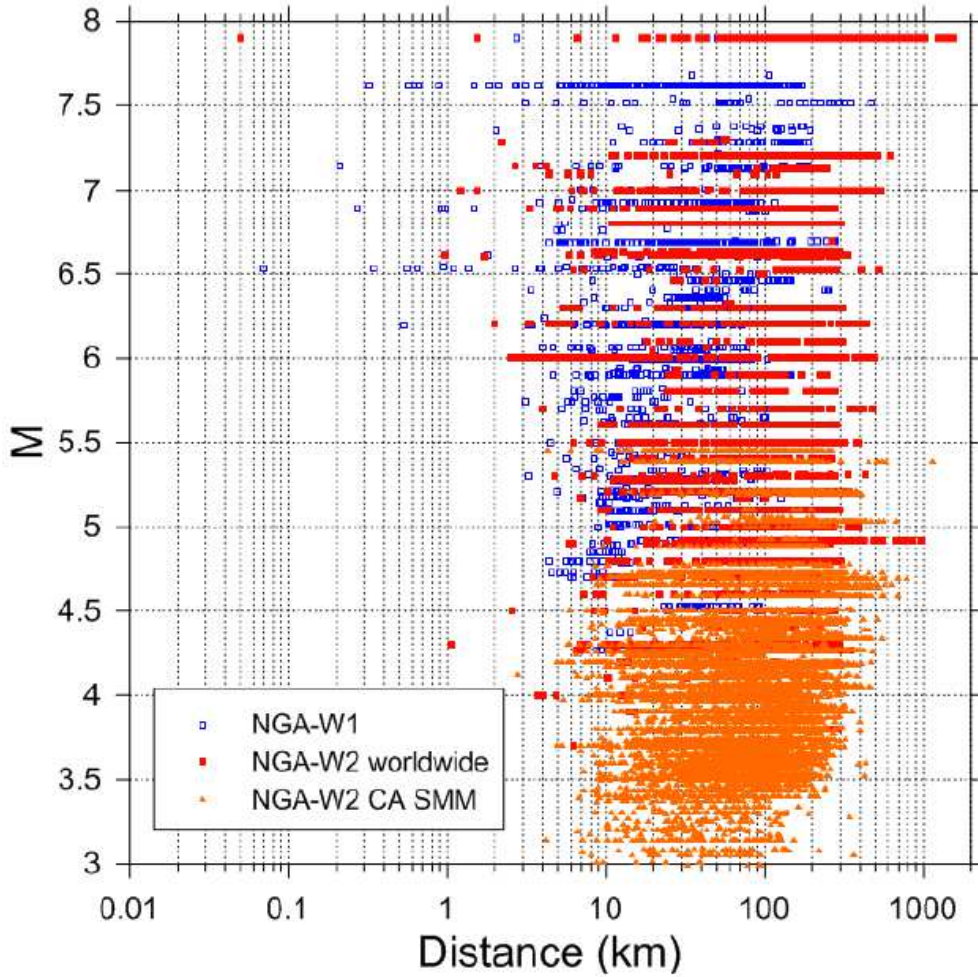


FIG. 28. Magnitude-distance distribution of strong motion records in the NGA-West2 database (magnitudes 3 to 7.9). Open blue squares are stations included in the NGA-West1. Solid red squares are stations added from worldwide events. Orange triangles are stations added from California only from small-to-moderate magnitude events (magnitudes 3 to 5.5). Reproduced with the permission from Ancheta et al., 2013 [92].

2.2. GROUND MOTION SIMULATIONS

Section 2.1.4.4 demonstrates that in some distance and magnitude ranges the data is sparse, even in one of the most densely populated data sets for GMPE development. Furthermore, there are many regions where there are few or no available records of strong ground shaking. It is increasingly common for simulations to be utilized to estimate the motion under these circumstances. The arguments for using simulations would be grounded in the belief that enough is known of the physics controlling strong ground motion that a simulation is subject to fewer uncertainties than the uncertainty in the parametric forms of equations used in GMPEs. Most of the physical factors controlling the ground motion have been studied individually, so models that are believed to be reliable are available. It needs to be noted that Fig. 28 of Section 2.1.4.4 can be misleading in estimates of data density, since it does not show for instance the site conditions (and weakly correlated value of κ), whether a near fault station is on a hanging wall, or whether it is subject to forward or backward directivity. As discussed, these are effects that have a strong impact on ground motions and their variability seriously dilutes the completeness of the database at short distances and large magnitudes.

Safety Report Series No. 85. [99] goes into details on simulations. However, it is worth mentioning some of the major approaches including their strengths and weaknesses.

Stochastic methods approximate the physics in the frequency domain. They start with a random time series, shape it in time to match envelopes of typical earthquake time series, then shape the spectrum of the frequency domain based on physical processes, before transforming back to the time domain with a reasonable synthetic seismogram. Examples of stochastic methods are given in Refs. [100–102]. These methods are relatively simple to construct and calibrate using small earthquakes in the target region. In this regard, they have been applied in several instances to help construct GMPEs (e.g. [103]).

Empirical Green's functions are small earthquakes that are used to describe the wave propagation from a source to a station. The strength is that they solve the wave propagation precisely. Weaknesses often include low signal-to-noise ratios at long periods and a frequent lack of small earthquakes on the faults that are capable of generating large events. Examples of this method include Irikura (1986) [104] and Irikura and Kamae (1994) [105]. To apply this approach, it is also necessary to create a reasonable source model in the time domain.

Since empirical sufficient Green's functions are not sufficiently available, these are frequently substituted with synthetic Green's functions. They can be computed using reasonable velocity models for the source station pairs where they are needed. The convenience of this approach makes it popular. Examples of this method include Irikura and Miyake (2011) [106].

Synthetic Green's functions cannot possibly be correct at high frequencies in a wiggle-for-wiggle sense. However, at lower frequencies the velocity model is generally known well enough to compute reasonably accurate synthetics. These can be merged with the stochastic approach at high frequencies. Examples of this method include Graves and Pitarka (2010) [107].

The procedure for using one of these synthetic approaches is straight forward in concept. The first one generates synthetics for source station pairs, where data is available, and uses those data to calibrate the model. Then the other one uses the simulation model to generate synthetic seismograms for source station geometries that are less constrained.

To illustrate synthetic ground motions, an example of the hybrid method of Graves and Pitarka (2010) [107] is useful. Most GMPEs are based on a 1-D assumption, meaning that the properties depend on depth, but not on location. This is not explicitly stated in the equations but this follows from equations in which the distance dependence is only a function of the distance itself, e.g. r_{fl} . This approximation is quite useful in Earth sciences, where a flat-layered (or radially layered) configuration is excellent for a first-order model. On a global scale, the Earth is well described as having a core, mantle and crust, for example. On regional scales, refraction studies resolve crustal thickness and layers in the crust that are very helpful to explain the travel times of the main phases seen on seismograms. Thus dependence of GMPEs only on r_{fl} is well motivated in the seismological literature.

The example shown in Fig. 29 shows the velocity field simulated by Graves et al (2011) [108] for a rupture on the San Andreas Fault east of Los Angeles, California. For this simulation, the flat-layered approximation has been replaced by a more realistic 3-D velocity model including high velocity mountains, low velocity basins and sharp boundaries between rock and basin at known major faults. The highest frequencies involved in this calculation are about 0.3 Hz. Figure 29 shows that early in the event the largest ground motions are propagating ahead of the rupture, as expected considering forward directivity. However, in the

images taken at 90 and 120 seconds the wave field has split, with a second region of equally severe shaking being guided by the alluvial basin that angles away from the fault. This is a low frequency effect of geological basins that can be understood and modelled using 3-D finite element codes (or equivalent), and geology that is reasonably well characterized with a resolution of ~ 100 meters.

Considering Fig. 29, it is evident that 3-D geology will introduce strong lateral variation in ground motions. Since current GMPEs generally do not include this information, the lateral variability will show up as an increased overall variability. The variability would be represented by lateral variations of δ_i'' . This shows that δ_i'' is partially caused by epistemic uncertainty, since this path effect is potentially knowable. Another important point in Fig. 29 is that the interface between the GMPE and the site response calculations is not as simple as it may seem from a casual consideration of Fig. 2. A site in a waveguide like the one in Fig. 29 is predicted to experience ground motions that have larger amplitudes and longer durations than will be generated by any 1-D velocity model.

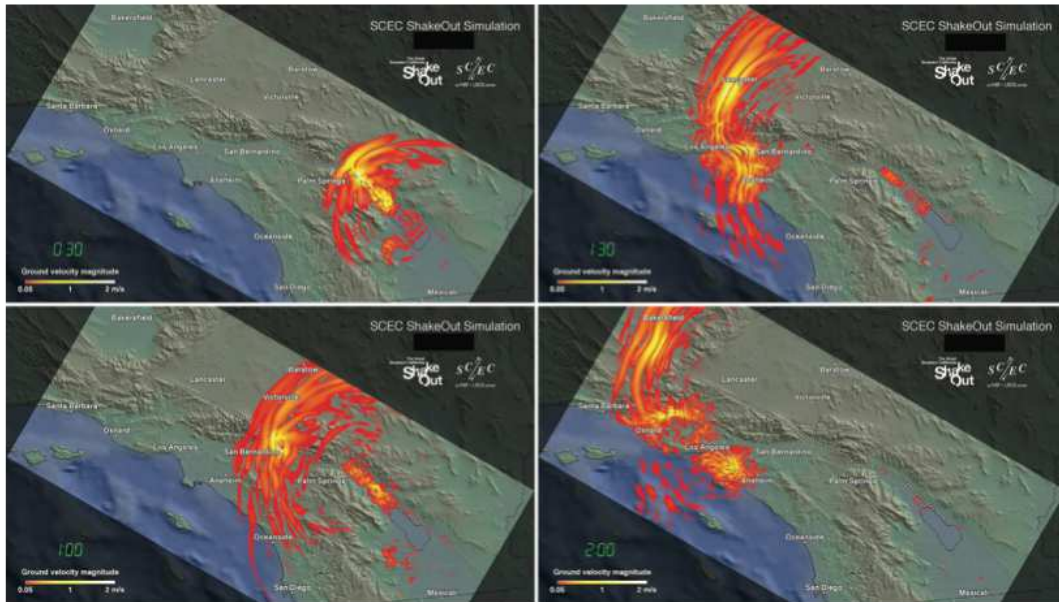


FIG. 29 Snapshots of the vector magnitude of the simulated ground velocity wave field at times of 30s (upper left), 60 s (lower left), 90 s (upper right) and 120 s (lower right) after the initiation of rupture. Reproduced with the permission from Graves et al., 2011 [108].

2.3. SELECTION OF GMPEs

2.3.1. Introduction

A great contribution to the overall uncertainties of a seismic hazard assessment is due to the uncertainty in GMPEs. Therefore, the selection of appropriate GMPEs and their treatment in a logic tree in order to consider epistemic uncertainties is an important task (e.g. [109]). A large number of GMPEs have been proposed by Douglas (2015) [110]. Differences between two GMPEs can be considerable, especially at short distances. Reasons for this can be, for instance, different path and site characterizations, varying parameter ranges of the regression

data set or different functional forms of the equation. In areas where regional GMPEs are available, these GMPEs are preferably included in the candidates of GMPEs. However, in many regions none or only a few regional GMPEs exist due to the lack of strong motion data and GMPEs from other areas need to be adopted and/or stochastic GMPEs need to be developed.

2.3.2. Priorities of criterion for the selection

The criteria on which basis GMPEs may be selected is a matter of discussion and partially depend on the target region and the available data. While some criteria are self-evident, like the GMPEs need to fit the required magnitude and distance range, the benefits of other criteria are debated. One needs to differentiate between active tectonic regions with available strong motion registrations, and regions with only rare strong motion data like stable tectonic regions. If possible, the selection of GMPEs needs to be strongly based on the comparison of strong motion observations, and preferably regional GMPEs need to be used. However, if a regional GMPE is poorly supported by data, it has to be decided whether GMPEs from other regions (eventually adjusted to the target region, see 2.4.6) might be preferred or given higher weights than the regional GMPE. Some example selection criteria for GMPEs are the following:

- Testing of candidate GMPEs against strong motion data: if sufficient strong motion data are available the GMPEs need to be compared with observations;
- Adequate ground conditions: GMPEs are valid for a certain shear wave velocity (V_{S30}) or shear wave velocity range. The mean V_{S30} of the GMPE need to fit to the ground conditions at the engineering bedrock. It is noted, that if the V_{S30} of the GMPE is much lower than the one at the engineering bedrock (e.g. 760 m/s and 1500 m/s) this can lead to an overestimation of the ground motion;
- Sufficient database: The database of the GMPE needs to contain sufficient records to constrain the dependence on magnitude and distance within the range of interest;
- Magnitude, distance and frequency range: The GMPE needs to cover the required range of magnitude and distance as well as the frequency range of interest. It is noted, that if the minimum magnitude of the GMPE dataset is higher than or around the minimum magnitude integration limit of the Probabilistic Seismic Hazard Analysis (PSHA), most likely the seismic hazard will be estimated incorrectly;
- Functional form: The equation needs to include a physically reasonable functional form for factors described in 2.1.1–2.1.2. However, since the functional form of GMPE is still debated, the testing of candidate GMPEs against strong motion data has a higher priority in the selection of GMPE.

For regions where well developed and constrained GMPEs are lacking, the above mentioned selection criteria may be applied less stringently in practice. For instance, if a regional GMPE exists that meets most but not all of the above listed criteria it might be decided to consider that GMPE. Or a GMPE that fits well to observations might be considered, even if for example the minimum magnitude is around or slightly above the minimum integration limit. In these cases the development of a logic tree considering several GMPEs to cover the epistemic uncertainties is particularly important. Using a logic tree, parameter consistency is important. This means, that all GMPE parameters like magnitude, distance or outcome

variables are consistent and refer to the same parameter definition. If not, a parameter conversion needs to be applied, which increases the uncertainty.

Further discussion and proposals on selection criteria and approaches can be found in the following references [111–114]. The development of regional GMPEs (empirically or based on stochastic simulations) may also be considered. Information about the adjustment of GMPEs is given in subsection 2.4.

2.3.3. On the methods of ranking GMPEs based on observation data

In the current practice of the selection of GMPE (e.g. [111, 114, 115]), the technique of ranking GMPEs based on the comparison of GMPEs and the observations is a key step for the selection of a GMPE. So far, several methods of ranking GMPEs have been proposed (e.g. [113, 116, 117]). Besides these methods, the evaluation method of goodness of fit simply based on the residual analysis of data and GMPE is also an option. Since there are differences in results derived by those ranking methods (e.g. [113, 117]), the uncertainty due to the ranking methods is also to be considered in the selection of GMPEs. Based on the discussion above, the following issues are suggested in the procedure of ranking GMPEs based on the observations. In the case when the local observation data are available, pre-selected GMPE can be directly compared with these data. In the case where there are not enough local data available, the comparison of GMPE with data can also be carried out by using data derived from regions with similar tectonic environments to the target region.

- Before comparing pre-selected GMPEs with data (as far as possible) in order to define weights for a logic tree, a procedure of adjusting the GMPEs (if needed) needs to be applied (c.f. Section 2.4). That is, the parameters needed for target GMPE needs to be provided or approximated by the dataset of observations;
- A procedure of comparison amongst different ranking methods is suggested if there is insufficient knowledge on the differences between the methods;
- Then, based on the results of the comparison of ranking methods, the selection of ranking method or a weighting system when using multi ranking methods can be considered;
- Newly proposed methods for ranking GMPEs need to be considered when revising the hazard evaluation.

2.4. ADJUSTMENT OF GMPES

2.4.1. Introduction

In classical seismic hazard assessment GMPEs contain significant uncertainties. In this context the selection and adjustment of GMPEs is an important task. After the appropriate GMPEs are selected, some adjustments for the application might be considered. The following subsections discuss the extrapolation to small magnitudes, the interpolation of available frequencies, style of faulting adjustment and path adjustment. A site adjustment is not discussed, because for nuclear facilities it is recommended to assess local site response by performing a site response analysis, which is discussed in Section 4.

2.4.2. Magnitude scale

Most recent GMPEs use the moment magnitude (M_W) in the equation. Different magnitude scales are introduced in Section 2.1.1.1 and the differences among them are illustrated. In order to be consistent, the earthquake statistics and the used GMPEs need to refer to a common magnitude scale (typically M_W). In case a magnitude conversion has to be considered for a GMPE, various formulas are available in the literature (e.g. [118–120]). If local magnitude (M_L) is used the selection of an appropriate conversion formula is very important and needs to be chosen carefully, because M_L is often dependent on the institution and therefore regionally dependent.

The scaling also depends on source mechanisms, since the source spectrum shape bends around the corner frequency, which varies with the source size. Relationships between the seismic moment and the local magnitudes that are relevant to the corner frequency were discussed in Ref [82]. The seismic moment can be converted to M_W by using the definition given in Ref [14]. The relationships are converted to that between M_W and the local magnitudes as shown in Fig. 30. The increase of the local magnitudes saturates with M_W similarity to the saturation shown in Fig. 3.

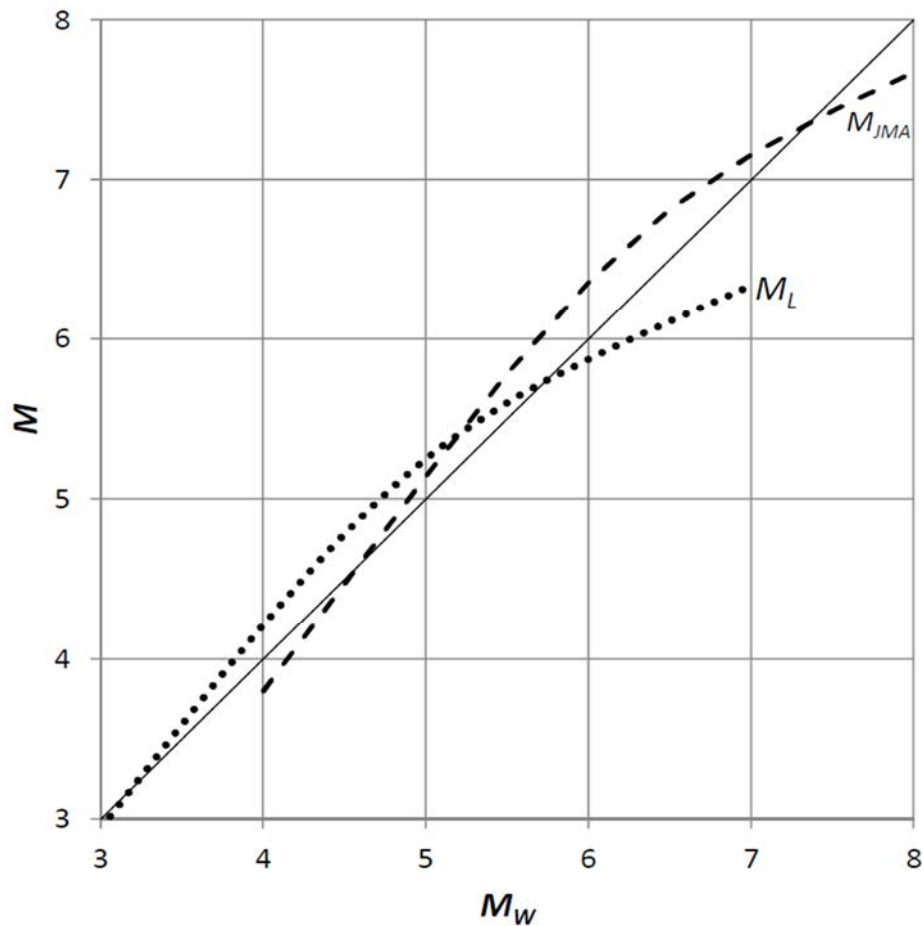


FIG. 30. Relation between the moment magnitude and other local magnitudes depending on the corner frequency. Broken and dotted lines are for M_{JMA} and M_L , respectively.

2.4.3. Extrapolation of GMPEs to small magnitudes

The median ground motions from small magnitude earthquakes in low to moderate seismicity regions are usually lower than would be predicted by extrapolating a global GMPE to small magnitudes. The extrapolated GMPE can overestimate the observed ground motions (e.g. [53, 121]). Even for magnitudes close to the minimum magnitude in the dataset of the GMPE, ground motions may be overestimated. Local data can be used to derive the necessary adjustment to small magnitudes [122]. The importance of this adjustment depends on the selected minimum magnitude integration limit. However, in future more and more GMPEs will consider small magnitude data to be used preferably.

2.4.4. Interpolation of supporting frequencies

If required structural frequencies are not supported by the selected GMPEs, models for the missing frequency points need to be developed. For GMPEs that do not give values for the requested frequency points, an interpolation procedure for the missing GMPE coefficients can be applied.

It needs to be assured that the highest supported frequency of the GMPE lies in the decreasing part of the response spectrum and not in the maximum amplification range. For very high frequencies (e.g. 100 Hz) the PGA ordinate from the GMPE may be adopted for that frequency if not provided by the GMPE.

2.4.5. Style of faulting

Not all GMPEs contain a style of faulting parameter. In this case, a consideration of the style of faulting might be added by applying adjustment factors to these GMPEs [29].

2.4.6. Source and path adjustment (V_s & κ)

Comparing two GMPEs developed for two different regions, source, path and site characteristics may lead to different predicted ground motions. If a GMPE developed for a certain region with specific seismic characteristics is used for the hazard calculation in another region, an adjustment to the site region might be considered. This subsection regards a source and path adjustment. A site adjustment is not needed if site response is assessed by site response calculations, like it is recommended in Section 4. The need for an adjustment depends on how different the two regions are from each other and the potential benefit that can be achieved. At least two parameters are important to be considered: shear wave velocity and damping.

At least an adjustment of the path can be considered, which accounts for the distance from a defined engineering bedrock level down to the seismic bedrock underneath the site (see Fig. 2 in Section 2.1.1). The engineering bedrock is shallower than the seismic bedrock at defined depth at the interface between deep sedimentary layers and surface layers, i.e. between the PSHA output and the input for the site response calculations. Here the shear wave velocity at the engineering bedrock is called reference shear wave velocity ($V_{s,ref}$). For the adjustment procedure a shear wave velocity profile from the engineering bedrock level down to the seismic bedrock (very hard rock) is needed for the GMPE and for the site.

The damping is often described as “kappa” (κ), a parameter for the high-frequency decay of the Fourier spectrum [65], see also earlier section. Shear wave velocity and kappa are not independent and they significantly influence the spectral shape and the amplification of the

response spectrum. The shear wave velocity profile influences the response spectral ordinates over a broad frequency band whereas kappa has an effect on high-frequency amplitudes.

GMPEs are valid or applicable for a certain shear wave velocity range. If $V_{S,ref}$ (for the site) differs much from the mean V_S of the GMPE, the spectral amplitudes will be under- or overestimated. For instance, if $V_{S,ref}$ for very hard rock conditions lies out of the GMPE V_S -range for rock, the spectral amplitudes will be overestimated. If the deeper site specific V_S profile is known, and also a generic V_S profile for the GMPE region is available, a partial adjustment of the GMPE can be introduced by accounting for the ratio between the rock amplification in the GMPE and the site. This may be achieved by different approaches, e.g. using the quarter wave length method given by Boore & Joyner (1997) [59].

In order to account for different damping characteristics in the local crust at the site, the parameter kappa can be used, as discussed in Section 2. According to Anderson & Hough (1984) [65], the shape of the Fourier spectrum $A(f)$ at high frequencies above a frequency f_E decays exponentially as in the Eq. 21.

$$A(f) = A_0 \exp(-\pi \kappa f) \quad (21)$$

Kappa evaluated for the free field contains source, path and site contributions. Further discussion about the origin of kappa can be found in Van Houtte et al. (2011) [71]. If the engineering bedrock lies on top of very hard rock, it is expected that the kappa for the site is different to the generic site condition for which the GMPE for “rock” was derived. In case of different kappas for the host region where the GMPE was developed and the site region, a correction of the GMPE can be performed.

A hybrid empirical method was proposed by Campbell (2003) [123], where the adjustment factors for the GMPEs are estimated using stochastic simulations. In this case, if only an adjustment of individual parameters is considered (e.g. V_S and κ) it is recommended not to apply this method directly, because the response spectral ratio cannot be obtained from the Fourier spectral ratio. For response spectral amplitudes the whole set of stochastic model parameters need to be known. Regarding the relationship between Fourier transform and response spectra see, e.g. [124].

A simple approach for a path adjustment can be achieved using 1-D soil profile calculations (e.g. by linear equivalent calculations or random vibration theory) considering damping and a generic V_S profile for the GMPE region and a specific V_S profile for the site. First, the rock spectrum is deconvolved with the generic GMPE V_S profile and damping to a depth where the velocity profile is similar to the rock beneath the soil column at the site or to the depth of the seismic bedrock. Then, the spectrum at depth is convolved with the site V_S profile and damping to the engineering bedrock level below the site. This approach enables a path adjustment taking into account V_S and damping. In this way, instead of κ , damping values for the soil/rock layers are considered. Alternatively, adjustment factors could be achieved by stochastic simulations and the comparison of the response spectra at the engineering bedrock level. However, the estimation of appropriate damping or κ values is not easy.

2.4.7. Single station sigma

Using sigma, like described in Section 2.1.3 on uncertainties in GMPEs, reduces the aleatory variability of ground motion, due to the elimination of the site-to-site variability term in the GMPE, and leads to lower seismic hazard values. However, the application of the single station sigma approach needs to be made carefully, and, as it requires a great effort to

determine and correctly implement a single station sigma, whether it is done needs to be related to the possible benefit. A model for single station standard deviation is presented by e.g. Rodriguez-Marek et al. (2013) [125]. Moreover, Morikawa et al. (2008) [90] demonstrated the single station standard deviation by restricting source areas.

2.4.8. Near-source ground motion

2.4.8.1. Introduction

Near-source ground motions often contain directivity pulses that may cause structural damages. Therefore it is important to take into account the rupture directivity in the design. The features of motions are described in the IAEA SR-85 [99]. According to the directivity effects, forward directivity is the most relevant for seismic design and the influence on the response spectrum as well as the time domain needs to be considered.

2.4.8.2. Long period motion and amplification of response spectrum

Directivity pulses cause long period motion. This affects the response spectra at long periods and leads to an amplification of the spectral ordinates around the pulse period. A narrow-band amplification of response spectra due to long period directivity pulses can be assessed using available rupture directivity models [40] providing response spectral scaling factors that can be applied to GMPEs or directly to the response spectrum. It needs to be noted that directivity effects may already be partially included in a GMPE since observed records consist of the pulse signals, which were used in the regression analysis to determine the GMPEs.

2.4.8.3. Non-stationary characteristics of near-source ground motion in the time domain

The forward propagating nature of ground motion (towards the site) causes directivity pulses that can be observed in the velocity time history. These ground motions cause higher seismic demands on structures than ground motions without directivity pulses. If the relevant eigenfrequencies of the structure are close to the period of the directivity pulse, the structural demands are even larger. Time histories are used for nonlinear analyses of structures. They have to cover the non-stationary characteristics of directivity pulse in the time domain. In this situation it is not sufficient to apply standard procedures to generate or match accelerograms according to the elastic response spectrum, even if the spectrum is amplified for near-source directivity like described above. Therefore, it is suggested to use real time histories containing directivity pulses. The records need to be selected according to the spectral form of the response spectrum and the rupture directivity parameters.

Selection of time histories

For the selection of ground motion records according to a near-source scenario earthquake two pulse parameters are important: the pulse period and the PGV. The pulse period (T_P) can be calculated from the magnitude with empirical relations ([126, 127]). The PGV value is a measure of the pulse impact and is known as a damage indicator for short distances. PGV may be estimated by GMPEs according to magnitude and distance of the near-source earthquake scenario. Furthermore, magnitude and distance may be used for the selection procedure. Potential candidate ground motion records containing directivity pulses are available in the used data by Somerville (2003) [41] and in the following literatures: Baker (2007) [126], NEHRP (2011) [128]. In addition, different classification schemes have been proposed for the identification of pulse-like time histories in these publications (e.g. [126, 128, 129]).

Scaling and matching of time histories

Scaling of selected ground motions to the required spectral ordinates is recommended in the scaling factor “within 0.5–2.0” (SSG–9, Para. 9.10). If spectrum matching techniques are applied, it has to be ensured that the pulse-like characteristics are preserved after matching. In order to achieve this, a qualitative visual check on the acceleration, velocity and displacement time histories and also on the normalized Arias intensity curve (the so called Husid diagram) need to be made. Spectrum matching may be done using a median response spectrum amplified by a narrow-band adjustment that accounts for the expected pulse period. A narrow-band adjustment would be preferred to a broadband adjustment that averages the effect of pulses. Alternatively, the velocity pulse can be extracted from the selected record before spectral matching and added later to the ground motion. In this case, T_P spectral amplification adjustment is not needed. Synthetic time histories could also be used, if desired pulse motions from observed time histories are added, following the generation of ground motions. In this context, it needs to be noted that time histories containing forward directivity pulses usually have shorter durations than other records. The strong motion duration can be estimated or adjusted by empirical relations.

Probability of pulse motions

Not all near-source records contain directivity pulses. Considering the number of required time histories for structural analyses, a representative percentage of pulse motions in a set may be considered using empirical relations [40]. The occurrence probability of a pulse motion depends on the site location relative to the fault geometry and decreases with rupture distance. Considering a simultaneous impact of two horizontal components of ground motion, it has to be considered that the rupture directivity pulse is oriented in the strike-normal direction and response spectra and time histories need to be specified separately in two horizontal directions. If the fault geometry and the source mechanism are known, the orientation of the pulse motion and its severity can be considered. Otherwise, the maximum pulse effect can be conservatively applied in one direction and a motion without a pulse in the orthogonal direction.

3. THE INTERFACE BETWEEN GMPES AND SITE RESPONSE

3.1. INTRODUCTION

For nuclear installations, the geotechnical characteristics of a site need to be incorporated into the design process. This section deals with the interface between the GMPes and detailed site response calculations. Since hazard curves and uniform hazard spectra developed in seismic hazard analyses generally do not make full use of geotechnical information, at the start of any project to design a nuclear installation the process for dealing with this interface needs to be recognized and defined very carefully. That is because the GMPE cannot be assumed to match the precise geotechnical conditions at the site.

Section 2 noted that GMPes are generally based on an Earth model that is assumed as 1-D layered model. The Earth properties depend on depth, but not on location, so the predicted ground motion is mainly a function of distance, e.g. r_{jt} . 1-D models do include a free surface. Thus it is reasonable to assume that there is an implicit model for site response embedded in the GMPE. Conceptually, that free surface is the reference site and serves as the interface between the GMPE and the site response model. It will have the properties of engineering or seismic bedrock. The site specific analysis needs to adjust from the conditions at the reference site to the actual conditions at the site. Approaches for doing this are discussed in Section 4.

3.2. APPROACHES TO DEALING WITH THE INTERFACE

In the traditional design approach of nuclear installation, source characteristics and propagation phenomena have to be accounted for. Propagation phenomena are generally considered as the combination of two main contributions. The first, large scale contribution accounts for geometric spreading and other relevant wave propagation effects from the source to the site vicinity as spherical wave. The second contribution accounts for near-site propagation effects, affected by small scale geological features in the subsoil configuration and surface morphology as plane wave.

In principle, physical modelling of large scale wave propagation can be performed to account for most of the relevant phenomena, at least at low frequencies. However, in many cases the information available to characterize the crustal configuration is not adequately known to model even the low frequency phenomena. For these cases and for high frequencies in general, the GMPes as reviewed in Section 2 play a crucial role.

GMPes take forms considering as independent variables source features (e.g. magnitude and fault geometry), site-source distance and site conditions. Parameters of these relationships are then determined by undertaking a statistical analysis of a number of relevant strong motion accelerograms or numerical simulations. In both cases, the expected ground motion is estimated for a reference site condition (generally a flat rock outcrop).

Site response may be partially accounted for in the GMPE. This simplified approach considers only very rough site characterization in terms of soil categories (e.g. [94, 128]) or synthetic parameters such as V_{S30} , Q or $Kappa$, as discussed in Section 2. In this case, the GMPE may be adjusted by introducing further parameters determined empirically considering accelerometric registrations at specified subsoil categories.

This approach cannot account for the large number of possible site configurations. Even on the regional scale, the result may only provide a first-order approximation. On the other hand, physical modelling of site response is a feasible task after a site specific

geometrical/geomechanical characterization at the scale of interest has been performed with available exploration tools. For this purpose, the GMPE and associated hazard tools are used to define the input motion to be considered for the physical modelling of site specific propagation phenomena.

The input motion will usually be applied at a defined reference soil configuration. It is noted that a consistent treatment of uncertainties in GMPEs and site response is important and needs to be warranted in order to avoid double counting of uncertainties. The second part of this section provides basic information and references for the characterization of site response.

3.2.1. Preliminary examples

To set the stage for Section 4, an example for the Yucca Mountain project [130] can be provided. In the seismic hazard analysis in the project, ground motions were estimated for a site on solid rock with $V_{S30}=1900$ m/s and $\kappa_0=0.0186$ sec. Subsequently, these motions were adjusted using methods following the principles described in Section 4 to ground motions at the locations of specific sites, incorporating relevant geotechnical observations of near surface geology relevant to the each site.

3.2.2. The concept of reference soil configuration

The interface between the GMPE domain (source and long range travel path effects) and site response (ground motion modifications induced by local geomorphological conditions) can be stated in the form of a specific reference interface. At this interface seismic ground motion resulting from source and long range propagation effect is assumed to be known by the application of GMPE. Below this interface, specific stiff soil conditions are assumed to hold at a reference soil configuration or “seismic bedrock” that allow an unequivocal and feasible experimental definition of the interface.

The definition of the reference interface such as the reference soil conditions or seismic bedrock is largely conventional. In principle, a physical definition is possible. It could be stated that the reference soil needs to be sufficiently extended in order not to show a significant small scale lateral variation of the recorded motion (except for the effect of geometrical spreading) and to behave elastically (i.e. without any significant loss of stiffness) under the most severe expected seismic motion. It could also be required that such a geological unit (the seismic bedrock) exists below (or around) the site. The statements above imply that the reference interface is dependent on the tectonic framework, in terms of geological bodies and seismic activity and therefore its definition may change at regional and at the near regional scale. On the other hand, since ground motion at the reference interface needs to be known from GMPEs, these need to be determined by selecting a large number of accelerometric stations representative of outcropping or buried reference interfaces.

It appears evident that all these conditions are difficult to be satisfied jointly. Thus, a more conventional definition for reference interface is adopted for common applications and corresponds to a flat surface of a stiff soil where no significant lateral variation is assumed to exist. Furthermore, in order to facilitate the identification of this interface, the relevant reference soil configuration is defined in terms of a simple parameter (e.g. V_{S30} larger than 800 m/s as in the case of Eurocode 8 [94]). It is worth noting that this definition does not imply the absence of any interference/reflection/refraction phenomena, which are able to enhance the local ground motion evaluation with respect to any other site conditions.

4. SITE RESPONSE

Site response plays a role at the local scale. Every site is different, so site conditions cannot be treated by simplified approaches. Hence, classification into soil categories (e.g. [94, 128]) or parameters such as V_{S30} or Kappa are not enough and the site response needs to be treated case by case. In fact, experiences from the IAEA-EBP Karisma benchmark showed that within the site of the Kashiwazaki-Kariwa nuclear installation the spectral acceleration recorded after the 2007 Niigataken-Chuetsu-Oki M6.6 Earthquake varied by a factor of three within few hundred meters. Modelling the seismic response of individual nuclear installations showed also how the motion is strongly influenced by 3-D geologic configurations, as the recorded motions were significantly different along the horizontal directions. Furthermore, soil structure-interaction effects, which cannot be neglected in the case of nuclear installations, can be properly taken into account only when the true nonlinear soil behaviour is considered and modelled. All the considerations above imply that incorporating the site response into GMPEs cannot be used as a tool for the assessment of the seismic loads for design purposes of nuclear installations.

The estimate of the site response function can be provided by considering two different approaches: the “theoretical/computational” one and the “empirical” one. In the first approach, the site response is deduced by physical modelling of wave propagation phenomena in the site surrounds. In the empirical approach, on the other hand, the response function is obtained empirically as the empirical spectral ratio between any observed input motion (i.e. the seismic ground motion observed at any site representative of the subsoil in the absence of the site response to be described) and the ground motion observed at the site of interest during the same past earthquake. In this last case the empirical response function can be used to forecast ground motion of future seismic events after a convolution with any expected future reference ground motion. Of course, both these approaches present advantages and drawbacks and need not be considered alternatives: a complementary application (whenever possible) is highly encouraged. These aspects will be discussed in some detail in the following sections. In particular, Section 4.2 will be devoted to the first approach and to basic elements to be considered for its application. In Section 4.3 the empirical approach will be discussed in its different applications. In the last section, some very general suggestions to practitioners will be provided.

4.1. BASICS OF SITE RESPONSE ASSESSMENT AND CRITICAL ASPECTS

A number of well-documented occurrences during past earthquakes worldwide testify that seismic ground motion may present significant variations within distance ranges that are very short with respect to the distance from the relevant seismic source. This implies that characteristics of seismic ground motion (peak values, spectral shape and duration) may be dramatically affected by the propagation pattern of seismic waves at local scale and that this can be crucial for remarkable lateral variations in the level of observed damages and other seismically-induced phenomena. A clear example [131] is summarized in Fig. 31 and concerns accelerometric observations carried out in Cesi (central Italy) during the seismic sequence that struck central Italy in 1997.

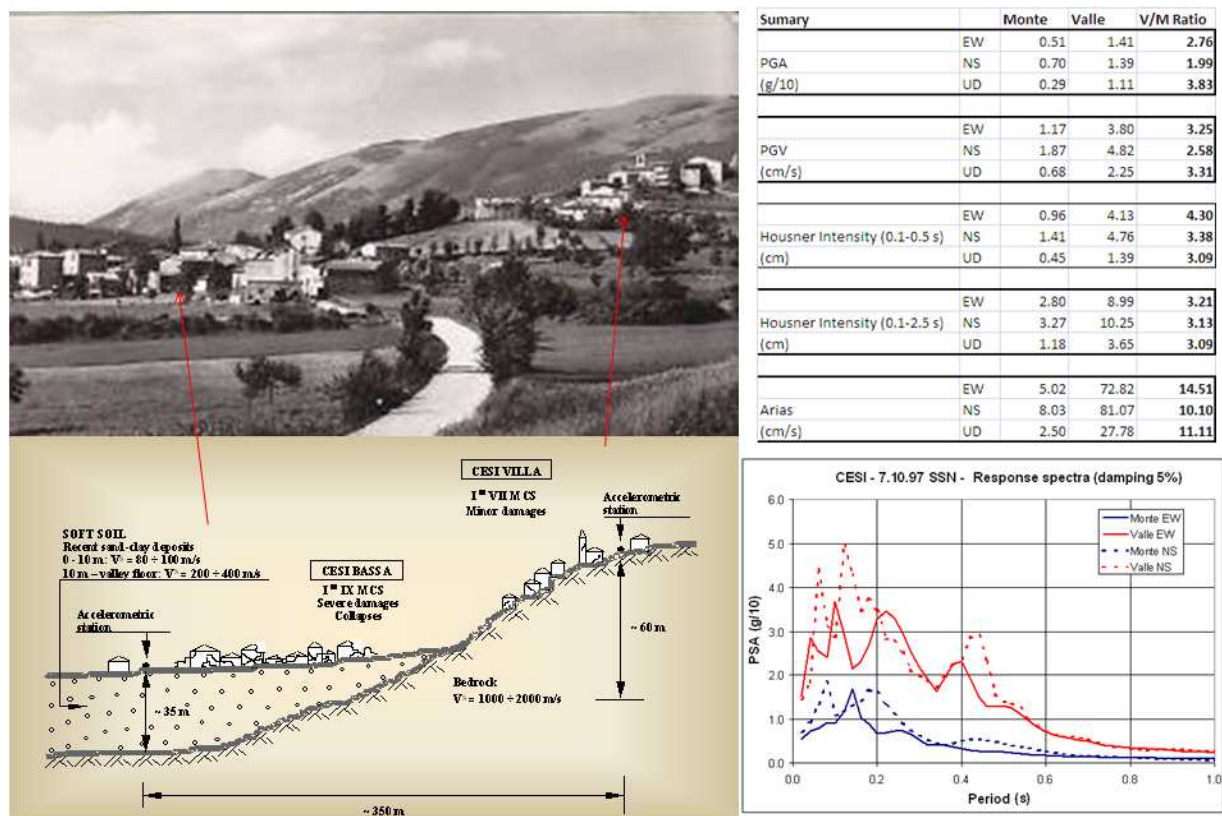


FIG. 31. Site response observed at Cesi (central Italy) during the seismic sequence that struck central Italy in 1997. On the left, geographical (up) and stratigraphical (bottom) situations at the two sites. On the right, accelerometric observations are reported relative to an aftershock (M_W 4.5) that occurred on 7 October 1997: representative numerical values at the top and spectral shapes at the bottom are reported for the Cesi Villa (Monte) and Cesi Bassa (Valle) accelerometric stations. Reproduced with the permission from Decanini et al., 2000 [131].

In general, such “site response” can be addressed as “surface soil formations and surface topography conditions responsible for modifications of the characteristics (amplitude, frequency content, duration) of the incoming wavefield resulting to the amplification or de-amplification of ground motion” [132]. “Site response analysis” is the quantitative characterization of this effect aiming at identifying, before any future potentially-damaging earthquakes, most critical situations and adopting suitable site specific design for structures. Other local seismic phenomena also occur that are related to high-strain seismic phenomena (landslides, rock falls, fracturing, liquefaction, etc.) that will not be considered in the following.

Differently from other aspects of hazard assessment, most phenomena associated to site response can be effectively assessed before earthquakes on the basis of affordable local scale geological/geotechnical observations and measurements. Furthermore, since in many cases site response may strongly affect ground motion amplitude and spectral content, seismic response studies may play a fundamental role in developing effective seismic hazard analysis and safety assessment strategies.

4.1.1. Physical interpretation of site response

From the physical point of view, near surface wave propagation includes reflection/refraction/dissipation processes controlled by the underground distribution of seismic impedance contrasts. Seismic impedance is the product of material density and phase velocity of the relevant seismic wave. In particular, in the near surface domain, reverberation of seismic waves trapped within geological bodies bounded by sharp impedance contrasts (the free surface being the most important one) is one of the key factors for amplification (Fig. 32).

Beyond such interference phenomena, the presence of laterally complex interfaces (edges, faults) also result in the production of locally generated new seismic phases (mainly surface waves), that make the expected wave field complex. Seismic resonance induced by the presence of sharp impedance contrasts below the flat free surface is the most important (and common) 1-D effect induced by seismic wave interference of up and down going seismic waves (mainly SH phases, i.e. S waves polarized horizontally). In this case, incoming waves, characterized by wavelengths comparable with the dimensions of the soft sedimentary cover, remain trapped in the soft layer below the surface and this produces large amplification of the observed ground motion at a frequency (resonance frequency) similar to $V_S/4H$, where V_S is the average shear wave velocity in the soft layer, and H is its thickness.

This simple relationship suggests that the effect of the sharp contrast is very effective when the dimension H of the layer is of the quarter wavelength order of the trapped wave.

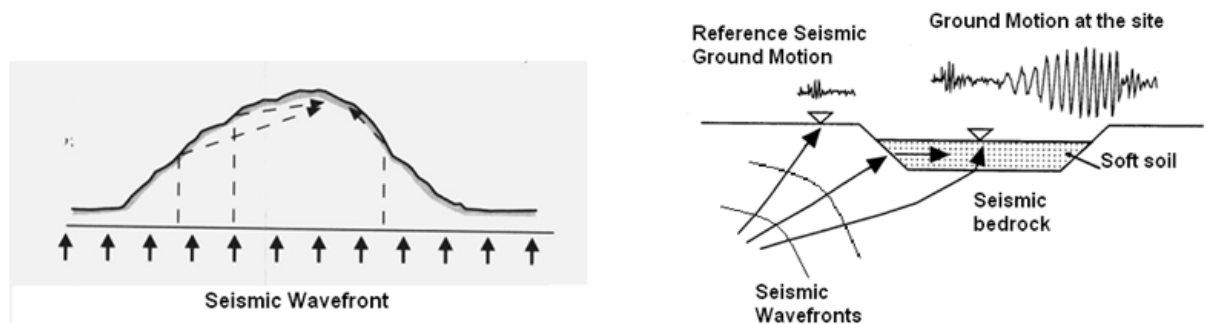


FIG. 32. Examples of interference phenomena induced by sharp seismic impedance contrasts. Reproduced with the permission from Lanzo and Silvestri, 1999 [133].

In general, site response can be seen both in spectral and time domains. In the spectral domain, site response results in spectral peaks at some frequencies (“Resonance Frequencies” generally speaking) and reducing spectral amplitudes at other frequencies. The most important spectral effects are those involving the frequency band of engineering interest (0.5–10 Hz). Typically, 50 m of soft sediments (V_S about 200–300 m/s) overlying a rigid bedrock produces 1-D resonance frequencies in the range of 1–1.5 Hz, while a 100 m thick layer is responsible for resonance frequencies in the range of 0.5–0.8 Hz. When lateral variations become relevant (e.g. in the case of deep basins where the semi-length of the soil deposit is comparable with its thickness) 2-D/3-D effects come into the play. In simple geometrical configurations (i.e. sinusoidal-shape alluvial valley) 2-D and 3-D effects induce a progressive shift of the resonance frequency towards higher values with respect to 1-D resonance [134]. Furthermore, in terms of amplification amplitudes, the difference between 1-D and 2-D effect

is smaller than that between the 2-D and 3-D configurations. In terms of frequency shift, however, the difference between 1-D and 2-D effect is larger than the one between 2-D and 3-D effects. It is worth noting, however, that these results only hold in the midpoint of the basin and that these effects cannot be generalized to the whole basin.

In the time domain, local subsoil conditions affect the ground motion peak amplitude (PGA and PGV), waveforms and duration especially in 2-D subsoil configurations. Observation and modelling suggest that for moderate acceleration levels ($<0.2\text{--}0.3\text{ g}$) the amplification of PGA is expected at soil sites compared to rock sites. Furthermore, the reverberation of trapped waves also increases the general duration of the wave motion.

Lateral heterogeneities also affect the configuration of the local wave-field by generating new seismic phases that also contribute to enhance amplitude and duration of the ground motion and significantly change its spectral structure. Experimental studies [135] indicate that during earthquakes, the presence of significant lateral variations of seismic impedance in the shallow subsoil may be responsible for the generation of high amplitude surface waves. Interference of these new seismic phases with the impinging ones may significantly increase the amplitude of the ground motion at the surface and elongate the duration of the earthquake.

Surface topography may also affect the expected ground motion. The occurrence of this effect depends on the following factors [136]:

- Incidence angle around the critical, especially for SV waves;
- Focusing and de-focusing of seismic waves along the topographic relief; and
- Diffraction of body and surface waves that propagate downwards and outwards from the topographic features and lead to interference patterns between direct and diffracted waves.

The respective role of these features depends on the specific situation and results in quite complex patterns. In general, numerical simulations reveal that surface morphology may play an important role only when the size of the surface irregularity is close to the range of incident wavelengths: this implies that the topographic effect is frequency dependent. The amplification is generally larger for the horizontal ground motion components than for the vertical ones. Furthermore, the amplification at the crest increases as the slope of its flanks steepens. A de-amplification is obtained at the base of the topographic irregularity. In general, numerical simulations predict a systematic amplification of the ground motion at convex topographies and a de-amplification over concave geometries.

These results, however, being the results of numerical modelling, cannot be easily generalized and strongly depend on the specific conditions considered in each case (topographic shape, incidence angle of impinging waves, seismic phases of concern, etc.). Observations are also available and testify the actual presence of such effects. However, in many cases it is not easy to separate the effect of subsoil rigidity variations and pure topographic effects.

4.1.2. Site domain concept depending on wave length

Physical intuition supported by numerical simulations suggests that a relationship exists between the wavelength of the seismic waves of concern and that of the impedance contrasts potentially responsible for significant perturbations of the relevant propagation pattern.

The link between the wavelength of the relevant seismic wave and that of the seismic impedance contrasts affecting their propagation pattern represents a basic tool for identifying the spatial scale of impedance contrast heterogeneities potentially responsible for significant perturbations in the propagation pattern. In particular, one can assume that lateral or vertical heterogeneities (surface morphology, loose soil overlying hard rocks, etc.) eventually presented at the scale L will be of main concern when L is of the same order as VT , where V is the local phase velocity of the seismic waves and T is the period of the structure potentially exposed to any future earthquake. This perspective is in line with the definition of the reference dimension that “shall be large enough to include all the features and areas that could be of significance in the determination of the natural and human induced phenomena under consideration and for the characteristics of the event” (as established in Ref. [1], para. 2.19 and quoted in para. 3.6 in SSG-9 [1]).

The above very simple rule of the thumb plays an important role in planning the subsoil surveys devoted to site response characterization and in selecting numerical codes for site response evaluation (see Sections 4.2.1 and 4.2.3). In particular, it can be used to define a sort of “site domain”, i.e. the size of site surrounds and of geological/geomorphological features to be considered for site response evaluations. In this perspective, the dimension of this “site domain” depends on the period of the structure, the seismic phase of concern and its average phase velocity in the site surrounds. As an example, the period of 1 s is of concern for structure and S waves component are of special interest (e.g. because these phases are expected to dominate near field horizontal ground motion components), the site domain will have the approximate size of several hundreds of meters if phase velocities of S waves are of the order of 200-300 m/s near the site. One can see that these dimensions largely exceed the typical size of building foundations. Please notice that if P waves are of concern (e.g. due to the importance attributed to vertical ground motion components), the size of the site domain for the above example significantly increases, since P waves phase velocities are larger than those of S phases. The above considerations also allow fixing a minimum resolution for information to be used for site characterization. In particular, subsoil features and morphologies characterized by typical dimensions much shorter than VT can be averaged out during the site response analysis.

In general, the size of the site domain described above, allows separating “local” and “long range” propagation phenomena, the former being ones those occurring within the site domain and the latter those occurring outside. In other terms, ground motion resulting from processes occurring outside this domain will be considered as an “input” motion for the definition of the site response in the frequency range of concern. The input motion can be also addressed as the “reference” motion.

4.1.3. The role of nonlinearity

From the physical point of view, wave propagation in the shallow subsoil, is a nonlinear process, in that constitutive equations describing soil behaviour (mainly when loose sediments are of concern) are sensitive to the level of strain induced by seismic waves. One kind of stress-strain relationships when shear is applied to a soil is shown in Fig. 33 (a). When a complete cycle of loading-unloading-reloading is applied, a hysteretic loop is described that accounts for the nonlinearity and the inelasticity of soil. The nonlinear behaviour is described by the backbone curve, through which different shear moduli G_i are derived: the differential increment of shear strain with stress is described by the tangent shear modulus (G_{tan}); when the increment is referred to the origin of the axes, the secant modulus is derived (G_{sec}); at very low strain, when the loop is negligible and the soil behaves elastically, the maximum (or initial) shear modulus is obtained (G_{max}).

Inelasticity is controlled by the area of the hysteretic loop, which describes the energy dissipated by the soil sample deforming internally. The amount of energy dissipated through work and heat is described by the internal damping, which ultimately accounts for the nonlinear inelastic behaviour of soils.

As the number of cycles increases, the area of the hysteretic loop increases in turn and moves towards the horizontal axis: this implies that as the shear strain increases the shear modulus decreases and the damping increases, as shown in Fig. 33 (b).

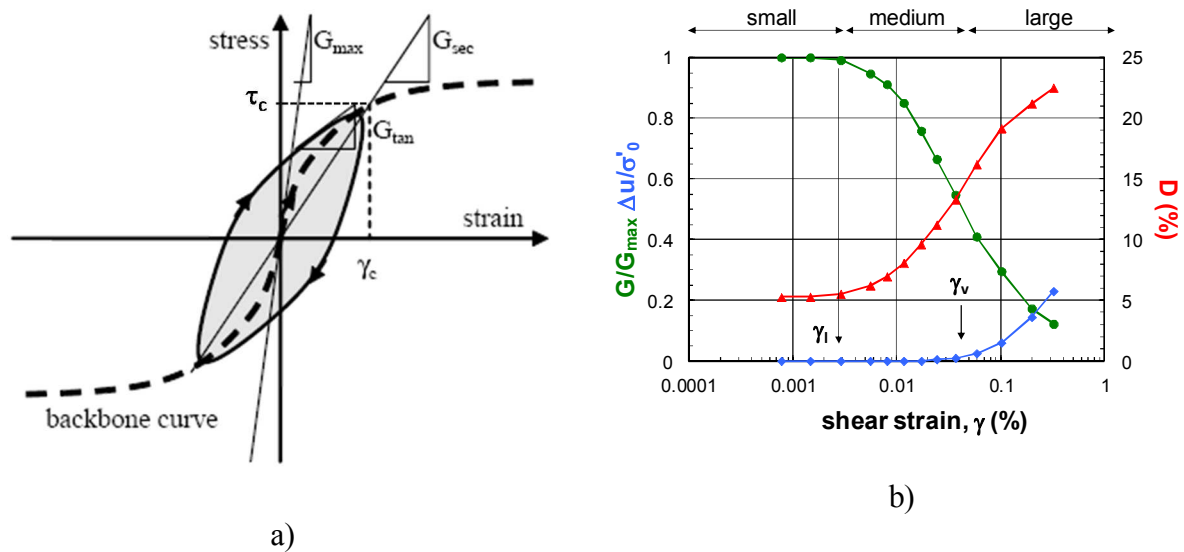


FIG. 33. Incremental shear stress versus shear strain: a) hysteretic loop; b) effect of shear strain ($\gamma\%$) on geotechnical properties of the soil: green circles: stiffness degradation (G/G_{max}); red triangles: damping ($D\%$); Diamonds: blue pore pressure ($\Delta u/\sigma'_0$).

The elastic strain threshold (γ_l) separates the field of linear elastic (at small strain) and nonlinear visco-elastic (at intermediate strain) soil behaviour; the volumetric strain threshold (γ_v) separates the nonlinear visco-elastic and the nonlinear elasto plastic (at large strain) behaviour, where irreversible deformations occur and the soil may undergo failure (e.g. liquefaction or displacements as a result of pore pressure increases or volumetric strain for, respectively, undrained or drained conditions). The presence of nonlinearity significantly

affects the local seismic response (Fig. 34). In fact, increasing strain reduces the rigidity of materials and increases material damping. As a consequence, the V_S values reduce and attenuation increases. Since the fundamental period of vibration linearly depends on the V_S values, their decrease shifts resonance towards higher periods. Furthermore, damping in the resonant layers affects constructive interference between up and down going trapped waves and reduce amplification phenomena.

In conclusion, the expected site response depends on the characteristics (time history, overall duration, spectral shape, etc.) of the ground shaking entering in the “site domain” (input ground motion) and these characteristics are due to source and long range propagation processes.

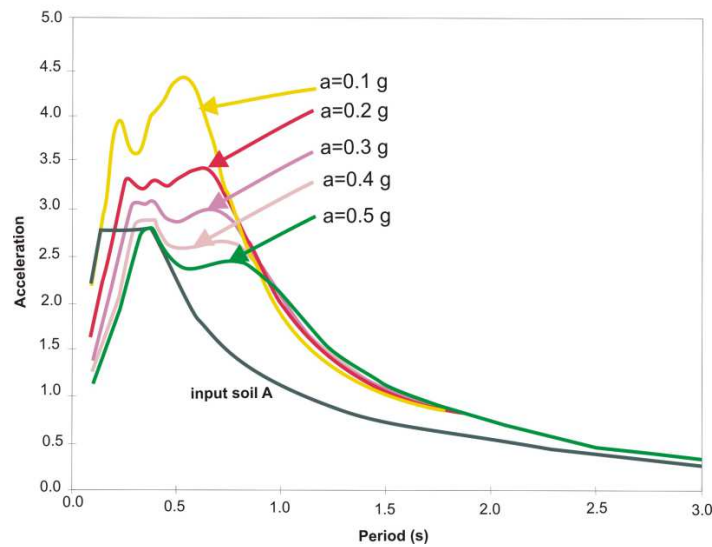


FIG. 34. Modelled effects of the ground motion level on the spectral shape of the response function at the top of a soft layer (V_S in the range 100-200 m/s) overlying a stiff reference soil (V_S equal to 800 m/s). The grey line indicates the response spectrum of the input reference motion. Colour lines describe the output response spectrum at the surface for increasing values of the input motion (in fractions of the gravity acceleration g). All the curves have been normalized at the same value for period equal to 0 (PGA). It becomes evident that increasing amplitude of the input motion changes the shape of the output motion by generally reducing amplification and displacing towards higher periods the maximum response. Reproduced with permission from Sanò and Pugliese, 2007 [137].

4.1.4. The parameterization of site response

The relationship between the Fourier or response spectra of the input ground motion and that of the ground motion of the site response (output ground motion) represents the so called “site response function”. Despite the fact that both Fourier and response spectral ratios are used in the common practice, one needs to be aware that they are not equivalent. The latter is the one most commonly applied in seismic engineering practice since it generally provides smoother patterns with respect to ratios computed from Fourier spectra, but, on the other hand, it lacks any simple physical interpretation.

Beyond this very generic definition, two possibilities are generally considered to parameterize the site response function:

- (1) **Transfer Function:** spectral ratios can be evaluated as the ratios between Fourier spectral amplitudes of input and output ground motions (Fourier spectral ratios). In some cases, however, this term is used to indicate the ratios of relevant response spectra computed at any fixed damping ratio: this use is discouraged to avoid possible misunderstandings. In the case of transfer function parameterization, the input is considered at depth, while the output is assumed to represent ground motion at the surface in correspondence of the site.
- (2) **Site Response Function (or amplification function):** spectral ratios (both in terms of ground motion or response spectra) are evaluated by considering as the reference the input motion at the outcrop. This parameterization is more representative of expected variations of the ground motion in the presence of laterally-varying geomorphological/seismostratigraphical conditions.

In general, these two parameterizations are equivalent (in that each representation can be directly converted into the other), but one needs to pay attention which site response function is considered when evaluating the expected ground motion at the site of interest.

Beyond these detailed representations of the site response, alternative more synthetic representations also exist. The simplest one concerns the ratio of peak parameters (e.g. PGA, corresponding to the response spectral acceleration for a period of 0 s) at the site and those of the input motion or of the input motion at any outcrop. This representation is rather incomplete since peak parameters are generally related to specific spectral component and could be not representative of the overall site response. An alternative are the so called site response factors (or amplification factors). In this case, the site response is the ratio between the integral intensity (e.g. [138]) input and ground motions output. In the case when Housner intensity is considered, a period range of potential interest for engineering and design is used for integration (e.g. 0.1–2.5 s). An example of such parameterization is shown in Eq. 22.

$$FA = \frac{\int_{0.1}^{2.5} PSV_{output}(T)dT}{\int_{0.1}^{2.5} PSV_{input}(T)dT} \quad (22)$$

where PSV is the response spectral pseudo velocity and terms of the fraction are Housner Intensities [138] associated to the input and output ground motion respectively. Such a rough parameterization of site response is of a little use in seismic design but is of great importance in extensive studies devoted to the identifications of most critical situations in urban planning (i.e. seismic microzoning).

4.2. THE THEORETICAL/COMPUTATIONAL APPROACH TO SITE RESPONSE EVALUATION

In this approach, site response (both in the form of transfer and site response functions) is computed numerically on the basis of physical modelling of the propagation process. In this kind of approach, the definition of the site response requires:

- The choice of any reference ground motion (seismic input);
- A geological, geophysical and geotechnical characterization of the subsoil and, in particular, of the site domain of concern; and
- Numerical tools for reproducing seismic waves propagation and to compute the expected ground motion at the surface or the relevant transfer functions.

The main advantage of this approach is that the site response can be evaluated everywhere information is available on the subsoil configuration and independently from the occurrence of previous earthquakes and the availability of seismic records at the site of interest. This can represent a great advantage in low seismicity areas or where accelerometric observations are scarce or unevenly distributed. Another advantage of this approach is the possibility it offers to evaluate the effect of different impinging earthquakes characterized by weak or strong motion and in this way have a better idea about possible future ground shaking phenomena.

Nevertheless, possible drawbacks affect this kind of approach. First of all, the correct representation of the propagation process is mandatory along with a good knowledge of the physical configuration of the subsoil. In addition, the effectiveness of the adopted modelling can be only checked “ex-post” on an empirical basis. Furthermore, since subsoil characteristics are uncertain, the resulting site response evaluation will be affected by uncertainty in its turn and this uncertainty needs to be accurately accounted for to avoid a possible underestimation of the expected ground motion. Though in most cases this problem is overlooked, the management of the relevant uncertainty needs to be an integral part of site response analysis.

4.2.1. The input ground motion

Due to the possible sensitivity of the site response to the amplitude of the seismic motion, the choice of input motion is essential for the site response assessment. Regarding one earthquake scenario, such an input motion is assumed to be representative of the “reference” or “controlling” ground motion, i.e. of the ground motion that is reasonably expected to produce the maximum level of shaking at the site of interest during a fixed exposure time. Usually more than one earthquake scenario is controlling the hazard at a site, especially in the case of diffuse seismicity. The standard output of a PSHA is a Uniform Hazard Spectrum (UHS), where the spectral ordinates for each period or frequency correspond to the same requested probability of exceedance, i.e. the maximum spectral accelerations of all contributing earthquakes (for that probability) act uniformly. Since the UHS does not correspond to any specific earthquake, it could result in physically not plausible but probabilistically adequate seismic loads. However, for a deterministic seismic design it is commonly used and practicable. Several approaches are suggested in the literature for evaluating the control of earthquake scenarios for design based (e.g. standardized spectral shapes [139] or conditional mean spectra [140]).

In principle, for site response analyses, this reference ground motion needs to be supplied in the form of an acceleration time history. However, in some cases, when site response computations are performed in the frequency domain (see Section 4.2.3) the input motion can also been supplied in the form of Fourier acceleration spectrum or in the form of a response spectrum.

Once the reference soil configuration is defined, the relevant time histories or response spectra representative of the input ground motion can be obtained in three ways [141] as follows:

- (1) Observations (several databases exist of observed accelerograms worldwide) more or less modified to fit the target reference response spectrum (real record);
- (2) Numerical simulation of the physical process responsible for ground motion at the reference interface including source and long range propagation features (synthetic time history); or
- (3) Random vibrations reshaped in the spectral domain to fit the reference response spectrum or by an application of the random vibration theory to retrieve a Fourier acceleration spectrum of the ground motion (artificial record).

All these possibilities present drawbacks and advantages that cannot be discussed here. Anyway, it is clear that, whatever the origin of the ground motion, it needs to be representative of the seismic hazard at the site.

The output can be a UHS, scenario based earthquakes or a deaggregation analysis [142, 143], giving the magnitude (M), source-site distance (R) and fractile (ε) of the controlling earthquakes. Then, the parameters M , R and ε are used to calculate the earthquake response spectra with GMPEs. The expected response spectrum can be used to define the input motion by following two approaches mentioned below.

- (1) A set of measured accelerograms relative to events of the same magnitude and the distance of the controlling earthquake that are also compatible (by also considering any slight rescaling), at least on average with the spectrum (Fourier or response) of the controlling earthquake (Design Spectrum), is used. The choice of a suite of accelerograms allows accounting for the relevant epistemic uncertainty that, at least on average, fit the spectral signature of the controlling earthquake [144].
- (2) The stochastic methods to provide the time history of input motion [101] are used. In this kind of approach parametric or functional descriptions of the ground motion's amplitude spectrum is combined with a random phase spectrum modified such that the motion is distributed over a duration related to the earthquake magnitude and to the distance from the source. The time series generated by the stochastic method can also be iteratively modified to fit any target response spectrum determined for probabilistic seismic hazard analysis [145]. Fourier amplitude spectra to be used for numerical simulations can be also retrieved for any reference response spectrum by the use of the inverse random vibration theory [146].

In the simple case that any single source can be identified as responsible for the reference input ground motion, this motion could also be deduced by available records from the same source, by deterministic modelling or artificial generation. In the first case, accelerograms need to be available at recording sites representative of the reference soil configuration of concern, which is rarely the case. More commonly, the reference earthquake has to be "reconstructed" by taking into account a possible site response at the recording site. In these cases, a deconvolution of the observed accelerograms has to be performed by suitable numerical procedures by eliminating the contribution of local site conditions. This requires a detailed knowledge of the subsoil configuration at the recording site down to reference soil configuration of concern and the use of numerical modelling. Otherwise, alternative empirical

approaches [147] can be also considered for this purpose. The question concerning the effectiveness of the use of observed or artificial accelerograms is debated. Obviously real accelerograms are preferred. However, finding suitable records is not always an easy task and in many cases the ones available only marginally or on average fit the features of the reference earthquake. Furthermore, to take into account epistemic uncertainty relative to the reference earthquake, several possible accelerograms need to be considered and this makes it even more difficult to define a suitable suite. To cope with that problem, spectral matching of real accelerograms can be applied [148, 149]. Alternatively, artificial accelerograms (both in terms of time histories or response/Fourier spectra) could be of help. It is noted, that if Fourier spectra are used, correction factors might be applied to avoid an overprediction of amplitudes [150]. In general, it could be of help to include both observed and artificial accelerograms in the suite of possible input motions in order to better account for epistemic uncertainty.

4.2.2. Site characterization

In order to simulate wave propagation in the site domain, relevant information concerning the subsoil configuration has to be provided. Of major concern are: the distribution of seismic impedance values for body waves in the subsoil, buried or outcropping morphology of major seismic impedance contrasts, geotechnical properties of the materials that constitute the geological bodies present in the site domain.

A basic aspect to be considered for collecting relevant information is the dimension of the site domain of concern and the size of morpho-stratigraphic features included in this domain. As stated above, this domain and the size of features of potential interest depend on the frequency range of concern and on typical phase velocities of seismic waves expected to affect the structure. When this structure is characterized by resonance frequencies around 1Hz and *S* waves with average phase velocities of the order of 200 m/s are expected to play a major role in possible damaging effects, the size of features of potential interest are typically in the range hundreds of meters. As one can see, this implies that any attempt at subsoil characterization would require surveys that are not restricted to building foundations.

The best way to approach the problem and to reduce costs is by a multilevel step by step procedure characterized by a progressive reduction of the scale of interest and a progression from qualitative to quantitative assessments.

A multilevel approach to the site characterization is straightforward in view of the optimization of the resources to be allocated and the geological and geotechnical problems to be addressed. Level one (mandatory) is aimed at the reconstruction of the geologic model of the site area and it is performed through the retrieving of existing information supplemented by extensive, usually low cost investigations from the ground surface. The main outcome of level one is to provide representative cross sections that capture the geological framework of the site area in terms of bedrock trends, thicknesses and lateral variations of surface deposits and morphological features of the site. The second level (mandatory, too) is the quantitative description of the soil and bedrock's geophysical and geotechnical properties, carried out by intensive in situ investigations (drilling and in situ testing). The main outcome of this level is the soil/bedrock characterization at low or intermediate strain and it could be exhaustive either in the case of a moderate seismicity affecting the site or the outcropping of relative stiff geological materials whose behaviour, under the worst expected seismic shaking, can be regarded as equivalent linear. The third level of investigation is aimed at the full nonlinear characterization of the soil behaviour and it is compulsory in the case of a strong seismicity affecting the site, or poor geotechnical properties of the surface deposits whose response may determine permanent soil displacements or imply strong soil-structure interaction effects. This

level of investigation is performed by taking samples from the drilling carried out in the second level of investigation and by carrying out laboratory testing. This is the most expensive level of investigation due to the cost of sampling and laboratory testing and implies also a consistent numerical modelling of the site response analysis.

Level one: Extensive survey.

The main goal of this extensive analysis is the reconstruction of a geological model of site vicinity, an area under study at a scale that is typically below 1:5000. Despite the qualitative character of information provided by typical geological reconstructions, the geological model represents the basic frame where other pieces of information will find a coherent allocation and interpretation. Obviously, to be useful, geological modelling needs to be well calibrated to the target. Evolutionary depositional and tectonic aspects will be of concern, but the focus needs to be on the identification and geometrical characterization of the major lithological units (both buried and outcropping). Particular attention needs to be devoted to recent bodies and formations (alluvial fans, loose sediments, etc.) that are generally of less concern in pure geological studies but become of paramount importance for site response evaluations. In fact, major impedance contrasts at the scale of tens to hundreds of meters mainly characterize contacts of these recent unconsolidated formations and the more competent geological bedrock. It is not expected that this kind of survey provides strictly quantitative evaluations about subsurface configuration; what is actually important is to provide a very rough estimate of the expected impedance contrast at the boundary of geological bodies (e.g. high, low and none) and of the depth of these contacts (e.g. meters, tens of meters and hundreds of meters), all over the area under study.

The geological survey, can take advantage of available borehole data (drilled for other purposes, such as water supply or foundations characterization) or of low cost geophysical prospecting techniques. Gravimetric measurements could be of great importance for extensive reconstructing geometry of deep sedimentary basins, while common resistivity and active refraction/reflection prospecting may help recognizing small scale lateral variations of seismic interfaces (e.g. at the boundaries of sedimentary basins where geological bedrock outcrops). Recent experience shows that passive seismic techniques [151, 152] (both single station and array configurations) may provide a valuable help in identifying the presence of sharp seismic impedance contrasts potentially responsible for a significant enhancement of seismic ground motion and supplying, in the framework of global geological view of the local situation, at least a very preliminary evaluation of respective depths via fast and ad-hoc approaches.

Information collected in this phase, will be of great importance to guide more detailed surveys to be carried out in the following phases. An outcome of particular importance at this level is a geological/lithotechnical section crossing the site domain, where major geological contacts potentially corresponding to significant seismic impedance contrasts are delineated.

Level two: Intensive survey

In this phase, the geological model developed in the first level will be considered to allocate intensive and more expensive measurements aiming at a more quantitative characterization of the essential features revealed at that level of analysis. The most important tool in this level is drilling [153]. From the geological point of view, this will provide a direct check of subsoil geometries revealed in the first level. In the case that a good and reliable first level analysis has been carried out, drilling can be restricted to more complex or unclear situations. Furthermore, exploration depths will be accurately calibrated to reach the most important buried geological bodies by avoiding unnecessary efforts and expenses.

A basic tool at this level is geophysical borehole prospecting. This kind of analysis basically aims at providing information about low strain behaviour of strata in the site domain. The two most important procedures to this purpose are downhole (DH) and crosshole (CH) tests of body wave velocities [154] and low strain ($<10^{-3}$) and high moderate frequency (10-100 Hz) material damping (initial material damping). In the DH procedure, the source is located at the surface near the borehole aperture, while three directional sensors located at depth in the well at varying depths. Controlled seismic waves generated at the surface, are monitored at depths and in this way *P*- and *S*-wave velocities can be estimated at the site. Due to this source sensor configuration, seismic measurements can be provided at depths shallower than 50-60 m. CH tests, instead, do not present such a limitation but is much more expensive. In this case, three parallel wells are drilled few meters apart. In the first well, seismic source is located at various depths. In the second and third wells, three directional seismic sensors are located at the same depth of the source. The system is progressively lowered measuring phase velocities and damping for in situ materials.

For deeper measurements, indirect procedures can be also considered, which are based on the inversion of active or passive seismic measurements at the surface [151]. In general, one could expect that outcomes of these indirect estimates are affected by uncertainties larger than those provided by borehole tests. However, one needs also to take into account that surface indirect estimates (e.g. reflection/refraction deep surveys, etc.) generally could sample larger subsoil volumes than borehole tests and this could be an advantage since seismic wave propagation for larger wavelength is much more sensitive to “average” seismic properties than to small scale variations. Furthermore, the fact that borehole measurements provides more direct estimates of the phase velocities with respect to surface measurements does not make the relevant outcomes error free. In all the cases, borehole measurements require interpretation (phase picking, hypotheses about seismic rays, etc.) that can bias results. Furthermore, due to drilling, the rocks surrounding the well cannot be considered as fully undisturbed. Moreover, casing may also play an important role: biased evaluations will be induced by bad well cementation. Other in hole tests exist that can overcome the problem of casing (e.g. the seismic cone test): but these cannot be applied everywhere and present severe limitations in terms of the exploration depth. In the same way, deviations from the vertical, lack of parallelism among wells in during CH tests (that is a very common problem when very deep wells are considered) may induce severe biases one needs to be aware that a basic assumption underlying borehole measurements is that 1-D heterogeneities (layering) are present only: if this is not the case, severe biases may occur. At last, one needs to be aware that borehole seismic measurements only concern the volume in the near surroundings of the well: any lateral extrapolation needs to be carried out in the framework of the overall geologic model determined in level one.

Despite drilling providing the most direct investigation for physical, mechanical and geophysical characterization of soil properties, it still may be time consuming and expensive when applied to an in depth characterization of large areas (within “site vicinity” according to IAEA SSG-9 [1]). In recent years the capability of taking multiple measurements through on site investigations based on direct pushing technologies has greatly increased. The most useful for the geotechnical and geophysical characterization of soils are the seismic piezocone: the Seismic Core Penetration Test (SCPTU) and the seismic flat dilatometer: the Seismic Dilato Meter Test (SDMT).

The full displacement penetrometer probe of SCPTU couples the ultimate strength of soils with the pore pressure dissipation and the onsite measurements of shear wave velocities, without the disadvantages of core drilling. Flat dilatometer (SDMT) on the other hand,

provides the deformability moduli of soils at low and medium strain for the serviceability limit states, coupled with borehole geophysics. Owing to the inexpensive and rapid performance of such surveys, they are suggested to be largely used for the site characterization aimed at finding the presence and properties of potentially amplifying soils.

Beyond these estimates, the empirical correlations of the geotechnical parameters and body wave velocities have been also proposed in the reference. Since these relationships are affected by large uncertainties, these need to be used very cautiously and just to support or extrapolate more direct estimates.

Level three: Geotechnical laboratory testing

At this level, the complete dynamical properties of the materials in the subsoil (e.g. nonlinear large strain behaviour) are determined by laboratory analyses carried out with rock samples obtained during drilling [153]). This kind of analysis is mandatory when strong seismic ground motion is expected and the nonlinear part of the constituent is presumed to play a role (see Section 4.1.3).

Laboratory testing is performed on small dimension specimens (size of the order of few cm to tens of cm) subjected to uniform initial stress and uniform changes in stress or strain conditions.

Two basic problems affect this kind of analysis. The first one concerns the actual possibility to replicate the initial and loading in situ conditions in the laboratory. Frequently, drilling significantly damages the sample and thus the specimens need to be reconstituted to reproduce original in-place conditions. In this last case, one can obtain realistic densities and applied stress, but the soil fabric would in many cases be different. The second one is the possibility that a small specimen is actually representative of the relevant geological body. Concerning this aspect, it is important to remember that seismic wavelengths of concern are of the order of tens to hundreds of meters and the actual representativeness of a ten cm specimen could be difficult to evaluate.

Both these problems makes difficult to compare laboratory results and in situ estimates. This makes the comparison of low strain and large strain evaluations mandatory in order to better reconstruct the relevant behaviour (see Fig. 33) and to evaluate the representativeness of laboratory results with respect to low strain in situ tests. For this purpose, low strain laboratory tests play a major role. Currently, few laboratory tests are actually available to cover such the low strain domain (resonant column, ultrasonic pulse and piezoelectric bender element). However, they only operate at frequencies >10 Hz, generally higher than those of interest for site response studies. On the other hand, the possibility to operate in the low frequency domain (cyclic triaxial, simple shear and torsional tests) would allow better simulation of the effect of fluids and pore pressure variations in drained and undrained conditions.

Laboratory testing is the most in depth approach for soil characterization, but the most expensive one, in turn. Thus, it needs to be used for small scale investigations (“site area” according to IAEA SSG-9 [1]) and the soil parameterization for the numerical modelling described in the following section. According to the level of shear stress induced by earthquake, different soil properties have to be investigated through appropriate laboratory tests, ranging from the intermediate level of strain (resonant column), to high level of strain (cyclic torsional and simple shear tests), up to the full volumetric deformation and pore pressure variation (cyclic triaxial test, Fig. 35).

Accordingly, the consistent mechanical model and the analysis method to simulate a site response can be chosen, once the induced shear strain level has been assessed and the proper soil properties investigated.






	Shear strain, γ [%] (approximate)					
Soil property (<i>parameters</i>)	10^{-4}	10^{-3}	10^{-2}	10^{-1}	1	10
	Low	Fair		High		Failure
Stiffness (G_0 , G)						
Damping (D_0 , D)						
Water overpressure (Δu)						
Permanent deformations (ϵ_v^p , ϵ_s^p)						
Stiffness reduction (δ_G , δ_D)						
Investigations	In-situ testing		resonant column→ cyclic shear→ cyclic triaxial			
Stress level	Vibratory machines			Earthquakes		
Mechanical model	Linear visco-elastic		Equivalent linear Visco-elastic		Nonlinear Elasto-plastic	
Analysis method	Linear Total stresses		Equivalent linear Total stresses		Incremental Effective stresses	

FIG. 35. Soil properties, investigations, stress levels, mechanical models and analysis methods as a function of the induced shear strain.

4.2.3. Numerical modelling

The analytical modelling of the site response needs to be consistent with the tectonic framework of the site area. This implies that a detailed geological characterization of the site has to be carried out, which characteristics and properties are compared to the level of seismicity that may affect the area in order to point out:

- (1) What kind of soil behaviour may be expected based on the seismic shaking, i.e. visco-elastic rather than elasto-plastic;
- (2) What geometrical and seismo-stratigraphical configurations needs to be taken into account (1-D stratigraphy and/or 2-D buried and outcropping morphologies)

Once the geological configuration and geotechnical models have been provided, the most appropriate method of analysis can be chosen depending on the level of strain (e.g. effective rather than total stress analysis), hydraulic conditions (e.g. volume strain rather than pore pressure increase) and geometrical framework (e.g. 1-D rather than multidimensional analyses).

Data relative to the seismic/geotechnical/geological features of the site domain and input motion (Sections 4.2.2 and 4.2.3) are considered to feed numerical models aimed at simulating seismic wave propagation in the shallow subsoil by considering respective kinematic equations. In general such models are expected to capture the most significant

aspects of the propagation process and this can be a very difficult task. The direct physical mathematical approach can provide closed form solutions just for the case when a purely linear behaviour is assumed to characterize the subsoil materials and the relevant bodies are characterized by simple geometries (e.g. flat Earth with parallel horizontal layers) [155]. In all the other cases, numerical methods become necessary and this makes the final result less constrained and controllable.

As a function of the numerical procedure adopted for evaluating site response one can distinguish: linear models, linear equivalent model and fully nonlinear models. With respect to geometries of seismic impedance interfaces in the site domain one can cite procedures dealing with 1-D, 2-D and 3-D configurations.

Numerical models range from simple and numerically cost effective procedures (1-D linear model) to most complex and computationally expensive (3-D fully nonlinear) models (Table 2.). Choosing among numerical models (from 1-D linear to 3-D nonlinear) depends on two aspects:

- (1) The strain expected during the earthquake; and
- (2) Geometries within the site domain relative to the frequency range of interest.

TABLE 2. OVERVIEW OF REPRESENTATIVE CODES FOR NUMERICAL ESTIMATE OF THE SITE RESPONSE [156]. EL: EQUIVALENT LINEAR; NL: NONLINEAR; TS: TOTAL STRESSES; ES: EFFECTIVE STRESSES. OPEN: SOURCE CODE AVAILABLE; FREE: FREWARE; SHARE: SHAREWARE; PAY: COMMERCIAL

Geometry	Computer code	Available	Analysis	
1-D	SHAKE 91(http://nisee.berkeley.edu/software/)	Open	EL	TS
	EERA (http://www.ce.memphis.edu/7137/eera.htm)	Free		
	STRATA (http://nees.org/resources/strata)	Free		
	PROSHAKE (http://www.proshake.com/)	Pay		
	NERA(https://sites.google.com/site/tt60898/home/software)	Free	NL	ES
	DEEPSOIL(http://deepsoil.cee.illinois.edu/), freeware	Free		
	DMOD2000(http://www.geomotions.com/), commercial	Pay		
2-D	QUAD-4 (http://nisee.berkeley.edu/software/)	Open	EL	TS
	QUAKE/W (http://www.geo-slope.com/)	Pay		
	OPENSEES (http://opensees.berkeley.edu/)	Open	NL	ES
	DYNAFLOW (http://www.princeton.edu/~dynaflow/)	Share		
3-D	FLUSH (http://nisee.berkeley.edu/software/)	Open	EL	TS
	PLAXIS (http://www.plaxis.nl/)	Pay	NL	ES
	FLAC (http://www.itascacg.com/)	Pay		

The choice among linear, linear equivalent and nonlinear models essentially depends on the strain expected during the earthquake in the site domain. Linear models can be considered useful just in the case that very small seismic waves are of concern (e.g. those provided by ambient vibrations induced by such as urban traffic).

Above this very low strain, linear equivalent numerical procedures can be used. In these procedures the medium is initially modelled assuming a pure visco-elastic (linear) behaviour with parameters corresponding to very low strain conditions (initial stiffness and damping). In this way, the strain is evaluated for each point. These preliminary strain evaluations are used to modify the seismic parameters according to the relevant reduction curve (see Fig. 33). Then, seismic wave propagation is modelled again by considering a new linear model with the modified parameters. This procedure is iterated until no further modification of the visco-

elastic parameters is necessary and full compatibility with the strain level is reached. Most common procedures for site response evaluations are of this kind. In general, the role of fluids is neglected and the methods operate by considering total stress only. In this kind of modelling, a time history is unnecessary and a reference earthquake can be represented in the form of the relevant spectrum (Fourier or response) since the computations are performed in the spectral domain by considering the amplitude variations of the monochromatic waves propagating in the model. Suitable correction factors are required to account for the finite duration of the reference earthquake. Otherwise, the spectral amplitudes could be over predicted [146].

When the strain exceeds the volumetric threshold, fully nonlinear modelling becomes crucial since equivalent nonlinear models are not able to provide realistic results. In this case, the kinematic equations are solved step by step by modifying the relevant parameters during the integration by also taking into account the role of fluids (effective stress is considered). This approach, beyond its apparent completeness, involves a number of assumptions (e.g. concerning the role of fluids) and requires a large number of numerical integrations and differentiations that can be responsible for significant numerical problems hampering the convergence of the relevant procedure to a realistic solution. To be correctly applied, the time history of the reference earthquake has to be provided. This makes the outcome sensitive to details of the accelerometric records, which have to be selected carefully. Both these features make the application of this kind of modelling quite troublesome, and this is why the linear equivalent approach remains the most used for common applications where relatively low strains are of concern.

The use of 1-D models implies that lateral variations in the seismic and geotechnical characteristics in the subsoil can be considered as negligible in the site domain or, equivalently, these are characterized by wavelengths much larger than those of the seismic waves of interest. A typical example of this kind is the site response expected at the centre of a flat, thin and large alluvial basin.

In this kind of model, the subsoil is assumed to be a stack of uniform horizontal layers overlying a half space, and only the impedance contrasts at each interface of layers are considered. It is also assumed that seismic waves (input motion) only travel vertically from the bottom of bedrock. In this case, propagation matrices approaches make the numerical solution of the problem quite fast and computationally simpler.

When the lateral variation becomes important, the application of 2-D and 3-D models is necessary. Typically this is the case with small and deep basins, where the ratio of thickness and lateral extension becomes small (generally <0.25) or where surface topography shows strong gradients. In these cases the topographic roughness at the wavelength of interest, the interference of the seismic waves becomes complex, with a strong role also played by the direction of impinging seismic waves. A number of numerical approaches exist to face the problem of 2-D–3-D modelling: FDM, Finite Element Method (FEM), Boundary Element Method (BEM), Spectral Element Method (SEM) and Hybrid methods that are combinations of the other methods. The main differences among these approaches are the possibility they offer to implement complex geometries and their computational efficiency.

Whatever the numerical procedure considered for modelling, a basic problem related to the discretization of the subsoil model exists. Most in soft soil seismic features (rigidity, etc.) present smooth patterns that cannot easily translate into uniform bodies separated by relatively sharp interfaces typical of numerical simulations. In some cases, these artificial interfaces may produce spurious and unrealistic interference phenomena that can bias site response evaluations. Furthermore, when linear equivalent numerical models are considered, the presence of unnecessary sharp interfaces may prevent the convergence of the underlying iterative procedure. To cope with this problem, discretization needs to be conducted carefully by taking into account that increasing the number of bodies to simulate smooth variations in the subsoil parameters also increases the numerical complexity, mainly when 2-D–3-D modelling is of concern. A rule of the thumb in this case could be to consider the smaller wavelength of concern λ_{\min} and to take this value as an upper bound for the scale of element size discretization δ , e.g. the minimum size of the bodies considered in the modelling.

4.2.4. Managing modelling uncertainty

Whatever numerical approach is considered to compute site response, the final outcomes have to be considered as affected by significant uncertainty. These depend on the imperfect knowledge of the soil geometry and the uncertain geotechnical parameterization in particular strain dependent damping factors. A further important source of uncertainty is the reference earthquake to be considered. A last source of uncertainty are approximations considered in the numerical modelling (1-D vs. 2-D–3-D; linear equivalent vs. nonlinear). Despite the fact that these sources of uncertainty may dramatically affect the computed site response, up to recent times, this aspect was simply overlooked.

The parameterization of such sources of uncertainty and of their effect is actually difficult to perform due to the strong nonlinearity of the computational procedure (in particular when linear equivalent and nonlinear procedures are considered) and to the possible interaction between the relevant parameters. In this situation, Monte Carlo approaches have been considered to evaluate the impact of uncertain input values on the final outcome. In the STRATA code [145], several sources of uncertainty are considered in the framework of a 1-D linear equivalent computational scheme. In this case, several possible input reference ground motions (real and artificial) are considered to explore the effect of input motion uncertainty. Uncertainty concerning geotechnical (backbone curve for stiffness and damping variations as function of strain), seismic (V_s values) and geometrical (thickness of the layers) properties are considered. For each run, the typical 1-D linear equivalent analysis is performed by considering the input motion and subsoil parameters computed by randomly varying the relevant values within a range defined by the operator and following a fixed probability distribution around the average values. Some constraints can be applied to reduce the interlayer variability that could result in unrealistic profiles. The whole procedure is performed a number of times (of the order of hundreds) in order to explore the possible range of solutions. In this way a number of site response evaluations (all compatible with available information and uncertainty ranges) can be obtained, which are representative of uncertainty affecting the final estimate (Fig. 36 as an example). As a result, depending on the applied guidelines and requested safety levels, mean site response estimates or conservative site response estimates can be computed.

The one here described represents a first attempt in the direction of a more conscious approach to numerical evaluations of the site response. In principle, this approach could be extended to other more complex computational schemes (2-D nonlinear, etc.) but it becomes very time consuming.

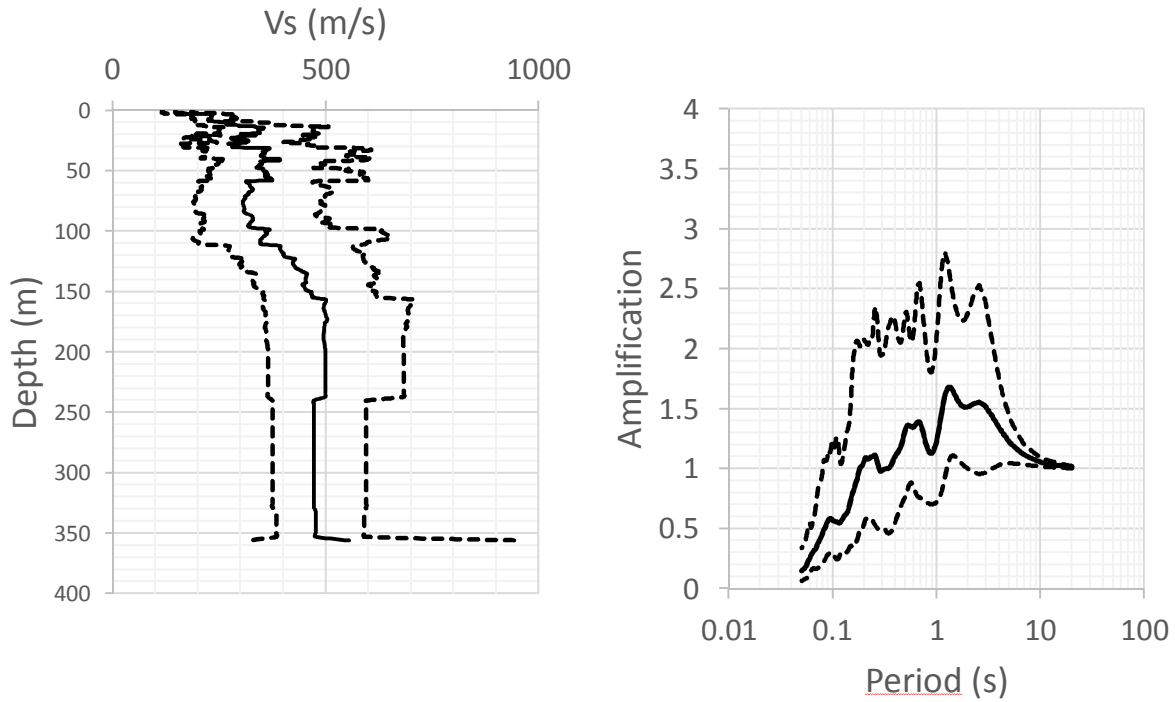


FIG. 36. The impact of uncertainty affecting the V_s profile (on the left) on the site response in terms of amplification function (on the right). Solid lines indicate the median value and dashed lines include the 68% of estimates. The simulation has been obtained by the software STRATA [145].

4.3. EMPIRICAL SITE RESPONSE EVALUATION

Several techniques have been proposed to evaluate the site response by the analysis of observed ground motion records [157]. All of them are based on the assumption that the subsoil linearly responds to waves produced by distant earthquakes: this limits their reliability when nonlinear behaviour of the soil comes into the play due to the size of ground shaking. Furthermore, 2-D–3-D effects cannot be easily identified on the basis of this approach. Anyway, beyond the doubtless importance of seismic monitoring at the sites of nuclear installation, these approaches play a fundamental role for site effect assessment since their outcomes represent a fundamental benchmark for theoretical/computational approaches. For this purpose, numerical analyses have to be repeated for weak input motions before being tested against empirical outcomes.

4.3.1. Standard Spectral Ratio

The most straightforward way to assess site response is by direct measuring lateral variations in the ground motion during earthquakes. In this regard, the Standard Spectral Ratio (SSR) technique [158] is the most popular one. In this approach, the ratio of Fourier amplitude spectra of a soil site earthquake record to that of a reference station for the same earthquake is considered as representative of the local seismic response. Here, the ground motion at the reference station is considered to be representative of the source and long range propagation effects. Effectiveness of this approach depends on a number of very restrictive prerequisites:

- A reference site exists that can be considered to be free from the site response to be determined;
- Simultaneous recordings exist at the soil site and at the reference station;
- Distance between the site and the reference station is small with respect to the hypocentral distance in order to consider that the propagating path is the same for the site and reference station; and
- Available observed recordings can be representative of the target ground motion.

First of all, the identification of the reference station nearby the site under study is of paramount importance. In general, when available, stations located on outcropping rocks are considered for this purpose. However, experimental evidence suggests [159] that rock sites are not always absent of site response due to a number of factors (e.g. near surface weathering and cracking and morphological irregularities). This implies that site response of the reference site has to be assessed in advance making the whole approach ineffective. Furthermore, the seismic bedrock below the site and reference outcrops could be represented by different geological units. The availability of borehole data (obtained by drilling into the buried local seismic bedrock) can overcome this drawback when the possible effect of the down going wave field and the resulting destructive interference is accounted for.

Another important problem arising in the SSR approach is the availability of earthquake records representative of the reference earthquake. To apply the SSR procedure, the deployment of relatively dense local seismic networks is necessary. In general, in low seismicity areas (where it is desirable that nuclear installations are located), long lasting seismic monitoring is necessary to capture strong ground motions. In many cases, however, only weak ground motions are recorded and thus, the eventual nonlinear behaviour induced by strong ground motion cannot be accounted for.

Results provided by the SSR approach to evaluate morphological effects need to be considered with caution. In fact, due the expected de-amplification at the base of relief resulting SSRs could be biased towards an overestimate of the relevant site response. Furthermore, the base of the hill is in many cases constituted by deposits coming from the erosion of outcropping rocks. This implies that site response at the reference station needs to be accounted for, along with the possible presence of regolith or alteration layers at the top of the relief.

The above features make the application of the SSR technique difficult for a correct and reliable evaluation of the site response both in the case of stratigraphical and morphological effects.

A possible alternative to overcome partially difficulties in the application of SSR with a reference site has been proposed by Si et al. (2010) [160]. In this case spectral ratios are performed by considering as reference spectral response deduced by suitable GMPEs. In particular, the empirical site response function $R(f)$ for the frequency f is given in the Eq. 23.

$$R(f) = \left(\sum_{i=1}^n \frac{O(f)}{O'(f)} \right) \frac{1}{n} \quad (23)$$

where the index i represents an observed record, n is the total number of records used for site effect estimation for each station, $O(f)$ is the root mean square of the two maximum horizontal components and $O'(f)$ is the predicted ground motion using a reference GMPE defined for the reference soil configuration. The effectiveness of this approach relies entirely on the effectiveness of the considered GMPE for the reference soil configuration and on the actual availability of earthquake records representative of the reference earthquake.

4.3.2. Receiver function

This approach aims at the definition of the local transfer function by using horizontal and vertical components of records at a single station [161]. The basic hypothesis underlying this approach is that, on average, the vertical component of observed ground motion relative to body waves contains more information on the source of ground motion than does the horizontal components. In fact, by following Langston [162], in the case of sub horizontal layering, the vertical component of teleseisms (e.g. earthquakes characterized by large epicentral distances) is assumed to be relatively uninfluenced by the local subsoil configuration, whereas the radial component contains P - to S -wave conversions from structural discontinuities below the site. In this view, spectral ratios between horizontal and vertical component are considered informative about the local transfer function. In particular, the maxima of the spectral ratio curves as a function of frequency are found to reveal the frequency dependence of the site response at the sediment sites, and the results for the seismic bedrock are relatively flat and near unity. On the other hand, with this approach it is not likely to correctly estimate the frequency dependent scaling factor, i.e. the actual amplitude of the transfer function. This approach mimics, on a different physical basis, the one proposed by Nakamura [163, 164], which is based on the analysis of horizontal vs. vertical average spectral ratios of ambient vibrations and also presents analogous limitations [165].

4.3.3. Blind deconvolution

An approximate site effect can be evaluated using the observed records at two different stations on the surface of the sediment layer. The advantage of the method is that it does not require any preliminary knowledge of the relevant seismic sources (the approach is *blind* in this sense). The explanation of the method is introduced further in Ref. [147] as following:

“The approach does not require recordings at depth nor at a nearby rock outcrop, and eliminates the need for any prior parameterization of source and site characteristics. It considers that the surface recordings are the result of the convolution of the ‘input motion at depth’ with transfer functions (channels) representing the characteristics of the transmission path of the waves from the input location to each recording station. The input motion at depth is considered to be the common component in the seismograms (same input in a statistical sense). The channel characteristics are considered to be the part in the seismograms that is non-common, since the travel path of the waves from the input motion location at depth to each recording station is different, due to spatially variable site effects. By means of blind deconvolution, the algorithm eliminates what is common in the seismograms, namely the input motion at depth, and retains what is different, namely the transfer functions of the site from the input location to each recording station. It estimates the site response in both frequency and time domains, and identifies the duration of the site’s transfer functions.”[147]

4.3.4. Spectral modelling

Another possibility to use weak motion data to characterize the site response at low strains when reference sites are not available is described is spectral modelling [166]. In this case, the site responses are determined by inverting seismograms relative to a number of weak earthquakes monitored by a seismic network. In this inversion, the Fourier velocity spectrum $\Omega_{ij}(f, r)$ observed at the j -th station located at hypocentral distance r from the point like seismic source of the i -th earthquake is represented as a function of the frequency f in the Eq. (24).

$$\Omega_{ij}(f, r) = 2\pi f E_i(f) B_{ij}(f) S_{ij}(r) T_j(f) I_j(f) \quad (24)$$

where $E_i(f)$ is the source model (the amplitude spectrum at the source), $B_{ij}(f)$ is attenuation along the ray path, $S_{ij}(r)$ is the amplitude decay with distance or apparent geometrical spreading, $T_j(f)$ is the site transfer function at the station and $I_j(f)$ is the instrument response function. Each of these components are then modelled by considering relatively simple functional forms depend on a number of parameters of to be determined empirically by considering a large set of weak motion data. A basic problem of this approach is that the simultaneous inversion of a large number parameters is fraught by trade-offs and ambiguities that require careful statistical analyses [166]). In the spectral modelling approach, $T_j(f)$ is considered in the Eq. (25) [167].

$$T_j(f) = A_j a_j(f) e^{-\pi f k_j} \quad (25)$$

where A_j is the average site response relative to the unknown reference site (the average site response over all frequencies), $a_j(f)$ is the frequency dependent site response function and k_j is a constant representative of the low strain damping at the site.

It is worth noting that in this approach, although appealing in principle, the site response contributions $T_j(f)$ are essentially the residuals of the inversion relative to the other contributions and hence are more susceptible to noise and instrument calibration errors. Furthermore, the site parameterization obtained this way only concerns low strain dynamical behaviour of soils and when obtained from weak motion measurements only, may provide estimates for site response during strong motion that may be significantly biased.

5. SUMMARIES

This publication deals with two topics that are commonly used in seismic hazard assessment: GMPE and site response analysis, and with the interface between these analyses. Both of these topics aim at forecasting characteristics of the ground motion induced at a site by a seismic source. The problem is addressed by focusing on the two main groups of features that characterize ground motion generation: the effect of source geometry and long range propagation of seismic waves (GMPEs), and that of small scale interference phenomena induced by local heterogeneities in the subsurface configuration and geomorphology near the site (local site response), respectively. The first group of features is approached by considering simplified models that are physically motivated and then parameterized empirically. The other group is approached by jointly considering numerical modelling and seismic observations that take advantage of geological, geophysical and geotechnical data available at the site of interest.

Despite inherent differences, GMPEs and site response studies are not independent and a clear boundary between them cannot be easily drawn. Furthermore, their harmonization is necessary to provide reliable seismic hazard estimates at a nuclear installation. In spite of this link, the main aspects of GMPEs and site response are necessarily described separately in the text.

5.1. GROUND MOTION PREDICTION EQUATION

For GMPEs the fundamental issues, including the treatment of the source, path and site conditions are introduced. The controlling independent variables, including their physical meanings and their limitations and some sample functional forms employed in GMPEs are described in this publication. The information is neither definitive nor comprehensive, but it is expected to be useful for readers to understand and apply GMPEs in seismic hazard assessment.

Another practical aspect for the application of GMPEs in the assessment of hazards for nuclear installations is the selection of GMPEs and when an appropriate local GMPE is not available, an adjustment of GMPEs from other regions where the models are well constrained. Fundamental but also practical information on these issues is introduced in the publication.

The importance of the interface between GMPEs and site response is addressed in this publication. The GMPEs only can estimate ground motion for site conditions implicit or explicit to the GMPE. The ground motion on the specific site condition at the nuclear installations will subsequently be estimated based on site response analysis.

Finally, the information on useful data resources on the seismic source, the sources of ground motion data and an example of practices of GMPE application for nuclear installation sites in Japan are introduced in the Appendix and Annex.

5.2. SITE RESPONSE

Both numerical and empirical approaches for the definition of the local seismic response are described in the text. These two approaches need to be seen as complementary, as each has its own distinctive advantages and drawbacks.

Numerical modelling of the site response requires a detailed knowledge of the subsurface configuration and surface morphology at a scale that is of the same order of the seismic wavelengths of main concern. A three level approach to the retrieval of this information has been described that includes: extensive geological surveys, in situ geophysical prospecting and laboratory analyses.

The importance of possible nonlinear dynamical behaviour of near surface materials to seismic loads is stressed and the importance of adopting correct simulation procedures is emphasized. Major aspects relative to such modelling are outlined.

Empirical methods devoted to the estimation of site response by direct monitoring of seismic ground motion are also presented. Despite the fact that in many situations seismic monitoring only allows evaluating seismic response of the local subsoil to relatively small earthquakes (generally smaller than the controlling earthquake to be used for the design), the importance of this kind of empirical analysis cannot be overlooked since it represents a fundamental benchmark for testing and tuning procedures considered for the numerical modelling of the site response.

APPENDIX: EXAMPLES OF AVAILABLE DATA

The Appendix presents examples of publicly available data as of end of 2015. Table 3 lists examples of strong motion data. The USA site classification is introduced in the Section 2 of this appendix and the site classification in EU is introduced in Table 4. Furthermore, examples of earthquake catalogue are given in Table 5 followed by a list of examples of fault rupture models, which are introduced in Table 6. Further increase of the available database is expected in the future, intending to greatly contribute to the reliability of the seismic hazard assessment.

1. Information on strong motion database

TABLE 3. IDENTIFIES SEVERAL WEB SITES THAT WERE ACTIVE IN 2015 AS SOURCES OF STRONG MOTION DATA

Global strong motion databases	
Organization	Web Site
PEER, Ground Motion Database	http://ngawest2.berkeley.edu/
CESMD, Center for Engineering Strong Motion Data	http://strongmotioncenter.org/
COSMOS, Strong Motion Virtual Data Center (VDC)	http://strongmotioncenter.org/vdc/scripts/default.pl
NGDC/NOAA, Earthquake Strong Motion Data Catalog (1933-1994)	http://www.ngdc.noaa.gov/nndc/struts/form?t=101650&s=34&d=34
Regional strong motion databases	
Organization	Web Site
ORFEUS/ESM, European Strong Motion DB	http://esm.mi.ingv.it/
RESORCE, Reference database for seismic ground motion prediction in Europe	http://www.resorce-portal.eu/
ESD, the European Strong Motion Database	http://www.isesd.hi.is/
ITACA, Italian Accelerometric Archive	http://itaca.mi.ingv.it/
SED, Swiss Seismological Service	http://arclink.ethz.ch/webinterface/
NIED, Japan Strong motion Seismograph Networks (K-NET, KiK-net)	http://www.kyoshin.bosai.go.jp/
Strong Ground Motion Database of Turkey	http://kyhdata.deprem.gov.tr/
ITSAK, Greek Strong Motion Data	http://www.itsak.gr/en/page/data/strong_motion/
GeoNet, New Zealand Strong Motion Data	http://info.geonet.org.nz/display/appdata/Strong-Motion+Data

CNSN, Canadian National Seismograph Network	http://earthquakescanada.nrcan.gc.ca/stnsdata/cnsn/
IES, Institute of Earth Sciences, Academia Sinica, Data management center for strong motion seismology	http://www.earth.sinica.edu.tw/~smdmc/
PESMOS, Indian Strong Motion Instrumentation Project	http://pesmos.in/2011/
BHRC-ISMB, Iran Strong Motion Network	http://site.bhrc.ac.ir/portal/ismnen/Home.aspx

Note: As for December 2015. The list may be incomplete due to temporarily unavailable networks

Some publicly available project databases provide a compilation, homogenization and sometimes even a reprocessing of strong ground motion data. Examples of such project databases are NGA, SHARE or SIGMA.

How the database used influences the GMPEs is described in Douglas et al (2014) [168] and Gregor et al (2014) [169].

2. Examples of site classification²

The Site Classes are defined as follows in NEHRP recommended provision.

- A Hard rock with measured shear wave velocity, $\bar{V}_s > 5,000$ ft/sec (1500 m/s)
- B Rock with $2,500$ ft/sec $< \bar{V}_s \leq 5,000$ ft/sec (760 m/s $< \bar{V}_s \leq 1500$ m/s)
- C Very dense soil and soft rock with $1,200$ ft/sec $< \bar{V}_s \leq 2,500$ ft/sec (360 m/s $< \bar{V}_s \leq 760$ m/s) or with either $N > 50$ or $\bar{s}_u > 2,000$ psf (100 kPa)
- D Stiff soil with 600 ft/sec $\leq \bar{V}_s \leq 1,200$ ft/sec (180 m/s $\leq \bar{V}_s \leq 360$ m/s) or with either $15 \leq \bar{N} \leq 50$ or $1,000$ psf $\leq \bar{s}_u \leq 2,000$ psf (50 kPa $\leq \bar{s}_u \leq 100$ kPa)
- E A soil profile with $\bar{V}_s < 600$ ft/sec (180 m/s) or with either $\bar{N} < 15$, $\bar{s}_u < 1,000$ psf, or any profile with more than 10 ft (3 m) of soft clay defined as soil with $PI > 20$, $w \geq 40$ per cent and $s_u < 500$ psf (25 kPa)
- F Soils requiring site specific evaluations:

² This site classification is based on Ref. [170].

1. Soils vulnerable to potential failure or collapse under seismic loading such as liquefiable soils, quick and highly sensitive clays, collapsible weakly cemented soils.

Exception: For structures having fundamental periods of vibration less than or equal to 0.5 second, site specific evaluations are not required to determine spectral accelerations for liquefiable soils. Rather, the Site Class may be determined in accordance with the stepwise classification and the site coefficient scheme by NEHRP.

2. Peat and/or highly organic clays ($H > 10$ ft [3 m] of peat and/or highly organic clay, where H = thickness of soil).

3. Very high plasticity clays ($H > 25$ ft [8 m] with $PI > 75$)

4. Very thick, soft/medium stiff clays ($H > 120$ ft [36 m]) with $\overline{s_u} < 1,000$ psf (50 kPa)

Note: \overline{N} is the standard penetration resistance; PI is the plasticity index; $\overline{s_u}$ is the undrained shear strength; w is the moisture content in percent; and $\overline{V_s}$ is the shear wave velocity average down to 100 ft (30m).

TABLE 4. SITE CLASSIFICATION IN EUROCODE 8 (Reproduced with permission from [94])

Subsoil	Description of stratigraphic profile	Parameters		
		$V_{s,30}$ [m/s]	N_{SPT} (blows/30cm)	c_u [kPa]
A	Rock or other rock like geological formation, including at most 5 m of weaker material at the surface.	> 800	—	—
B	Deposits of very dense sand, gravel, or very stiff clay, at least several tens of meters in thickness and characterized by a gradual increase of mechanical properties with depth.	360 – 800	> 50	> 250
C	Deposits of very dense sand, gravel, or very stiff clay, at least several tens of meters in thickness and characterized by a gradual increase of mechanical properties with depth.	180 – 360	15 – 50	70 – 250
D	Deposits of loose to medium non cohesive soil (with or without some soft cohesive layers), or of predominantly soft to firm cohesive soil.	< 180	< 15	< 70
E	A soil profile consisting of a surface alluvium layer with V_s values of type C or D and thicknesses varying between 5 m and 20 m, underlain by stiffer materials with $V_s > 800$ m/s.			
S ₁	Deposits consisting or containing a layer at least 10 m thick of soft clays/silts with high plasticity index ($PI > 40$) and high water content.	< 100	—	10 – 20
S ₂	Deposits of liquefiable soils, sensitive clays, or any other soil profile not included in types A-E or S ₁ .			

3. Databases of source information

TABLE 5. EXAMPLES OF AVAILABLE CATALOGUES OF SEISMIC SOURCE INFORMATION

Organization	Website
The Global Centroid Moment Tensor (CMT) Project	http://www.globalcmt.org/
Incorporated Research Institutions for Seismology	http://www.iris.edu/seismon/
U.S. Geological Survey	http://earthquake.usgs.gov/earthquakes/search/
Japan Meteorological Agency	http://www.seisvol.kishou.go.jp/eq/mech/index.html (Japanese website with information in English)
F-NET by National Research Institute for Earth Science and Disaster Prevention	http://www.fnet.bosai.go.jp/event/joho.php?LANG=en
International Seismological Centre (ISC)	http://www.isc.ac.uk/

TABLE 6. EXAMPLES OF AVAILABLE SOURCES FOR FINITE SOURCE MODEL AND RELATED PARAMETERS

Organization	Website
Finite source rupture model database operated by Paul Martin Mai	http://equake-rc.info/srcmod/
Earthquake Research Institute, the University of Tokyo	http://www.eri.u-tokyo.ac.jp/sanchu/Seismo_Note/
Earthquake and Volcano Research Center, Nagoya University	http://www.seis.nagoya-u.ac.jp/sanchu/Seismo_Note/
The Pacific Earthquake Engineering Research Center (PEER)	http://peer.berkeley.edu/nga/flatfile.html
The Pacific Earthquake Engineering Research Center (PEER)	http://peer.berkeley.edu/ngawest2/databases/

REFERENCES

- [1] INTERNATIONAL ATOMIC ENERGY AGENCY, Seismic Hazards in Site Evaluation for Nuclear Installations, IAEA Safety Standards Series No. SSG-9, IAEA, Vienna (2010).
- [2] CAMPBELL, K.W., Strong motion attenuation relations: a ten year perspective, *Earthq. Spectra* **1** 4 (1985) 759–803.
- [3] FUKUSHIMA, Y., Survey of recent studies on attenuation relation of strong ground motion (Empirical Prediction Relation) *J. Seismol. Soc. Jpn.*, Zisin II, **46** 3 (1993) 315–328 (in Japanese with English abstract).
- [4] ABRAHAMSON, N.A., SHEDLOCK, K.M., Overview, *Seismol. Res. Lett.* **68** 1 (1997) 9–23.
- [5] CAMPBELL, K.W., “A contemporary guide to strong motion attenuation relations” in *International Handbook of Earthquake and Engineering Seismology*, (LEE, W.H.K., KANAMORI, H., JENNINGS, P.C., KISSLINGER, C., Eds) Academic Press, London (2002a).
- [6] DOUGLAS, J., Earthquake ground motion estimation using strong motion records: a review of equations for the estimation of peak ground acceleration and response spectral ordinates, *Earth-Sci. Rev.* **61** (2003) 43–104.
- [7] ABRAHAMSON, N., et al., Comparisons of the NGA ground motion relations, *Earthq. Spectra* **24** 1 (2008) 45–66.
- [8] MIDORIKAWA, S., Ground motion attenuation relations, *J. Seismol. Soc. Jpn.* **61** (2009) S471–S477 (in Japanese).
- [9] SI, H., MIDORIKAWA, S., New attenuation relationships for peak ground acceleration and velocity considering effects of fault type and site condition, *J. Struct. Construct. Eng. AIJ* **523** (1999) 63–70 (in Japanese with English abstract).
- [10] RICHTER, C.F., An instrumental earthquake magnitude scale, *Bull. Seismol. Soc. Am.* **25** (1935) 1–32.
- [11] HEATON, T.H., TAJIMA, F., MORI, A.W., Estimating ground motions using recorded accelerograms, *Surv. Geophys.* **8** (1986) 25–83.

- [12] GUTENBERG, B., Amplitudes of surface waves and magnitude of shallow earthquakes, *Bull. Seismol. Soc. Am.* **35** (1945) 3–12.
- [13] TSUBOI, C., Determination of the Gutenberg-Richter magnitude of earthquakes occurring in and near Japan, *J. Seismol. Soc. Jpn. Zisin II*, **7** (1954) 185–193.
- [14] HANKS, T.C., KANAMORI, H., A moment magnitude scale, *J. Geophys. Res.* **84** (1979) 2348–2350
- [15] CROUSE, C.B., VYAS, Y.K., SCHELL, B.A., Ground motion from subduction-zone earthquakes, *Bull. Seismol. Soc. Am.* **78** 1 (1988) 1–25.
- [16] MOLAS, G.L., YAMAZAKI, F., Attenuation of earthquake ground motion in Japan including deep focus events, *Bull. Seismol. Soc. Am.* **85** 5 (1995) 1343–1358.
- [17] YOUNGS, R.R., CHIOU, S.-J., SILVA, W.J., HUMPHREY, J.R., Strong ground motion attenuation relationships for subduction zone earthquakes. *Seismol. Res. Lett.* **68** 1 (1997) 58–73.
- [18] KANNO, T., NARITA, A., MORIKAWA, N., FUJIWARA, H., FUKUSHIMA, Y., A new attenuation relation for strong ground motion in Japan based on recorded data, *Bull. Seismol. Soc. Am.* **96** 3 (2006) 879–897.
- [19] ZHAO, J.X., et al., Attenuation relations of strong ground motion in Japan using site classification based on predominant period, *Bull. Seismol. Soc. Am.* **96** 3 (2006) 898–913.
- [20] ABRAHAMSON, N., SILVA, W., Summary of the Abrahamson & Silva NGA ground motion relations, *Earthq. Spectra* **24** 1 (2008) 67–97.
- [21] CAMPBELL, K.W., BOZORGNI, Y., NGA ground motion model for the geometric mean horizontal component of PGA, PGV, PGD and 5% damped linear elastic response spectra for periods ranging from 0.01 to 10s, *Earthq. Spectra* **24** 1 (2008b) 139–171.
- [22] CHIOU, B.S.-J., YOUNGS, R.R., An NGA model for the average horizontal component of peak ground motion and response spectra. *Earthq. Spectra* **24** 1 (2008) 173–215.

- [23] STEWART, J.P., et al., Selection of ground motion prediction equations for the global earthquake model, *J. Earthq. Spectra* **31** (2015) 19–45.
- [24] ALLMANN, B.P., SHEARER P.M., Global variations of stress drop for moderate to large earthquakes, *J. Geophys. Res.* **114** B013110 (2009).
- [25] MITCHELL, B.J., CONG, L., EKSTROM, G., A continent-wide map of 1-Hz Lg coda Q variation across Eurasia and its relation to lithospheric evolution, *J. Geophys. Res.* **113** B04303 (2008).
- [26] PAYSANOS, M., A lithospheric attenuation model of North America, *Bull. Seism. Soc. Am.* **103** (2013).
- [27] ATKINSON, G.M., BOORE, D.M., Earthquake ground motion prediction equations for eastern North America, *Bull. Seismol. Soc. Am.* **96** 6 (2006) 2181–2205.
- [28] SI, H., MIDORIKAWA, S., TSUTSUMI, H., WU, C., MASATSUKI, T., NODA, A., Preliminary analysis of attenuation relationship for response spectra on bedrock based on strong motion records including the 2011 M_w 9.0 Tohoku earthquake, (Proc. 10th Int. Conf. Urban Earthq. Eng. March 1–2, 2013) Tokyo Institute of Technology, Tokyo, Japan (2013) 113–117.
- [29] BOMMER, J.J., DOUGLAS, J., STRASSER, F.O., Style-of-faulting in ground motion prediction equations, *Bull. Earthq. Eng.* **1** (2003) 171–203.
- [30] BOORE, D.M., ATKINSON, G.M., Ground-motion prediction equations for the average horizontal component of PGA, PGV and 5%-damped PSA at spectral periods between 0.01s and 10.0s, *Earthq. Spectra* **24** 1 (2008) 99–138.
- [31] SOMERVILLE, P.G., SMITH, N.F., GRAVES, R.W., ABRAHAMSON, N.A., Modification of empirical strong ground motion attenuation relations to include the amplitude and duration effects of rupture directivity. *Seismol. Res. Lett.* **68** 1 (1997) 199–222.
- [32] AGUIRRE, J., IRIKURA, K., Source characterization of Mexican subduction earthquakes from acceleration source Spectra for the prediction of strong ground motions, *Bull. Seismol. Soc. Am.* **7** (2007) 1960–1969.

- [33] BALTAY, A.S., HANKS, T.C., BEROZA, G.C., Stable stress drop measurements and their variability: implications for ground motion prediction, *Bull. Seismol. Soc. Am.* **103** 1 (2013).
- [34] HANKS, T.C., f_{\max} , *Bull. Seismol. Soc. Am.* **71** (1982) 1867–1879.
- [35] KATAOKA, S., KUSAKABE, T., Attenuation relations of acceleration response spectrum using stress drop as a regressor, *JSCE, J. Earthq. Eng.* **27** (2003) 51 (in Japanese with English abstract).
- [36] RADIGUET, M., COTTON, F., MANIGHETTI, I., CAMPILLO, M., DOUGLAS, J., Dependency of near-field ground motions on the structural maturity of the ruptured faults, *Bull. Seismol. Soc. Am.* **99** (2009) 2572–2581.
- [37] DAN. K., MUTO, M., TORITA, H., OHASHI, Y., KASE, Y., Basic examination on consecutive fault rupturing by dynamic rupture simulation, *Annual Report on Active Fault and Paleo earthquake Researches, AIST, Geol. Surv. Jpn* (2007) 7 259–271 (in Japanese with English abstract).
- [38] ABRAHAMSON N.A., SOMERVILLE, P.G., Effects of the hanging wall and footwall on ground motions recorded during the Northridge earthquake. *Bull. Seismol. Soc. Am.* **86** 1B (1996) S93–S99.
- [39] SPUDICH, P., CHIOU, B.S.J., Directivity in NGA earthquake ground motions: analysis using isochrone Theory. *Earthq. Spectra* **24** 1 (2008) 279–298.
- [40] SPUDICH, P., et al., Final Rep. NGA-West2 Directivity Working Group, PEER (2013) http://peer.berkeley.edu/publications/peer_reports/reports_2013/webPEER-2013-09-Spodich.pdf.
- [41] SOMERVILLE, P.G., Magnitude scaling of the near-fault rupture directivity pulse, *Phys. Earth Planet. Int.* **137** (2003) 201–212.
- [42] KAGAWA, T., IRIKURA, K., SOMERVILLE, P., Differences in ground motion and fault rupture process between surface and buried rupture earthquakes, *Earth Planets Sp.* **56** (2004) 3–14.
- [43] ABRAHAMSON, N., SILVA, W., Empirical response spectral attenuation relations for shallow crustal earthquakes, *Seismol. Res. Lett.* **68** 1 (1997).

- [44] OHNO, S., OHTA, T., IKEURA, T., TAKEMURA, M., Revision of attenuation formula considering the effect of fault size to evaluate strong motion spectra in near field. *Tectonophysics* **218** 8 (1993) 69–81.
- [45] OHNO, S., TAKAHASHI, K., MOTOSAKA, M., Empirical estimation of horizontal and vertical motions based on California earthquake records and its application to Japan inland earthquakes, *J. Struct. Constr. Eng. (Transactions of AIJ)* 544 (2001) 39–46 (in Japanese with English abstract)
- [46] NODA, S.H., et al., Response Spectra for Design Purpose of Stiff Structures on Rock Sites, OECD/NEA Workshop on the Relations Between Seismological Data and Seismic Engineering, Istanbul, 16–18 October 2002.
- [47] DHAKAL, Y.P., TAKAI, N., SASATANI, T., Empirical analysis of path effects on prediction equations of pseudo-velocity response spectra in northern Japan, *Earth. Engng. Struct. Dyn.* **39** (2010) 443–461.
- [48] MORIKAWA N., KANNO T., NARITA A., FUJIWARA H., FUKUSHIMA Y., Additional Correction Terms for Attenuation Relations Corresponding to the Anomalous Seismic Intensity in Northeast Japan, *J. Jpn. Assoc. Earthq. Eng.* 3-1 (2003) 14–26 (in Japanese with English abstract).
- [49] MIDORIKAWA, S., OHTAKE, Y., “Attenuation relationships of peak ground acceleration and velocity considering attenuation characteristics for shallow and deeper earthquakes”, *Proc. 11th Japan Earth. Eng. Symp.* (2002) 20–22 (in Japanese with English abstract).
- [50] NISHIMURA, T., HORIKE, M., The attenuation relationships of peak ground accelerations for the horizontal and the vertical components inferred from Kyoshin network data, *J. Struct. Construct. Eng. (Transactions of AIJ)* **571** (2003) 63–70 (in Japanese with English abstract).
- [51] HORIKE, M., NISHIMURA, T., Attenuation relationships of peak ground velocity inferred from the Kyoshin network data, *J. Struct. Construct. Eng. (Transactions of AIJ)* **575** (2004) 73–79 (in Japanese with English abstract).
- [52] COTTON, F., POUSSE, G., BONILLA, F., SCHERBAUM, F., On the discrepancy of recent European ground motion observations and predictions from empirical models:

analysis of KiK-net accelerometric data and point-sources stochastic simulations, Bull. Seismol. Soc. Am. **98** (2008) 2244-2261.

[53] ATKINSON, G., MORRISON, M., Observations on regional variability in ground motion amplitudes for small-to-moderate earthquakes in North America, Bull. Seismol. Soc. Am. **99** 4 (2009) 2393–2409.

[54] CHIOU, K., YOUNGS, R., ABRAHAMSON, N., ADDO, K., Ground-motion attenuation model for small-to-moderate shallow crustal earthquakes in California and its implications on regionalization of ground motion prediction models. Earthq. Spectr. **26** 4 (2010) 907–926.

[55] SI, H., KOKETSU, K., MIYAKE H., IBRAHIM, R., “High attenuation rate for shallow, small earthquakes in Japan”, Proc. 15th World Conference on Earthquake Engineering, Paper No. 3097 (2012).

[56] ANDERSON, J.G., Expected shape of regressions for ground motion parameters on rock, Bull. Seismol. Soc. Am. **90** (2000) S43–S52.

[57] BORCHERDT, R.D., GLASSMOYER, G., On the characteristics of local geology and their influence on ground motions generated by the Loma Prieta earthquake in the San Francisco Bay region, California, Bull. Seismol. Soc. Am. **82** (1992) 603–641.

[58] MIDORIKAWA, S., FUKUSHIMA, Y., Evaluation of site amplification factors based on average characteristics of frequency dependent Q^{-1} of sediment strata, J. Struct. Constr. Eng. Transaction of Architectural Institute of Japan, **460** (1994) 37–46.

[59] BOORE, D.M., JOYNER, W.B., Site amplifications for generic rock sites, Bull. Seismol. Soc. of Am. **87** 2 (1997) 327–341.

[60] FIELD, E.H., PETERSEN, M.D., A test of various site-effect parameterizations in probabilistic seismic hazard analyses of southern California, Bull. Seismol. Soc. Am **90** (2000) S222–S244.

[61] STEIDL, J.H., Site response in southern California for probabilistic seismic hazard analysis, Bull. Seismol. Soc. Am. **90** (2000) S149–S169.

[62] CHOI, Y., STEWART, J.P., Nonlinear site amplification as function of 30m shear wave velocity. Earthq. Spectra, **21** 1 (2005) 1–30.

- [63] MASUI, D., MIDORIKAWA, S., Site amplification characteristics due to deep ground structure in earthquake motions on engineering bedrock, *Doboku Gakkai Ronbunshuu*, **62** 2 (2006) 225–232 (in Japanese with English abstract).
- [64] KTENIDOU, O.J., COTTON, F., ABRAHAMSON, N.A., ANDERSON J.G., Taxonomy of κ : a review of definitions and estimation approaches targeted to applications, *Seismol. Res. Lett.* **85** (2014) 135–146.
- [65] ANDERSON, J.G., HOUGH, S.E., A model for the shape of the Fourier amplitude spectrum of acceleration at high frequencies, *Bull. Seismol. Soc. Am.* **74** (1984) 1969–1993.
- [66] ANDERSON, J.G., Implication of attenuation for studies of the earthquake source (EWING, M., Ed), *Geophysical Monograph 37* (Maurice Ewing Series 6), Reprinted from *Earthquake Source Mechanics*, American Geophysical Union, Washington DC (1986) 311–318.
- [67] ANDERSON, J.G. A preliminary descriptive model for the distance dependence of the spectral decay parameter in southern California, *Bull. Seismol. Soc. Am.* **81** (1991) 2186–2193.
- [68] PURVANCE, M.D., ANDERSON J.G., A comprehensive study of the observed spectral decay in strong motion accelerations recorded in Guerrero, Mexico, *Bull. Seismol. Soc. Am.* **93** (2003) 600–611.
- [69] BIASI, G.P., ANDERSON, J.G., Measurement of the parameter kappa and re-evaluation of kappa for small to moderate earthquakes at seismic stations in the vicinity of Yucca mountain, Nevada, Final Technical Report TR-07-007, Nevada System of Higher Education, Univ. Nev., Univ. Las Vegas (2007) 232 pp.
- [70] KILB, D., et al., A comparison of spectral parameter kappa from small and moderate earthquakes using southern California ANZA seismic network data, *Bull. Seismol. Soc. Am.* **102** (2012) 284–300.
- [71] VAN HOUTTE, C., DROUET, S., COTTON, F., Analysis of the origins of κ (Kappa) to compute hard rock to rock adjustment factors for GMPEs, *Bull. Seismol. Soc. Am.* **101** 6 (2011) 2926–294.

- [72] LAURENDEAU, A., COTTON, F., KTENIDOU, O.J., BONILLA, L.F., HOLLENDER, F., Rock and stiff-soil site amplification: dependency on V_{S30} and κ_0 , Bull. Seismol. Soc. Am. **103** (2013) 3131–3148.
- [73] WALLING, M., SILVA, W. J., ABRAHAMSON, N. A., Nonlinear site amplification factors for constraining the NGA models, Earthq. Spectra **24** (2008) 243–255.
- [74] ABRAHAMSON, N.A., SILVA, W. J., KAMAI, R., Update of the AS08 Ground-Motion Prediction Equations Based on the NGA-West2 Data Set, Pac. Earthq. Eng. Res. Cent. (2013).
- [75] BOORE, D.M., STEWART, J.P., SEYHAN, E., ATKINSON, G.M., NGA-West2 equations for predicting response spectral accelerations for shallow crustal earthquakes, Pac. Earthq. Eng. Res. Cent. (2013).
- [76] CAMPBELL, K.W., BOZORGNIA, Y., NGA-West2 Campbell-Bozorgnia ground motion model for the horizontal components of PGA, PGV and 5%-damped elastic pseudo-acceleration response spectra for periods ranging from 0.01 to 10 sec, Pac. Earthq. Eng. Res. Cent. (2013).
- [77] CHIOU, B.J., YOUNGS, R.R., Update of the Chiou and Youngs NGA ground motion model for average horizontal component of peak ground motion and response spectra, Pac. Earthq. Eng. Res. Cent. (2013).
- [78] TRIFUNAC, M.D., Preliminary analysis of the peaks of strong earthquake ground motion— dependence of peaks on earthquake magnitude, epicentral distance and recording site conditions, Bull. Seismol. Soc. Am. **66** 1 (1976) 189–219.
- [79] BOORE, D.M., JOYNER, W.B., FUMAL, T.E., Estimation of response spectra and peak accelerations from western north American earthquakes, Interim Rep. U.S. Geol. Sur. Open-File Rep. (1993) 93–509 pp.
- [80] FUKUSHIMA, Y., MIDORIKAWA, S., Prediction of velocity response spectra for seismic motions in and on rock site considering nonlinear scaling of M_w^2 Term, J. Struct. Construct. Eng, AIJ **447** (1993) 39–49 (in Japanese with English abstract).

- [81] DOUGLAS, J., JOUSSET, P., Modeling the difference in ground motion magnitude-scaling in small and large earthquakes, *Seismol. Res. Lett.* **82** (2011) 504–508.
- [82] FUKUSHIMA, Y., Scaling relations for strong ground motion prediction models with M^2 terms, *Bull. Seismol. Soc. Am.* **86** 2 (1996) 329–336.
- [83] ANDERSON, J.G., KAWASE, H., BIASI, G.P., BRUNE, J.N., AOI, S., Ground motions in the Fukushima Hamadori, Japan, Normal-Faulting Earthquake, *Bull. Seismol. Soc. Am.* (2013) **103** 1935–1951.
- [84] YUZAWA, Y., NAGUMO, H., KUDO, K., “Empirical shake map for long period(1-15 sec) ground motion in Japan”, *Proc. 15th World Conf. on Earthquake Engineering*, Paper No. 1724 (2012).
- [85] CAMPBELL, K.W., Near-source attenuation of peak horizontal acceleration, *Bull. Seismol. Soc. Am.* **71** 6 (1981) 2039–2070.
- [86] IDRIS, I. M., An NGA empirical model for estimating the horizontal spectral values generated by shallow crustal earthquakes, *Earthq. Spectra* **24** (2008) 217–242.
- [87] SI, H., KUYUK, H.S., KOKETSU, K., MIYAKE, H., Attenuation characteristic of peak ground motion during the 2011 Tohoku, Japan, earthquake, *Seismol. Res. Lett.* **82** (2011) 460
- [88] STRASSER, F.O., BOMMER, J.J., ABRAHAMSON, N.A., Truncation of the distribution of ground motion residuals, *J. Seismol.* **12** (2008) 79-105.
- [89] KAWASE, H., MATSUO, H., Relationship of S-wave Velocity Structures and Site Effects Separated from the Observed Strong Motion Data of K-NET, KiK-net and JMA Network, *J. Jpn. Assoc. Earthq. Eng.* **4** 4 (2004).
- [90] MORIKAWA, M., et al., Strong motion uncertainty determined from observed records by dense network in Japan. *J. Seismol.* **12** (2008) 529–546.
- [91] AL ATIK, L., et. al., The variability of ground motion prediction models and its components, *Seismol. Res. Lett.* **81** 5 (2010).
- [92] ANCHETA, T.D., et. al., PEER NGA-West2 Database, Pacific Earthquake Engineering Research Center (2013).

- [93] PACOR, F., R. et al., Overview of the Italian strong motion database ITACA 1.0, *Bull. Earthq. Eng.* **9** 6 (2011) 1723–1739.
- [94] CEN, Eurocode 8: Design of Structures for Earthquake Resistance—Part 1: General rules, seismic actions and rules for buildings, NE 1998-1 (2004) CEN, Brussels.
- [95] BUILDING SEISMIC SAFETY COUNCIL, NEHRP recommended provisions for seismic regulations for new buildings and other structures: Part 1 – provisions and part 2 – commentary, Federal Emergency Management Agency, Washington DC (2003).
- [96] SANDIKKAYA, M.A., YILMAZ, M.T., BAKIR, B.S., YILMAZ, Ö., Site classification of Turkish national strong motion stations. *J. Seismol.* **14** (2010) 543–556.
- [97] BRADY, A.G., TRIFUNAC, M.D., HUDSON, D.E., Analyses of strong motion earthquake accelerograms – response spectra, Technical Report, Earthq. Eng. Res. Lab. California Institute of Technology (1973).
- [98] BOORE, D.M., BOMMER J.J., Processing of strong motion accelerograms: needs, options and consequences, *Soil Dyn. Earthq. Eng.* **25** (2005) 93-115.
- [99] INTERNATIONAL ATOMIC ENERGY AGENCY, Ground Motion Simulation Based on Fault Rupture Modelling for Seismic Hazard Assessment in Site Evaluation for Nuclear Installations, Safety Reports Series No. 85, IAEA, Vienna (2015).
- [100] BOORE, D.M., Stochastic simulation of high-frequency ground motions based on seismological models of the radiated spectra, *Bull. Seism. Soc. Am.* **73** 6 (1983) 865–1894.
- [101] BOORE, D.M., Simulation of ground motion using the stochastic method, *Pure Appl. Geophys.* **160** (2003) 635–676.
- [102] MOTAZEDIAN, D., ATKINSON, G.M., Stochastic finite-fault modelling based on a dynamic corner frequency, *Bull. Seismol. Soc. Am.* **95** 3 (2005) 995–1010.
- [103] RIETBROCK, A., STRASSER, F., EDWARDS, B., A stochastic earthquake ground-motion prediction model for the United Kingdom, *Bull. Seismol. Soc. Am.* **103** (2013) 57–77.

- [104] IRIKURA, K., “Prediction of strong acceleration motion using empirical Green's function”, Proc. 7th Japan Earthq. Eng. Symp., Tokyo (1986) 151–156.
- [105] IRIKURA, K., KAMAE, K., “Simulation of strong ground motion based on fractal composite faulting model and empirical Green's function”, Proc. of the 9th Japan Earthquake Engineering Symposium, **3** (1994) E019–024.
- [106] IRIKURA, K., MIYAKE, H., Recipe for predicting strong ground motion from crustal earthquake scenarios, Pure Appl. Geophys. **168** (2011) 85–104.
- [107] GRAVES, R. W., PITARKA, A., Broadband ground motion simulation using a hybrid approach, Bull. Seism. Soc. Am. **100** (2010) 2095–2123.
- [108] GRAVES, R.W., AAGAARD, B.T., HUDNUT, K.W., The shakeout earthquake source and ground motion simulations, Earthq. Spectra **27** 2 (2011) 273–291.
- [109] BOMMER, J.J., SCHERBAUM, F., BUNGUM, H., et al., On the use of logic trees for ground motion prediction equations in seismic-hazard analysis, Bull. Seismol. Soc. Am. **95** (2005) 377–389.
- [110] DOUGLAS, J., Ground motion prediction equations 1964–2015, <http://www.gmpe.org.uk/>
- [111] BOMMER, J.J., On the selection of ground motion prediction equations for seismic hazard analysis, Seismol. Res. Lett. **81** 5 (2010).
- [112] GRAIZER, V.M., Comment on “On the Selection of Ground-Motion Prediction Equations for Seismic Hazard Analysis” by Bommer, J.J., et al., Seismol. Res. Lett. **82** 2 (2011) 233–236.
- [113] KALE, U., AKKAR, S., A new procedure for selecting and ranking Ground-Motion Prediction Equations (GMPEs): the Euclidean Distance-Based Ranking (EDR) method, Bull. Seismol. Am. **103** 2A (2013) 1069–1084.
- [114] DELAVAUD, E., et. al., Toward a ground motion logic tree for probabilistic seismic hazard assessment in Europe, J. Seismol. **16** 3 (2012) 451–473.
- [115] STEWART, J. P., et. al., GEM-PEER Task 3 Project: Selection of a global set of ground motion prediction equations, Pac. Earthq. Eng. Res. Cent. (2013).

- [116] SCHERBAUM, F., COTTON, F., SMIT, P., On the use of response spectral reference data for the selection and ranking of ground motion models for seismic hazard analysis in regions of moderate seismicity: the case of rock motion, *Bull. Seismol. Soc. Am.* **94** (2004) 216–2185.
- [117] SCHERBAUM, F., DELAVALD, E., RIGGELSEN, C., Model selection in seismic hazard analysis: an information-theoretic perspective, *Bull. Seismol. Soc. Am.* **99** (2009) 3234–3247.
- [118] UTSU, T., Relationships between Magnitude Scales, *International Handbook of Earthquake and Engineering Seismology–Part A* (LEE, W.H.K., KANAMORI, H., JENNINGS, P.C., KISSLINGER, C., Ed.) (2002) 733–746.
- [119] GRÜNTAL, G., WAHLSTRÖM, R., An M_W based earthquake catalogue for central, northern and northwestern Europe using a hierarchy of magnitude conversions, *J. Seismol.* **7** 4 (2003) 507–532.
- [120] ALLMANN, B., EDWARDS, B., BETHMANN, F., DEICHMANN, N., Determination of M_W and calibration of M_L (SED) - M_W regression. - Appendix A to: Fäh, D., et. al., ECOS-09 Earthquake Catalogue of Switzerland, Release 2011, Report and Database, Public catalogue, 17.04.2011, Swiss Seismological Service ETH Zurich, Report SED/RISK/R/001/20110417 (2010).
- [121] BEAUVAL, C., et al., On the testing of ground motion prediction equations against small magnitude data, *Bull. Seismol. Soc. Am.* **102** 5 (2012) 1994 – 2007.
- [122] ATKINSON, G.M., BOORE, D.M., Modifications to existing ground motion prediction equations in light of new data, *Bull. Seismol. Soc. Am.* **101** 3 (2011) 1121–1135.
- [123] CAMPBELL, K.W., Prediction of strong ground motion using the hybrid empirical method and its use in the development of ground motion (Attenuation) relations in Eastern North America, *Bull. Seismol. Soc. Am.* **93** 3 (2003) 1012–1033.
- [124] UDWADIA, F.E., TRIFUNAC, M.D., The Fourier transform, response spectra and their relationship through the statistics of oscillator response, Rep. No. EERL 73-01, California Institute of Technology, Earthquake Engineering Research Laboratory (1973).

- [125] RODRIGUEZ-MAREK, A., et. al., A model for single station standard deviation using data from various tectonic regions, *Bull. Seismol. Soc. Am.* **103** 6 (2013) 3149–3163.
- [126] BAKER, J.W., Quantitative classification of near-fault ground motions using wavelet analysis, *Bull. Seismol. Soc. Am.* **97** 5 (2007) 1486–1501.
- [127] SHAHI, S.K., BAKER, J.W., An empirically calibrated framework for including the effects of near-fault directivity in probabilistic seismic hazard analysis, *Bull. Seismol. Soc. Am.* **101** 2 (2011) 742–755.
- [128] NATIONAL EARTHQUAKE HAZARDS REDUCTION PROGRAM, Selecting and Scaling Earthquake Ground Motions for Performing Response-History Analyses, Prepared for U.S. Department of Commerce, National Institute of Standards and Technology, NIST GCR 11-917-15 (2011).
- [129] BRAY, J.D., RODRIGUEZ-MAREK, A., Characterization of forward-directivity ground motions in the near-fault region, *Soil Dyn. Earthq. Eng.* **24** 11 (2004) 815–828.
- [130] STEPP, J.C., et. al., Probabilistic seismic hazard analyses for ground motions and fault displacement at Yucca Mountain, Nevada, *Earthq. Spectra* **17** 1 (2001) 113–149.
- [131] DECANINI et al., Some remarks on the Umbria-Marche earthquakes of 1997, *Eur. Earthq. Eng.* **3** (2000) 18–48.
- [132] PITILAKIS, K., “Site effects”, Recent advances in earthquake geotechnical engineering and microzonation (ANSAL, A., Ed), Springer (2006) 139–197.
- [133] LANZO, L., SILVESTRI, F., *Risposta Sismica Locale* , Hevelius Edizioni, Benevento, 1999, Italy.
- [134] BARD, P.Y., RIEPL-THOMAS, J., “Wave propagation in complex geological structures and local effects on strong ground motion”, *Wave Motion*, (KAUSEL, E., MANOLIS, G.D., Ed.) *Earthq. Eng.*, WIT Press (1999) 38–95.
- [135] PITILAKIS, K., RAPTAKIS, D., LONTZETEDIS, K., TIKA-VASSILIKOU, T.H., JONGMANS, D., Geotechnical and geophysical description of EURO-SEISTEST using field, laboratory tests and moderate strong motion recordings. *J. Earthq. Eng.* **3** 3 (1999) 381–409.

- [136] BARD, P.Y., Microtremor Measurements: A tool for effect estimation? State-of-the-art paper, II Int. Symp. on the Effects of Surface Geology on Seismic Ground Motion. Yokohama, Dec. 1–3, (IRIKURA, K., KUDO, K., OKADA, H., SASATANI, T., Ed.) Balkema **3** (1999) 1251–1279 pp.
- [137] SANÒ, T., PUGLIESE, A., “La risposta sismica locale” (ROMEO, R., Ed.) Monographs of the Int. Centre for Mechanical Sciences, Udine (2007) 151–188 (in Italian).
- [138] HOUSNER, G.W., “Spectrum intensities of strong motion earthquakes”, Proc. Symp. on Earthquake and Blast Effects on Structures, Earthq. Eng. Res. Ins. (1952) 21–36.
- [139] NEWMARK, N.M., HALL, W.J., Earthquake spectra and design, Earthq. Eng. Res. Ins. Monographs, Berkeley, California (1982).
- [140] BAKER, J.W., Conditional mean spectrum: tool for ground motion selection, J. Struct. Eng. **137** (2011) 322–331.
- [141] BOMMER, J.J., ACEVEDO, A.B., The use of real earthquake accelerograms as input for dynamic analysis, J. Earthq. Eng. **8** Special Issue 1 (2004) 43–91.
- [142] McGUIRE, R.K., Probabilistic seismic hazard analysis and design earthquakes: closing the loop, Bull. Seism. Soc. Am. **85** 5 (1995) 1275–1284.
- [143] BAZZURRO, P., CORNELL, C.A., Disaggregation of seismic hazard, Bull. Seism. Soc. Am. **89** 2 (1999) 501–520.
- [144] SMERZINI, C., GALASSO, C., IERVOLINO, I., PAOLUCCI, R., Ground motion record selection based on broadband spectral compatibility, Earthq. Spectra (2013) 1427–1448.
- [145] KOTTKE, A.R., RATHJE, E.M., Technical Manual for Strata, PEER Report 2008/10, Pacific Earthq. Eng. Res. Cent., College of Engineering, University of California, Berkeley.
- [146] RATHJE, E.M., KOTTKE, A.R., Procedures for random vibration theory based seismic site response analyse: A White Paper Prepared for the Nuclear Regulatory Commission, Geotechnical Engineering Report GR08-09, Geotechnical Engineering

Center, Department of Civil, Architectural and Environmental Engineering, University of Texas at Austin, TX, (2008).

[147] ZERVA, A., PETROPULU, A.P., BARD, P.Y., Blind deconvolution methodology for site-response evaluation exclusively from ground-surface seismic recordings, *Soil Dyn. Earthq. Eng.* **18** (1999) 47–57.

[148] HANCOCK, J., et. al., An improved method of matching response spectra of recorded earthquake ground motion using wavelets. *J. Earthq. Eng.* **10** 1 (2006) 67–89.

[149] AL ATIK L., ABRAHAMSON, N., An improved method for nonstationary spectral matching, *Earthq. Spectra* **26** 3 (2010) 601–617.

[150] KOTTKE, A.R., RATHJE, E.M., Comparison of time series and random-vibration theory site-response methods, *Bull. Seism. Soc. Am.* **103** 3 (2013) 2111–2127.

[151] FOTI, S., PAROLAI, S., ALBARELLO, D., PICOZZI, M., Application of surface wave methods for seismic site characterization, *Surv. Geophys.* **32** 6 (2011) 777–825.

[152] OKADA, H., The microtremor survey method. *Geophys. Monogr. Ser.* **12**, Society of Exploration Geophysicists (2003) 129.

[153] MAYNE, P.W., COOP, M.R., SPRINGMAN, S., HUANG, A-B., ZORNBERG, J., “State-of-the-art paper (SOA-1): geomaterial behavior and testing”, *Proc. 17th Intl. Conf. Soil Mechanics & Geotechnical Engineering*, 4 (ICSMGE, Alexandria, Egypt), Millpress/IOS Press Rotterdam (2009) 2777–2872.

[154] KRAMER, S.L., *Geotechnical Earthquake Engineering*, Prentice Hall, New Jersey, (1996) 653 pp.

[155] TSAI, N.C., A note on the steady-state response of an elastic layered half-space, *Bull. Seism. Soc. Am.* **60** 3 (1970) 795–808.

[156] BARDET, J.P., ICHII, K., LIN, C.H., EERA, A., Computer program for equivalent-linear earthquake site response analysis of layered soil deposits, Department of Civil Engineering, University of Southern California (2000).

[157] SAFAK, E., Models and methods to characterize site amplification from a pair of records, *Earthq. Spectra* **13** (1997) 97–129.

- [158] BORCHERDT, R.D., Effects of local geology on ground motion near San Francisco bay, *Bull. Seism. Soc. Am.* **60** (1970) 29–61.
- [159] STIEDL, J.H., TUMARKIN, A.G., ARCHULETA, R.J., What is a reference site? *Bull. Seism. Soc. Am.* **86** (1996) 1733–1748.
- [160] SI, H., TSUTSUMI, H., MIDORIKAWA, S., Evaluation of hanging wall effects on ground motion attenuation relationship correcting the site effects (Proc. 9th U.S. Natl. 10th Can. Conf. on Earthq. Eng.) Paper No. 647 (2010).
- [161] LERMO, J.L., CHAVEZ-GARCIA, F.J., Site effect evaluation using spectral ratios with only one station. *Bull. Seism. Soc. Am.* **83** (1993) 1574–1594.
- [162] LANGSTON, C.A., Structure under Mount Rainier, Washington, inferred from teleseismic body waves, *J. Geophys. Res.* **84** (1979) 4749–4762.
- [163] NAKAMURA, Y., A method for dynamic characteristics estimation of subsurface using microtremor on the ground surface, *Quarterly Report of Railway Technical Research Institute* **30** 1 (1989) 25–33.
- [164] NAKAMURA, Y., Clear identification of fundamental idea of Nakamura's technique and its applications, (Proc. of the 12th world Conf. Earthq. Eng. Auckland, New Zealand) Paper 2656 (2000).
- [165] COUTEL, F., MORA, P., Simulation-based comparison of four site-response estimation techniques, *Bull. Seism. Soc. Am.* **88** (1998) 30–42.
- [166] EDWARDS, B., RIETBROCK, A., BOMMER J.J., BAPTIE, B., The acquisition of source, path and site effects from microearthquake recordings using Q tomography: application to the United Kingdom. *Bull. Seism. Soc. Am.* **98** 4 (2008) 1915–1935.
- [167] POGGI, V., EDWARDS, B., FÄH, D., Derivation of a reference shear wave velocity model from empirical site amplification, *Bull. Seism. Soc. Am.* **101** 1 (2011) 258–274.
- [168] DOUGLAS, J., et al., Comparisons among the five ground motion models developed using RESORCE for the prediction of response spectral accelerations in Europe and the Middle East, *Bull. Earthq. Eng.* **12** 1 (2014) 341–358.

[169] GREGOR, N., Comparison of NGA-West2 GMPEs, Earthquake Spectra **30** 3 (2014) 1179–1197.

[170] NATIONAL EARTHQUAKE HAZARDS REDUCTION PROGRAM, NEHRP Recommended provisions for seismic regulations for new buildings and other structures (FEMA 450) 2003 edition, Part 1: Provisions, Building Seismic Safety Council, National Institute of Building Sciences, Washington DC (2004) 47–49.

DEFINITIONS

(The following definitions apply in this publication only.)

Attenuation

The decrease in amplitude of the seismic waves with distance from the earthquake source due to geometrical spreading, energy energy partition at interfaces, absorption (reflection/refraction phenomena) and wave scattering.

Controlling earthquake

Earthquakes used to determine spectral shapes or to estimate ground motions at the site for some methods of dynamic site response. There may be several controlling earthquakes for a site. As a result of the PSHA, controlling earthquakes are characterized as mean magnitudes and distances derived from a deaggregation analysis of the mean estimate of the PSHA.

Damping

Process responsible for energy dissipation during periodic oscillations of any dynamical system.

Design basis earthquake

The earthquake for which the structures, systems and components of nuclear installation will remain intact without any damage.”

Engineering bedrock

Synonymous with reference soil condition used in common engineering practice.

Input (seismic or motion)

The seismic signal at the boundary of a geological or engineering structure of which the seismic response has to be assessed.

Nonlinear behaviour

Stress-strain relationship depending on the level of strain and on the number of loading unloading cycles.

Reference earthquake

Synonymous at controlling earthquake.

Reference interface

Buried or outcropping surface bounding reference soil conditions.

Response spectrum

Represents the maximum response of a single degree of freedom damped system (mimicking a standard building) to ground motion as function of the natural frequency and damping ratio of the system. This parameter is widely used in engineering practice to evaluate inertial loads induced in the building during an earthquake.

Seismic bedrock

Generic term indicating any sound unaltered and unweathered rock represented by a geological body extending at depth without strong seismic impedance contrasts inside, either outcropping or underlying soil layers. Materials constituting this formation are assumed to behave linearly under the seismic load.

Uniform hazard spectrum (UHS)

Response spectrum whose ordinates are characterized by a uniform exceedance probability.

Reference soil conditions

Any subsoil configuration where seismic input ground motion used for site response analysis is assumed to be known.

Seismic impedance

Product of density and seismic wave velocity. This parameter controls refraction reflection phenomena at seismic interfaces.

Seismic microzoning

Procedures devoted to delineating zones with homogeneous site effects.

Site response

The modification in terms of amplitude, duration and frequency content of the seismic signal due to the local geological conditions (stratigraphy, lithology, morphology and buried geological bodies).

Site effects

Seismic response of a site to the seismic input either in terms of local site response or ground instabilities (liquefaction, landslides, ground cracks and settlements).

Site response factor

A single value parameterization of site response; it is generally determined as the ratio of integral spectral representations of ground motion intensity (e.g. Housner intensity) at the surface and at outcropping reference interface.

Site response function

Ratios of spectral amplitudes of ground motion at the surface of any geological body and those of the ground motion entering in the body measured at any outcropping reference interface. In some cases, the term amplification function is used instead of site response function: however, since site response also includes de-amplification and frequency /phase changes, this last term could be misleading.

Transfer function

Ratios of Fourier spectral amplitudes of ground motion at the surface of any geological body and the ones of the ground motion entering in the body at the reference interface.

ANNEX: DEVELOPMENT OF GMPE: JAPANESE EXAMPLE FOR VERY HARD ROCK CONDITION

In the Annex, a practice of Japan on the derivation of database and GMPE of strong ground motion on very hard rock is introduced. This introduction shows that strengthening the seismic observation network plays a very important role in deepening the understanding of input strong ground motion for nuclear installations.

A-1. GMPE ON HARD ROCK

In Japan, taking advantage of the vertical array observation network in which many underground seismographs are located on hard rock basement with V_S larger than 2 km/s, a database of response spectra on hard rock with V_S larger than 2 km/s has been established [A-1, A-2]. Based on these data, a GMPE for response spectra on hard rock is directly estimated [A-3]). This GMPE thus can avoid the possible influence of trade-offs between site response and path, source effects and makes the prediction of ground motion by GMPE more precise.

A-1.1. Database on hard rock

Si et al. (2013) [A-2]) chooses 34 earthquakes with M_W from 5.5 to 9.1. Three or more records per event on hard rock are obtained, to establish the new GMPE for response spectra on very hard rock. Among these earthquakes, there are 14 crustal earthquakes, 11 interplate earthquakes and 9 intraplate earthquakes in the database. Figure A-1 shows the histogram with respect to the earthquake type and a plot of moment magnitude against the focal depth.

The strong motion data used in this study come from stations in the KiK-net, K-NET and F-NET networks of the National Research Institute for Earth Science and Disaster Prevention (NIED), RK-NET by Central Research Institute of Electric Power Industry (CRIEPI) and the dam observation stations by Japan Commission on Large Dams (JCOLD), National Institute for Land and Infrastructure Management (NILIM) and the Miyagi prefecture. Only data recorded or estimated on hard rock are used.

For the strong motion data coming from KiK-net, the stations at which the bottom seismograph is located on bedrock with $V_S \geq 2$ km/s are selected for estimating the strong motion on hard rock. Generally, the strong motion observation system at KiK-net stations is a vertical array observation system, where at each station seismographs are

installed both at the ground surface and on the bottom of the borehole. In this study, the stations where the bottom of the borehole reaches very hard rock with shear wave velocity over 2 km/sec are selected as the candidate stations for the estimation of strong motion. For this purpose, firstly the properties of the soil materials in the borehole were identified by fitting the transfer function defined as the ratio of the Fourier spectra of the seismic wave recorded at the ground surface and the bottom of the borehole. Then the strong motions on very hard rock are estimated from the records on the ground surface of the borehole. Almost all the records from KiK-net stations are derived by using this method. Figure A –2 shows an example of the result of the identification of material of the borehole and the estimated strong motion on seismic very hard rock.

Finally, for the 34 target earthquakes, about 600 records on very hard rock are collected. In the database, the distance definitions used are fault distance and the EHD. Here, only the results for horizontal component and fault distance were shown.

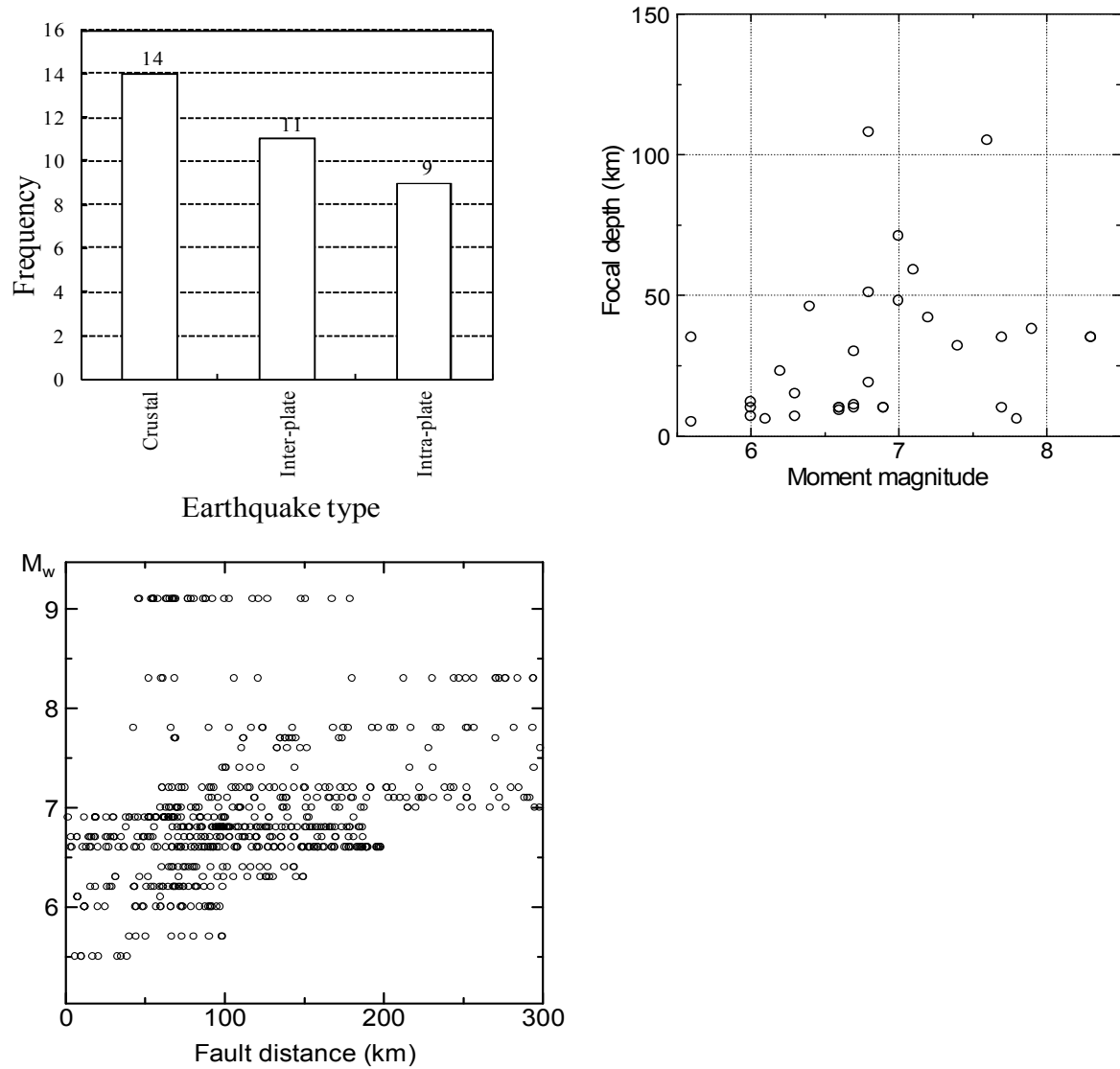


FIG. A-1. Left top: histogram of the earthquake type; Right top: plot of moment magnitude vs. the focal depth; bottom: Distribution of M_w vs fault distance. Reproduced with permission from H. Si.

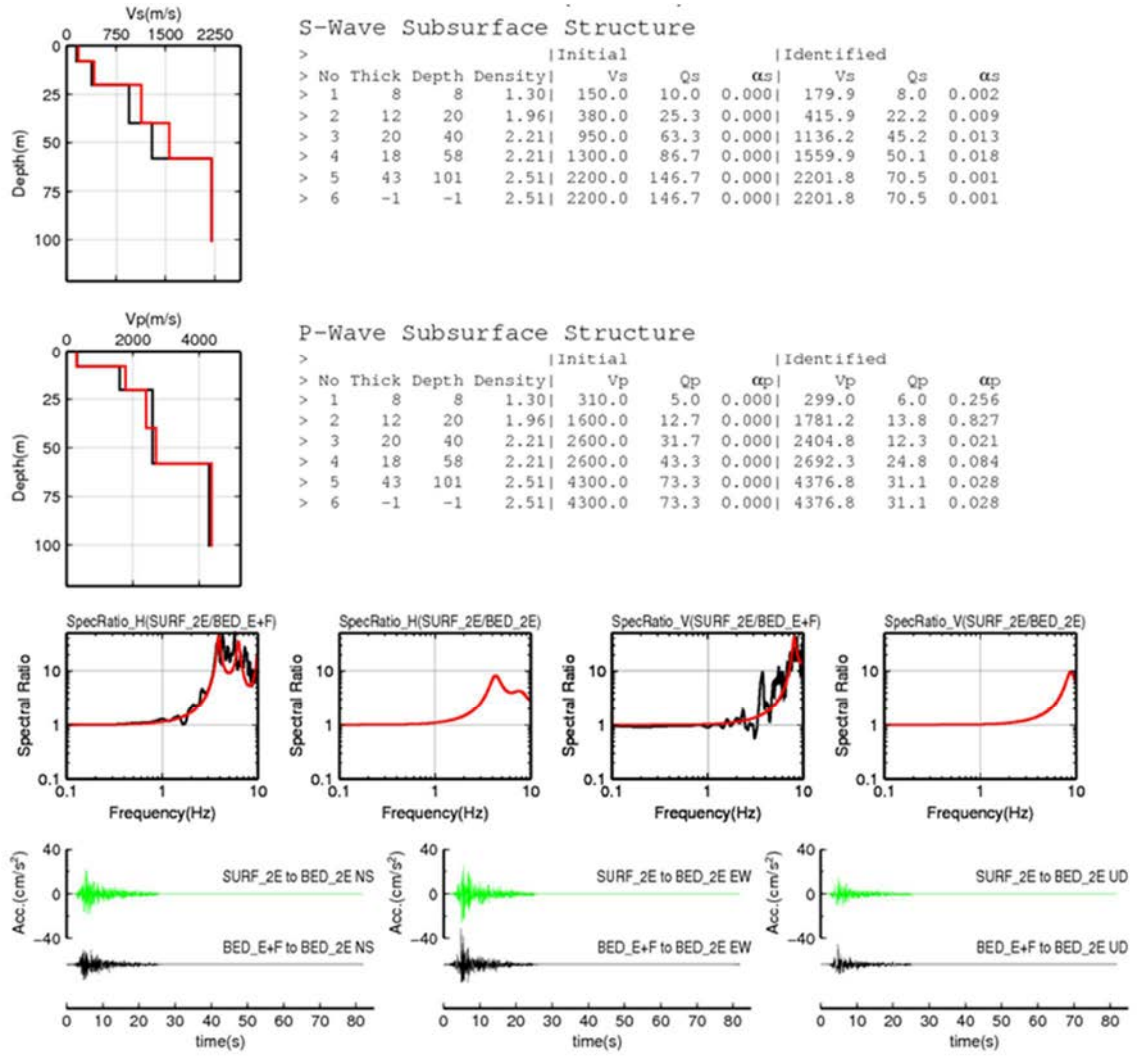


FIG. A-2. Examples of estimated ground motion on very hard rock at AICH17 station of KiK-net. Upper two rows: identified S and P wave velocity profiles. Third rows: estimated transfer function (SpecRatio_H: Horizontal; V: Vertical). Fourth row: estimated ground motions on very hard rock (coloured green). Reproduced with permission from H.Si.

A-1.2. GMPE estimated for very hard rock sites

The derived GMPEs for very hard rock sites are shown in Eq. (A-1).

$$\begin{aligned}
 \log SA(T) &= b(T) + g(X) - k(T)X + \varepsilon(T) \\
 g(X) &= \begin{cases} -\log(X + C(T)); D \leq 30 \text{ km or } D > 30 \text{ km} \& X < 1.7D \\ 0.6\log(1.7D + C(T)) - 1.6\log(X + C(T)); D > 30 \text{ km} \& X \geq 1.7D \end{cases} \\
 k(T) &= 0.003, T \leq 0.3s \\
 &= 0.002, T \geq 0.6s \\
 C(T) &= 0.0055 \cdot 10^{0.5M_w}, T \leq 0.3s \\
 &= 0.0028 \cdot 10^{0.5M_w}, T \geq 0.6s
 \end{aligned} \tag{A-1}$$

Where $SA(T)$ uses the GMTRot150 definition of the horizontal component, an average response spectra proposed by Boore et al. (2006) [A-4]) for horizontal components and response spectra for vertical components, X is fault distance or EHD and $b(T)$ is defined by Eq. (A-2) as follows:

$$b(T) = \begin{cases} a_1(T)M_w + \sum d_i(T)S_i + h(T)D + e(T) + \varepsilon_1(T) \\ Mw < 8.3 \text{ if } T < 2s \text{ or } M < 7.5 \text{ if } T \geq 2s \\ a_2(T)M_w + \sum d_i(T)S_i + h(T)D + e(T) + \varepsilon_2(T) \\ Mw \geq 8.3 \text{ if } T < 2s \text{ or } M \geq 7.5 \text{ if } T \geq 2s \end{cases} \tag{A-2}$$

Where D equals the focal depth, s_i is a category variable accounting for the earthquake type defined as crustal, inter and intraplate earthquake. The same definition as the one used by Si and Midorikawa (1999) [A-5].

Figure A-3 shows the coefficients for magnitude dependence derived in this study.

From the figure, $a_1(T)$ increases with period T ; $a_2(T)$ is zero for the case of FD (Fault Distance), showing the saturation with M_w for EHD.

Figure A-3 also shows the comparison of the coefficient of M_w , $a_1(T)$ derived in this study and those in the other recent studies. From the figure, the results in this study show similar tendencies to the others (e.g. [A-6, A-7]) that the coefficient increases with the period.

Figure A–4 shows ground motion predicted by GMPEs derived in this study. The prediction for response spectra are calculated for different earthquake with M_W of 6, 7 and 8. From the results, it can be found that: (1) the amplitudes increase with M_W ; (2) amplitudes for intraplate earthquake are generally larger than those from crustal and interplate earthquake; and (3) for long period, amplitudes from crustal earthquake are larger than from interplate earthquake.

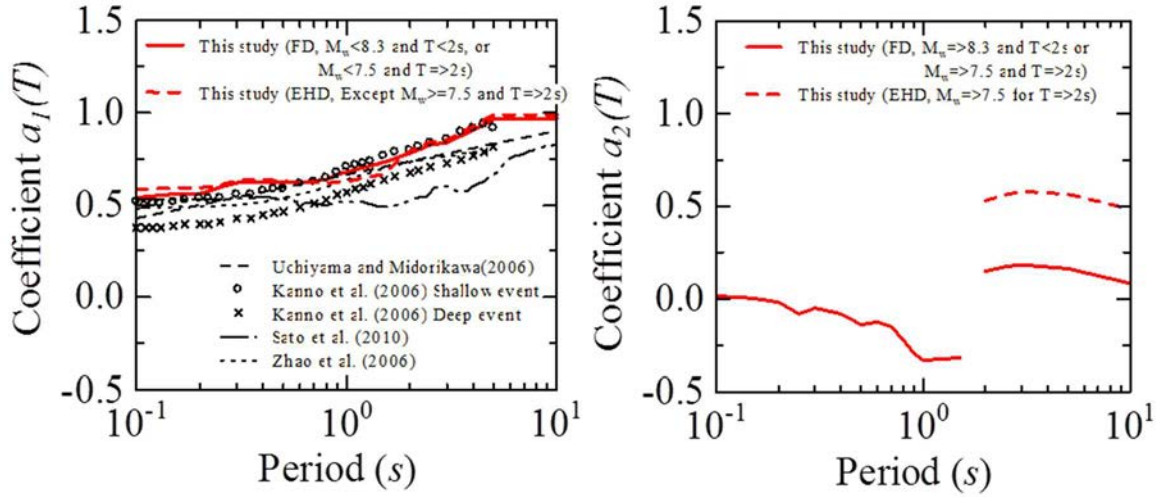


FIG. A–3. Coefficient of $a_1(T)$ and $a_2(T)$ for the scaling of magnitude and strong ground motion. Reproduced with permission from H. Si.

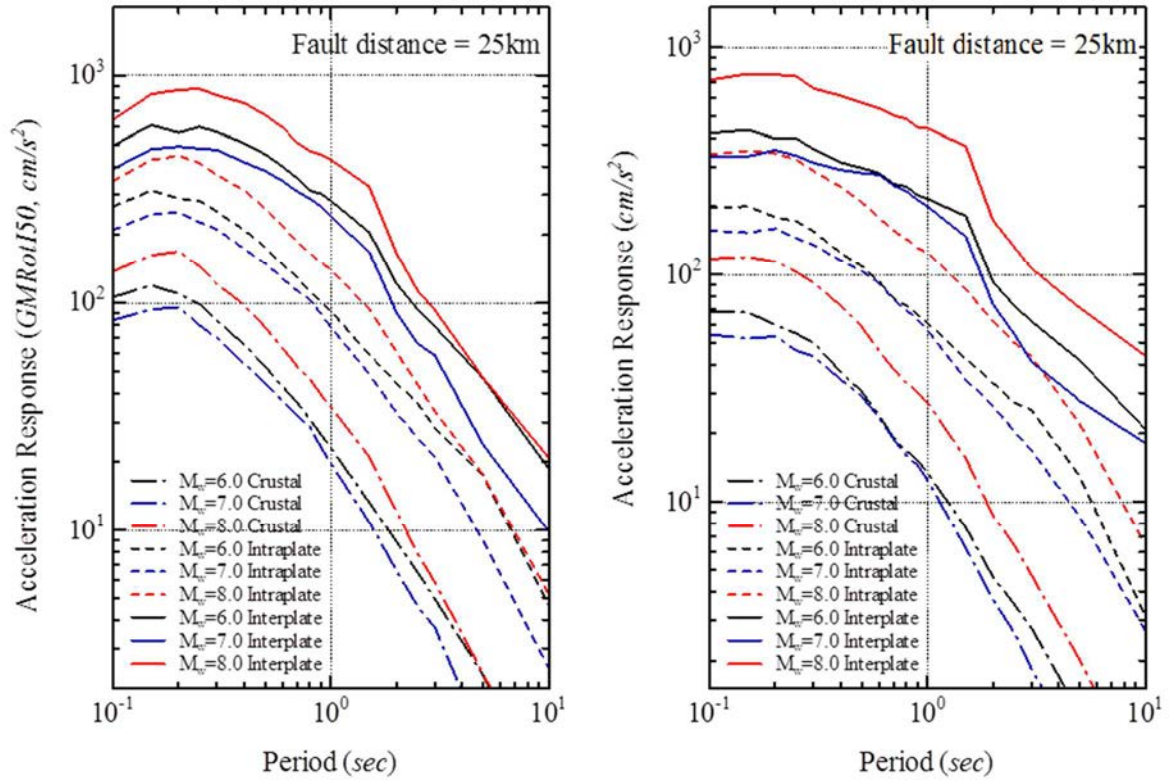


FIG. A-4. Predicted response spectra based on the results. (Left: horizontal component; Right: vertical component). Reproduced with permission from H. Si.

A-1.3. Validation and conclusion

In order to validate the GMPE developed in [A-2], observation data from earthquakes not included in the database used for this development are used for the comparison with the prediction of the GMPE.

The observation data from two recent earthquakes are used. These earthquakes are well recorded and are representative earthquakes for crustal events.

- 1994/1/17 Northridge, California M_W 6.7
- 2008/5/12 Wenchuan M_W 7.9

Observation data and site information including V_{S30} and $Z2.0 = (Z1.5 + Z2.5)$ for 1994 Northridge earthquake are provided by the NGA flat file. Observation data for 2008 Wenchuan earthquake are provided by the CSMNC of the Chinese Earthquake

Administration. Since no V_{S30} data and depth to hard rock are available, only data observed on rock site indicated by CSMNC are used.

Based on the above data, the ground motion at each site is calculated by coupling the GMPE developed in this study and the site response factors Amp of Si et al. (2013) [A–2] shown in Eq. (A–3).

$$\begin{aligned} Amp &= (1 - a (1 - V_{S30}RT)^b) (c + dH) & (0.6s \leq T \leq 5s) \\ Amp &= 1 - a (1 - V_{S30}RT)^b & (\text{otherwise}) \end{aligned} \quad (A-3)$$

where, $V_{S30}RT = V_{S30}/V_{S\text{ BASE}}$, H is the depth of sediments. a , b , c and d are regression coefficients.

The results are compared with the seismic data from the earthquakes. Figures A–5 and A–6 show comparisons of the calculated and the observed motions. The results show that the observations are consistent with the predictions.

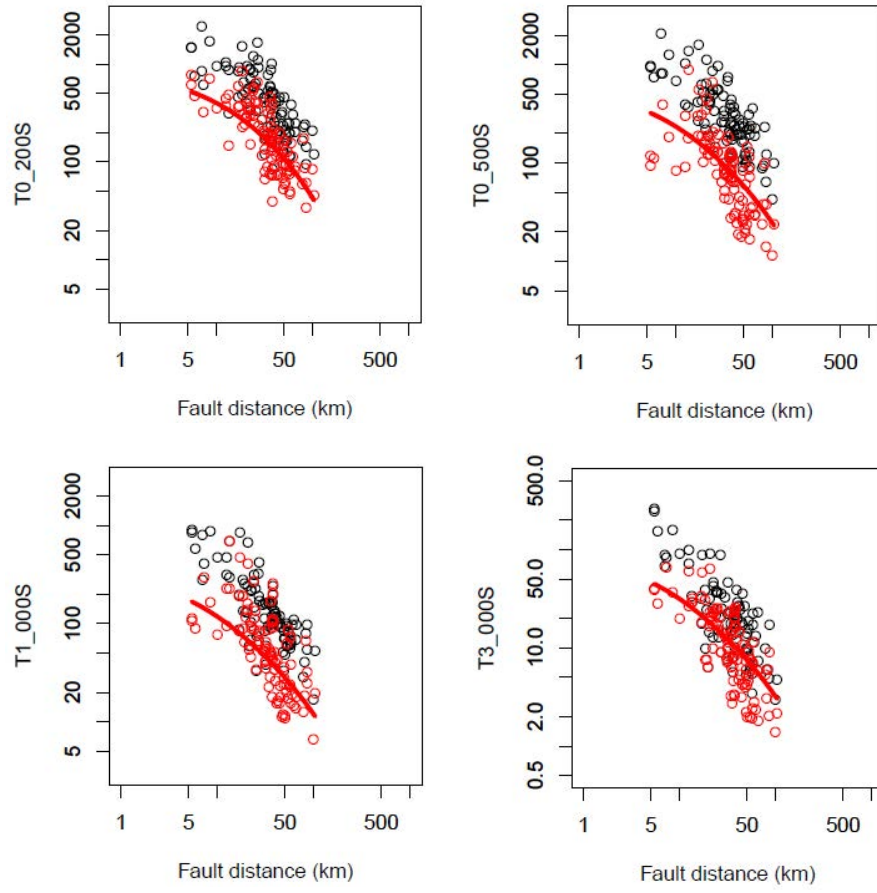


FIG. A-5. Comparison between observed and predicted response spectra Northridge. Reproduced with permission from Si et al., 2013 [A-3].

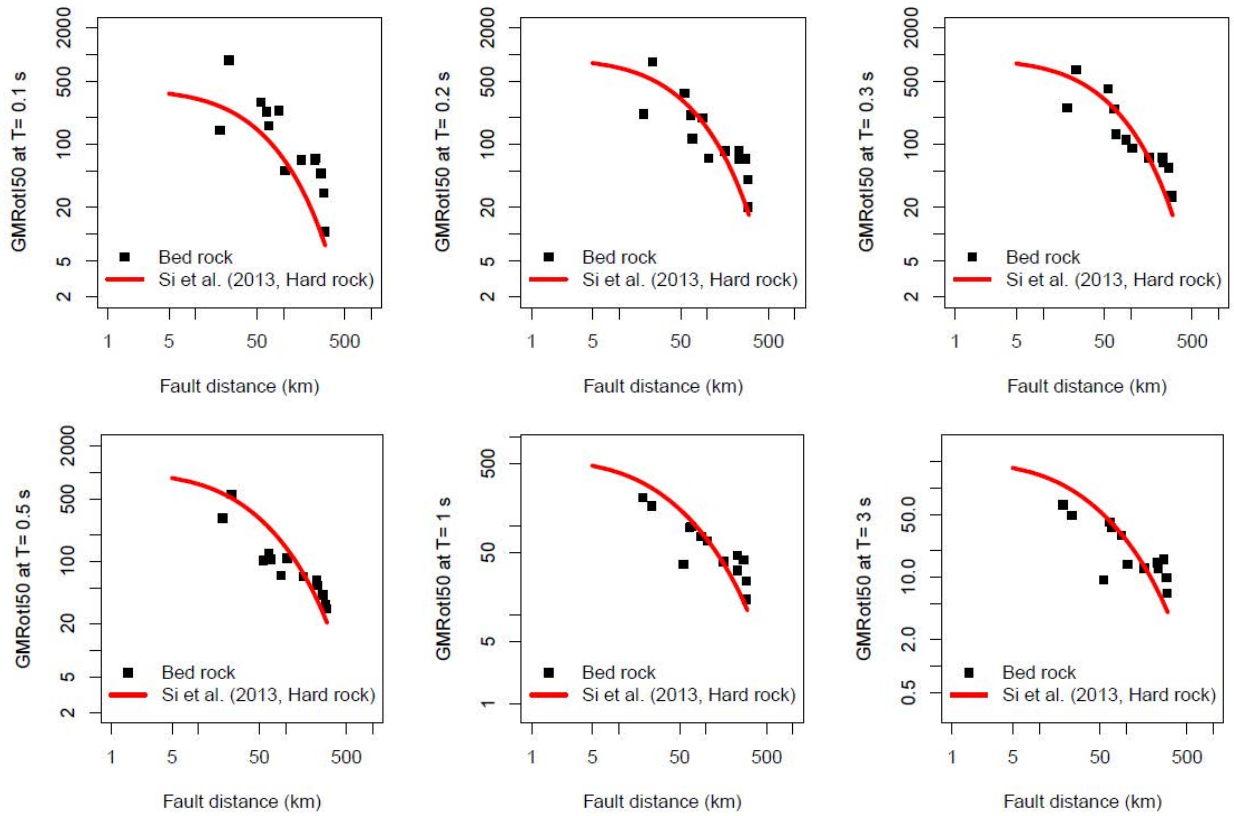


FIG. A-6. Comparison between observed and predicted response spectra Wenchuan. Reproduced with permission from Si et al., 2014 [A-8]

REFERENCES OF ANNEX

- [A-1] SI, H., MIDORIKAWA, S., TSUTSUMI, H., NODA A., MASATSUKI, T., Preliminary Study of new attenuation relationship for response spectra on seismic bedrock including near source data, Proc. 8th Int. Conf. on Urban Earthq. Eng. March 7-8, 2011) Tokyo Institute of Technology, Tokyo, Japan (2011) 75–78.
- [A-2] SI, H., MIDORIKAWA, S., TSUTSUMI, H., WU, C., MASATSUKI, T., NODA. A., Preliminary analysis of attenuation relationship for response spectra on bedrock based on strong motion records including the 2011 M_w 9.0 Tohoku earthquake, Proc. 10th Int. Conf. Urban Earthq. Eng., Tokyo Institute of Technology, Tokyo, Japan (2013) 113–117.
- [A-3] SI, H., TSUTSUMI, H., SAIJO, Y., TAJIMA, R., MURATA, R., A study on the evaluation of amplification factor for response spectra, Summaries of technical papers of Annual Meeting, Architectural Institute of Japan, B-2, 20092, (2013) (in Japanese).
- [A-4] BOORE, D.M., WATSON-LAMPREY, J., ABRAHAMSON, N.A., GMRotD and GMRotI: Orientation-independent measures of ground motion, Bull. Seismol. Soc. Am. **96** (2006) 1502–1511.
- [A-5] SI, H., MIDORIKAWA, S., New attenuation relationships for peak ground acceleration and velocity considering effects of fault type and site condition, J. Struct. Construct. Eng. AIJ, **523** (1999) 63–70 (in Japanese with English abstract).
- [A-6] UCHIYAMA, Y., MIDORIKAWA, S., Attenuation relationship for response spectra on engineering bed rock considering effects of focal depth, J. Struct. Constr. Eng., Transaction of Architectural Institute of Japan, **606** (2006) 81–88 (In Japanese).
- [A-7] KANNO, T., NARITA, A., MORIKAWA, N., FUJIWARA, H., FUKUSHIMA, Y., A new attenuation relation for strong ground motion in Japan based on recorded data, Bull. Seismol. Soc. Am. **96** 3 (206) 879–897.
- [A-8] SI, H., KOKETSU, K., MIYAKE, H., LI, X., Empirical evaluation of ground motion for the Wenchuan and Lushan earthquakes, Earthq. Eng. Eng. Dyn. **34** 4 (2014) (in Chinese with English abstract).

CONTRIBUTORS TO DRAFTING AND REVIEW

Albarelo, D.	University of Siena, Italy
Anderson, J.	University of Nevada, United States of America
Berge-Thierry, C.	Alternative Energies and Atomic Energy Commission, France
Cotton, F.	GFZ, Helmholtz Centre Potsdam, Germany
Crespo, M.J.	Principa, Spain
Douglas, J.	University of Strathclyde, United Kingdom
Fukushima, Y.	International Atomic Energy Agency
Gülen, L.	T.C. Sakarya University, Turkey
Irikura, K.	Aichi Institute of Technology, Japan
Martin, C.	Geoter-Fugro, France
McDuffie, S.M.	Department of Energy, United States of America
Petersen, M.	United States Geological Survey, United States of America
Renault, P.	Swissnuclear, Switzerland
Romeo, R.	University of Urbino, Italy
Sánchez Cabañero, J.G.	Nuclear Safety Council, Spain
Schmitt, T.	TÜV SÜD, Germany
Seber, D.	Nuclear Regulatory Commission, United States of America
Senfaute, G.	Électricité de France, France
Si, H.J.	Seismological Research Institute Inc., Japan
Somerville, P.G.	AECOM, United States of America
Thiry, J.M.	AREVA, France
Tran, M.T.	Vietnam Academy of Science and Technology, Vietnam
Varpasuo, Pentti E.J.	PVA Engineering Services, Finland
Wu, C.J.	Nuclear Regulation Authority, Japan

Working Group and/or Consultants Meetings

Vienna, Austria: 11–13 July, 2012
Tokyo, Japan: 12–16 November, 2012
Vienna, Austria: 13–17 May, 2013
Tokyo, Japan: 06–11 July, 2013
Vienna, Austria: 16–19 September, 2013
Rockville, MD, USA: 02-04 December, 2013



IAEA

International Atomic Energy Agency

No. 24

ORDERING LOCALLY

In the following countries, IAEA priced publications may be purchased from the sources listed below or from major local booksellers.

Orders for unpriced publications should be made directly to the IAEA. The contact details are given at the end of this list.

BELGIUM

Jean de Lannoy

Avenue du Roi 202, 1190 Brussels, BELGIUM

Telephone: +32 2 5384 308 • Fax: +32 2 5380 841

Email: jean.de.lannoy@euronet.be • Web site: <http://www.jean-de-lannoy.be>

CANADA

Renouf Publishing Co. Ltd.

22-1010 Polytek Street, Ottawa, ON K1J 9J1, CANADA

Telephone: +1 613 745 2665 • Fax: +1 643 745 7660

Email: order@renoufbooks.com • Web site: <http://www.renoufbooks.com>

Bernan Associates

4501 Forbes Blvd., Suite 200, Lanham, MD 20706-4391, USA

Telephone: +1 800 865 3457 • Fax: +1 800 865 3450

Email: orders@bernann.com • Web site: <http://www.bernann.com>

CZECH REPUBLIC

Suweco CZ, s.r.o.

SESTUPNÁ 153/11, 162 00 Prague 6, CZECH REPUBLIC

Telephone: +420 242 459 205 • Fax: +420 284 821 646

Email: nakup@suweco.cz • Web site: <http://www.suweco.cz>

FRANCE

Form-Edit

5 rue Janssen, PO Box 25, 75921 Paris CEDEX, FRANCE

Telephone: +33 1 42 01 49 49 • Fax: +33 1 42 01 90 90

Email: fabien.boucard@formedit.fr • Web site: <http://www.formedit.fr>

Lavoisier SAS

14 rue de Provigny, 94236 Cachan CEDEX, FRANCE

Telephone: +33 1 47 40 67 00 • Fax: +33 1 47 40 67 02

Email: livres@lavoisier.fr • Web site: <http://www.lavoisier.fr>

L'Appel du livre

99 rue de Charonne, 75011 Paris, FRANCE

Telephone: +33 1 43 07 43 43 • Fax: +33 1 43 07 50 80

Email: livres@appeldulivre.fr • Web site: <http://www.appeldulivre.fr>

GERMANY

Goethe Buchhandlung Teubig GmbH

Schweitzer Fachinformationen

Willstätterstrasse 15, 40549 Düsseldorf, GERMANY

Telephone: +49 (0) 211 49 874 015 • Fax: +49 (0) 211 49 874 28

Email: kundenbetreuung.goethe@schweitzer-online.de • Web site: <http://www.goethebuch.de>

HUNGARY

Librotrade Ltd., Book Import

Pesti út 237. 1173 Budapest, HUNGARY

Telephone: +36 1 254-0-269 • Fax: +36 1 254-0-274

Email: books@librotrade.hu • Web site: <http://www.librotrade.hu>

INDIA

Allied Publishers

1st Floor, Dubash House, 15, J.N. Heredi Marg, Ballard Estate, Mumbai 400001, INDIA

Telephone: +91 22 4212 6930/31/69 • Fax: +91 22 2261 7928

Email: alliedpl@vsnl.com • Web site: <http://www.alliedpublishers.com>

Bookwell

3/79 Nirankari, Delhi 110009, INDIA

Telephone: +91 11 2760 1283/4536

Email: bkwell@nde.vsnl.net.in • Web site: <http://www.bookwellindia.com>

ITALY***Libreria Scientifica "AEIOU"***

Via Vincenzo Maria Coronelli 6, 20146 Milan, ITALY

Telephone: +39 02 48 95 45 52 • Fax: +39 02 48 95 45 48

Email: info@libreriaaeiou.eu • Web site: <http://www.libreriaaeiou.eu>

JAPAN***Maruzen-Yushodo Co., Ltd.***

10-10, Yotsuyasakamachi, Shinjuku-ku, Tokyo 160-0002, JAPAN

Telephone: +81 3 4335 9312 • Fax: +81 3 4335 9364

Email: bookimport@maruzen.co.jp • Web site: <http://maruzen.co.jp>

RUSSIAN FEDERATION***Scientific and Engineering Centre for Nuclear and Radiation Safety***

107140, Moscow, Malaya Krasnoselskaya st. 2/8, bld. 5, RUSSIAN FEDERATION

Telephone: +7 499 264 00 03 • Fax: +7 499 264 28 59

Email: secnrs@secnrs.ru • Web site: <http://www.secnrs.ru>

UNITED STATES OF AMERICA***Bernan Associates***

4501 Forbes Blvd., Suite 200, Lanham, MD 20706-4391, USA

Telephone: +1 800 865 3457 • Fax: +1 800 865 3450

Email: orders@bernan.com • Web site: <http://www.bernan.com>

Renouf Publishing Co. Ltd.

812 Proctor Avenue, Ogdensburg, NY 13669-2205, USA

Telephone: +1 888 551 7470 • Fax: +1 888 551 7471

Email: orders@renoufbooks.com • Web site: <http://www.renoufbooks.com>

Orders for both priced and unpriced publications may be addressed directly to:

IAEA Publishing Section, Marketing and Sales Unit

International Atomic Energy Agency

Vienna International Centre, PO Box 100, 1400 Vienna, Austria

Telephone: +43 1 2600 22529 or 22530 • Fax: +43 1 2600 29302

Email: sales.publications@iaea.org • Web site: <http://www.iaea.org/books>

International Atomic Energy Agency
Vienna
ISBN 978-92-0-105516-3
ISSN 1011-4289